MICRORNA CONTROLS OF NEVEROUS SYSTEM DEVELOPMENT AND FUNCTIONS IN *DROSOPHILA MELANOGASTER*

WENG RUIFEN

(B. Sci. (Hons.), NUS)

A THESIS SUBMITTED

FOR THE DEFREE OF DOCTOR OF PHILOSOPHY

DEPARTMENT OF BIOLOGICAL SCIENCES

NATIONAL UNIVERSITY OF SINGAPORE

2013

DECLARATION

I hereby declare that this thesis is my original work and it has been written by me in its entirety.

I have duly acknowledged all the sources of information, which have been used in the thesis.

This thesis has also not been submitted for any degree in any university previously.

WENG Ruifen

21 January 2013

Acknowledgement

First and foremost, I would like to thank my advisor, Stephen Cohen. Steve has been a wonderful mentor who has been incredibly supportive, understanding and encouraging throughout these years. I appreciate the freedom that I was given to explore and experiment, and the immense scientific insight that Steve has never failed to provide me during the course of this study. I have been deeply indebted to all the time he has spent nurturing my scientific development, the valuable guidance and advices he has given me during the ups and downs of the graduate years.

Secondly, I have to thank my collaborator, Joanne Yew. Joanne has been an amazing person to work with. I treasure all the generous advices she has given me, all the fun sciences and non-science chitchats that we have had. I have learnt tremendously from her and really appreciate her help and encouragement.

I would like to thank my graduate committee members, Dr. Pernille Rorth, Dr. Joanne Yew and Dr. Lim Kah-Leong, for their invaluable advices and timely feedback.

I would also like to thank past and present members of the Cohen lab. I would like to thank everyone in the Cohen lab for the incredible scientific atmosphere in the lab, for their patience with me when I have asked for help, and for making our interactive group meetings such a joy to attend.

Over the years, I have met and learnt from many great people in the lab, in TLL and in IMCB. I am grateful to Adam Cliff for being my great ‘fly genetics encyclopedia’

in the first and subsequent years of my PhD studies when I had absolutely no idea how to recognize the TM2 balancer or how to do a genetic recombination! I am absolutely indebted to Adam for providing me the listening ears and for sharing his opinions on many matters whenever I was in doubt. I would also like to thank Ville Hietakangas, Valerie Hilgers, David Foronda, Hector Herranz, Jishy Varghese, Lynette Foo and Dan Zhang for the great scientific discussion and wonderful friendship. I am grateful to Phing Chian Chai for his patience when I have asked for help with the millions of questions in *Drosophila* neuroblasts. I appreciate greatly his generosity in sharing his knowledge in the filed and the useful reagents. It has been a great experience working with Jacqueline Chin on the pheromone project, and I thank Jac for the wonderful friendship, the great many interesting discussion we have had and her help with many of the experiments. The same gratitude goes towards Shruti Shanker and Wan Chin Ng for the discussion on *Drosophila* behavior; and to Weibin Zhang and Lynette Foo for reading this thesis.

Last but not least, I would like to thank my family for their selfless love and support throughout the good and bad times of these years.

List of Publication

Weng, R., Chen, Y.W., Bushati, N., Cliffe, A., and Cohen, S.M. (2009). Recombinase-mediated cassette exchange provides a versatile platform for gene targeting: knockout of miR-31b. **Genetics** *183*, 399-402.

Chen, Y.W., Weng, R., and Cohen, S.M. (2011). Protocols for use of homologous recombination gene targeting to produce microRNA mutants in Drosophila. **Methods Mol Biol** *732*, 99-120

Ge, W., Chen, Y.W., Weng, R., Lim, S.F., Buescher, M., Zhang, R., and Cohen, S.M. (2012). Overlapping functions of microRNAs in control of apoptosis during Drosophila embryogenesis. **Cell Death Differ** 19, 839-846.

Weng, R., and Cohen, S.M. (2012). Drosophila miR-124 regulates neuroblast proliferation through its target anachronism. **Development** *139*, 1427-1434.

Vodala, S., Pescatore, S., Rodriguez, J., Buescher, M., Chen, Y.W., Weng, R., Cohen, S.M., and Rosbash, M. (2012). The oscillating miRNA 959-964 cluster impacts Drosophila feeding time and other circadian outputs. **Cell Metab** *16*, 601-612.

Kugler J-M, Chen Y.W., Weng, R. and Cohen S.M. (2013) miR-989 is required for border cell migration in the Drosophila ovary. **PLOS ONE** (2013 Submitted)

Weng, R., Chin, JS. J., Yew J.Y., Bushati, N. and Cohen S.M. (2013) miR-124 limits sex-specific splicing factor traF expression to control pheromone production in Drosophila. **PNAS** (2013 Submitted)

Garg D., Chen Y.W., Weng, R., Ler S.H., Gunaratne J., and Cohen S.M. (2013) microRNA mediated control of superoxide metabolism promotes male reproductive success at the cost of accelerated age-related decline in brain function. **Science** (2013 Submitted)

Table of Contents

Summary

miRNAs have been implicated as post-transcriptional regulators of central nervous system (CNS) development and function. *miR-124* is an evolutionarily ancient, CNS-specific miRNA. On the basis of the evolutionary conservation of its nucleotide sequence and CNS-specific expression in the CNS, *miR-124* is expected to have an ancient conserved functional role in the nervous system across phyla. This thesis describes the context-dependent roles of *miR-124* in the control of neural development and function in *Drosophila melanogaster*.

First I report on the investigation of *miR-124* function using a targeted knockout mutant and present evidence for a role during larval central brain neurogenesis in *Drosophila melanogaster*. I show that *miR-124* activity in the larval central brain neuroblast lineage is required to support levels of neural progenitor proliferation by limiting the expression of *anachronism*, which encodes for a secreted inhibitor of neuroblast proliferation, in the neuroblast lineage.

The second session of this thesis describes the role of *miR-124* in adult function and present evidence for a role in conferring sexual identity and reproductive fitness, apparently acting in both the CNS and the peripheral tissues to influences male pheromone production. I show evidence that *miR-124* acts in the sex determination pathway to control leaky *transformer* expression. In *miR-124* loss-of-function, mutant males express elevated level of tra^{F}, which leads to aberrant production of a subset of male-specific pheromones. As a result, chemical communications are impaired, leading to abnormal courtship and aggression behaviors.

List of Tables

List of Figures

List of Abbreviations and Symbols

Chemicals and reagents

dNTP	Deoxynucleoside triphosphate
EDTA	Ethylene-diamine-tetra-acetate
HCl	Hydrochloric acid
LiCl	Lithium chloride
Gly	Glycine
MgCl2	Magnesium chloride
NaCl	Sodium chloride
PBS	Phosphate buffered saline
PMSF	Phenylmethylsulfonylfluoride
SDS	Sodium dodecylsulphate
Tris	Tris (hydroxymethyl)-aminomethane
ALH	After larval hatching

Units and measurements

°C	Degree Celsius
µg	Microgram(s)
µl	Microlitre(s)
µM	Micromolar
Ct	Threshold cycle
bp	Base pair(s)
g	Gram(s)
h	Hour(s)
kb	Kilo base-pairs
kDa	Lilo Dalton(s)
M	Molar
min	Minute(s)
ml	Mililitre(s)
mM	Milimolar
ng	Nanogram(s)
OD600nm	Absorbance at wavelength 600 nm
rpm	Revolution per minute
sec	Second(s)
U	Unit(s)

v/v	Volume per volume
w/v	Weight per volume

Others

ALH	After larval hatching
Ase	Asence
BrdU	5-bromo-2'deoxyuridine
CDS	Coding sequence
CNS	Central nervous system
DNA	Deoxyribonucleic acid
Dpn	Deadpan
Elav	Embryonic Lethal Abnormal Vision
et al.	Et alii (and others)
i.e.	That is
GMC	Ganglion mother cell
Insc	Inscuteable
MARCM	Mosaic analysis of a repressible marker
Mira	Mirdanda
miRNA	MiRNA
mRNA	Messenger RNA
NB	Neuroblast
nt	Nucleotide(s)
ORF	Open reading frame
PCR	Polymerase chain reaction
PH3	Phospho-histone H3
PON	Partner of Numb
pre-miRNA	Precursor miRNA
pri-miRNA	Primary miRNA
Pros	Prospero
RMCE	Recombinase-mediated cassette exchange
RNA	Ribonucleic acid
RNAi	RNA interference
RT	Reverse transcription
RT-qPCR	RT-based quantitative polymerase chain reaction
SD	Standard deviation of the sample
SDS-PAGE	SDS Polyacrylamide Gel Electrophoresis

UAS	Upstream activating sequence
UTR	Untranslated region
w	White
WT	Wild-type

1 Introduction

1.1 Gene targeting in *Drosophila melanogaster*

Almost a century on since the birth of classical genetics, when Thomas Hunt Morgan began using *Drosophila melanogaster* to establish the chromosome theory of heredity [1], this tiny insect has remained one of the most popular model organisms for genetic studies. This is partly due to the availability of a wide variety of genetic tools for genome manipulations.

Over the last few decades, biological research in *Drosophila* has been greatly facilitated by our ability to manipulate DNA sequences *in vivo,* thanks to the explorations of novel techniques in fly genetics. In particular, the introduction of homologous recombination-based gene targeting in 2000 has greatly enhanced the repertoire of tools available for genome manipulation in this model organism [2-4]. Prior to this, gene deletions relied mainly on conventional chemical mutagenesis or the flanking deletion strategy based on imprecise *P*-element excision or male recombination [2-7]. While often effective, the strategy based on chemical mutagenesis is relatively inefficient. By contrast, the flanking deletion strategy suffers from its strict dependence on the proximity of a *P*-element to the gene of interest. It is, therefore, of limited usefulness in cases where no nearby *P*-element insertions are available or when the gene of interest is close to another gene. The advent of gene targeting by ends-out homologous recombination has provided a direct way to target specific loci, by creating precise user-defined deletions [8-13].

The ends-out homologous recombination strategy is a multi-generation process involving the contribution of several enzymatic reactions. A routine ends-out targeting experiment typically consists of three major steps. These include the cloning of a gene-targeting construct; the generation of a so-called donor fly containing the targeting construct and the induction of homologous recombination *in vivo* to initiate gene targeting. This strategy allows the generation of a specific knockout of the gene of interest. The steps involved in generating a targeted allele based on this strategy are outlined by the schematic overview provided in Figure 1.1.

Using this method, gene specific targeting events can be made in about 4-5 months with reported efficiencies ranging from 1 in 200 to 1 in 350,000, depending on the size and chromosomal location of the targeted loci [15-16]. However, bearing in mind the time and effort needed for the entire gene targeting procedure, improvements should be implemented to enhance its efficiency for use in global gene targeting projects.

In addition, the current homologous recombination-based gene targeting vectors do not allow repeated targeting of a single locus to create the variant alleles of target gene. Each variant requires starting from the beginning with a new targeting vector.

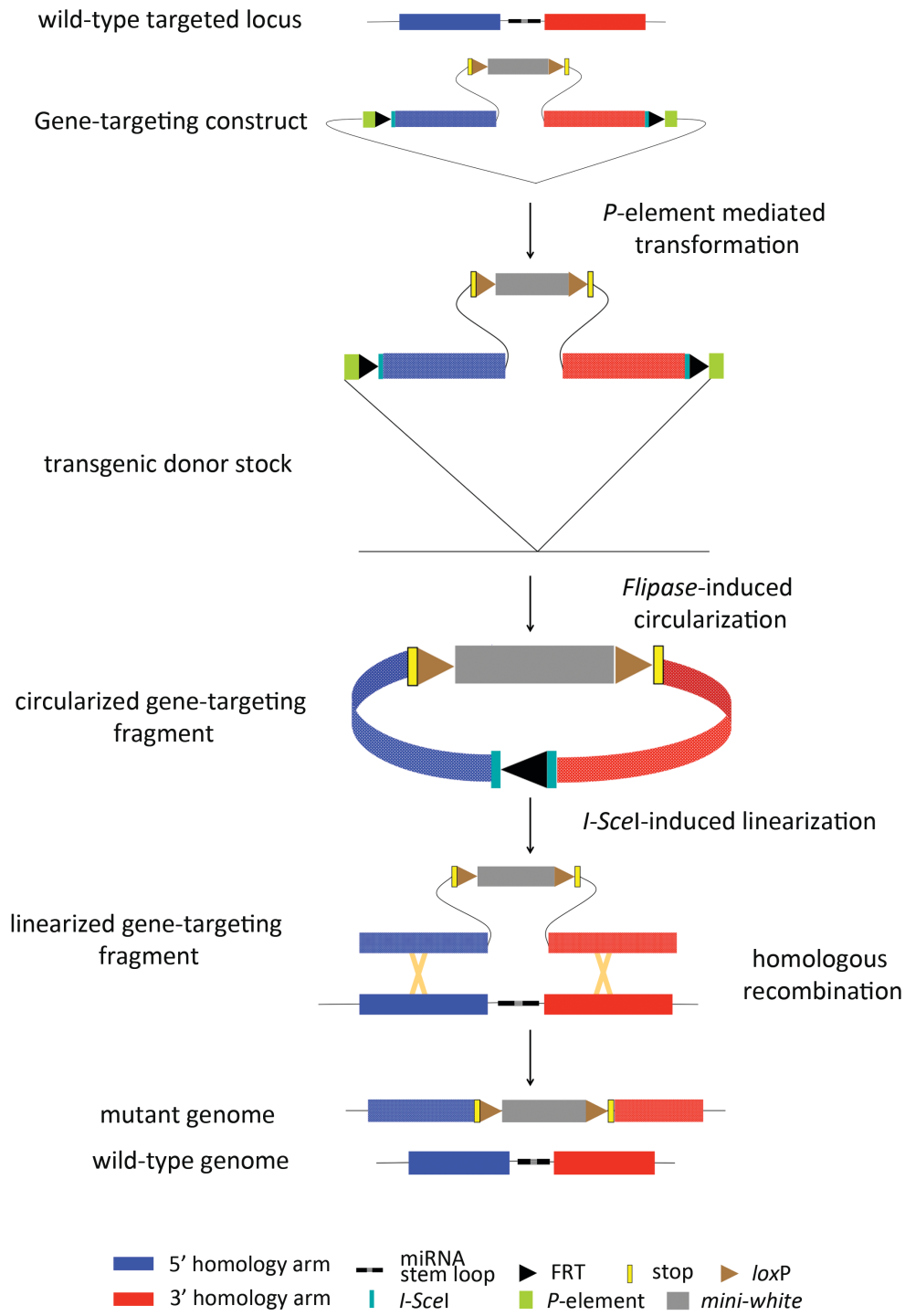

Figure 1.1 Schematics of ends-out gene targeting by homologous recombination.

3kb to 4kb homology sequences flanking the target gene are cloned into the targeting vector (shown here is the pW25 vector developed by Rong and Golic [11]. P-element-mediated transformation gives rise to transgenic donor containing the targeting cassette. Induction of FLP recombinase is used to excise a circular DNA molecule containing the targeting vector, which is then linearized by cleavage with the *I-SceI* endonuclease. The linearized targeting vector can then recombine with the chromosomal target locus, replacing the endogenous gene with *mini-white* and generating a mutant heterozygous for the targeted gene.

Recently, an integration strategy called recombinase mediated cassette exchange (RMCE) has been developed for site-specific recombination [14, 15]. In this system, the donor and target sequences are each flanked by inverted recognition sites for the bacteriophage φC31 integrase. Double crossover events occurring on both sides of the donor and target sequences result in a clean exchange of the target sequence cassette with the donor cassette, as illustrated in Figure 1.2.

To this end, the bacteriophage φC31 integrase-mediated RMCE has been shown to facilitate directional site-specific transformation, which leads to a clean exchange of target cassette with a donor cassette with reasonable efficiency [15]. First developed for use in cell culture, RMCE has since been demonstrated in several model organisms, including fission yeast, flies and mice [19-22]. Therefore, the RMCE strategy may provide a means to overcome some of the limitations of the current gene targeting strategy. This would then allow repeated genomic manipulation once an initial gene-targeting event has been created at the locus of interest.

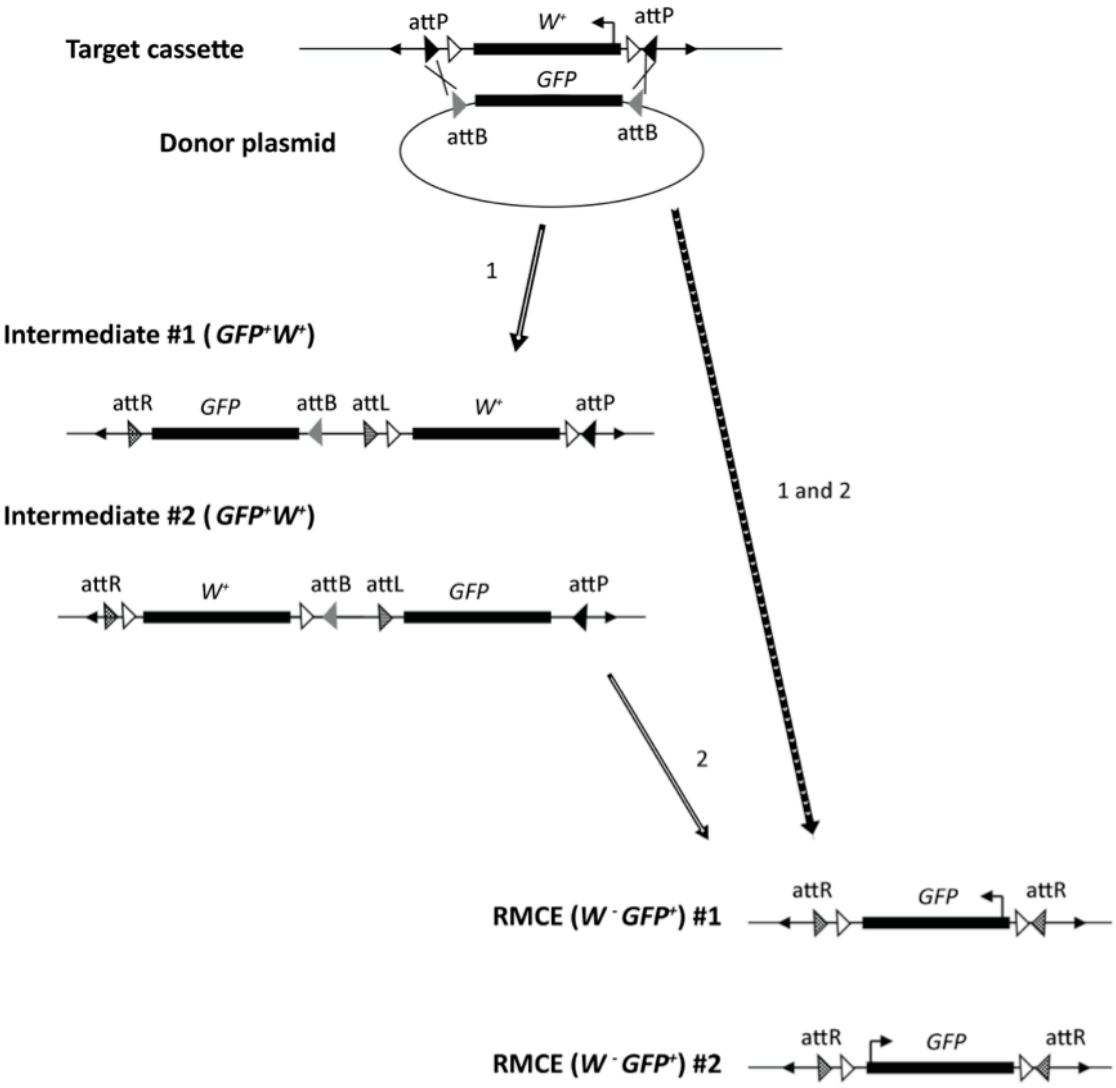

Figure 1.2 Site-specific integration by φC31-mediated RMCE.

The target *mini-white* cassette is flanked by inverted attP sites within a genomic *P*-element, and the donor *gfp* cassette is flanked by inverted attB sites on a plasmid. Crossovers at both ends of the two aligned cassettes result in an exchange of *mini-white* for *gfp*. Alternatively, a single crossover at one end of the aligned cassettes creates an intermediate that integrates the entire donor plasmid, resulting in the carry over of both *mini-white* and *gfp* (intermediate #1). Similarly, a single crossover may occur at the other attP/attB pair, resulting in a similar structure in which *mini-white* is inserted to the left of *gfp* (intermediate #2). Either of the two intermediates may then resolve into an RMCE event by a subsequent crossover between the remaining attP/attB pair within the intermediate structure. Thick solid line, transcription unit; small arrowheads, *P*-element ends; triangles, att sites (features not drawn to scale).

1.2 Biogenesis and Functions of animal miRNAs

1.2.1 Biogenesis of animal microRNAs

MicroRNAs (miRNAs) are endogenous non-coding RNAs of ~22 nucleotides (nt) in length that regulate gene expression in animals and plants. Animal miRNAs were first discovered in 1993 when the small RNA, *lin-4*, was found to regulate *C. elegans* larval developmental timing through its control on the expression of the *lin-14* messenger RNA (mRNA) [23-24]. Since then, computational predictions and deep sequencing efforts have identified hundreds of miRNAs in many multicellular organisms, including mammals (Reviewed in [16]).

In *Drosophila*, transcription of most miRNA genes is carried out by RNA polymersase II, resulting in the production of the primary miRNAs (pri-miRNA) with a length varying from several hundreds nt to several kilobases (kb). Most pri-miRNAs exist as autonomous transcript units with a polyadenylated 3' end and a 5' 7-methylguanosine cap [17, 18]. In some other cases, such as intronic miRNA genes, the pri-miRNA can be located in another transcript (e.g. [19]).

For the pri-miRNAs that exist as independent transcripts, a stable hairpin structure formed by the folding back of the pri-miRNAs is endonucleolytically cleaved by the nuclear RNase III enzyme, Drosha, and the double-stranded RNA-binding domain (dsRBD) protein, Partner of Drosha (Pasha). Cleavage of the pri-miRNA by the Drosha/Pasha complex occurs co-transcriptionally [20], leading to the formation of a ~70 nt long hairpin precursor miRNA (pre-miRNA). In cases where pri-miRNAs are derived from short intronic hairpins, the so-called mirtrons, the nuclear biogenesis by Drosha cleavage is bypassed. Instead, the splicing machinery that releases pre-

miRNA-like hairpins from the host transcripts results in the generation of these intron-derived miRNAs [21, 22].

Regardless of the nature of the molecular processing of the pri-miRNAs, the pre-miRNAs formed are then exported into the cytoplasm by the combined efforts of Ran-GTP and the export receptor Exportin-5 [23]. This allows the cleavage of the precursor miRNA by the cytoplasmic Dicer-1/Loquacious complex [24, 25]. This then gives rise to the mature miRNA:miRNA* duplex of ~22 nucleotides, where miRNA* denotes the passenger strand that is degraded, in most cases, in the final step of miRNA processing. Finally, the mature single-stranded miRNA is incorporated into an Argonaute (Ago) protein-containing RNA-induced silencing complex (RISC) [26-28] (Figure 1.3).

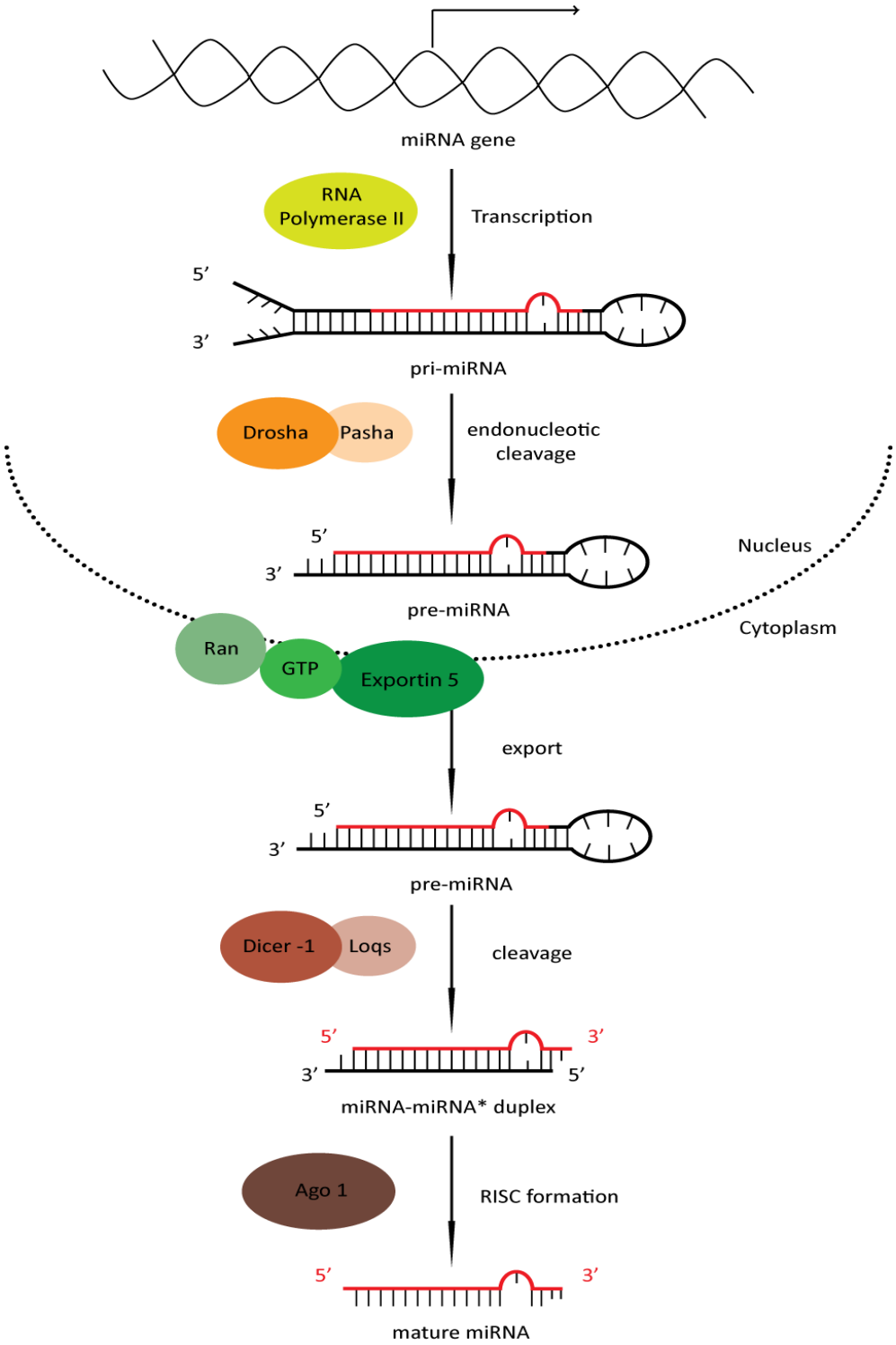

Figure 1.3 Cartoon diagrams showing the biogenesis of miRNAs.

Transcription of the miRNA locus by RNA polymerase II results in the primary miRNA (pri-miRNA), which is processed by the Drosha/Pasha complex into precursor miRNA (pre-miRNA). Followed by exportation from the nucleus to the cytoplasm by Exportin-5, the pre-miRNA is further processed by Dicer and Loquacious into a miRNA:miRNA* duplex (where miRNA* duplex denotes passenger strand). Only the mature miRNA is loaded on the Agronaute-containing complex called the RNA-induced silencing complex (RISC).

1.2.2 Regulation of miRNA biogenesis

Similar to protein-coding genes, production of miRNAs can be regulated at both transcriptional and post-transcriptional levels.

The transcriptional regulation of pri-miRNA genes is largely similar to that of protein-coding genes. These involve recognition of enhancer and terminator elements by the RNA polymerase-containing transcription machinery [17, 18], and motif-specific recognition of transcription factors [29].

By contrast, post-transcriptional control of miRNA biosynthesis depends mainly on the mechanisms that regulate the cleavage of the pri-miRNA by the Drosha/Pasha complex. One well-characterized example is negative regulation of the mouse miRNA, *let-7*, by its target LIN-28. Competitive binding of LIN-28 to *let-7* prevents binding of *let-7* to Drosha, therefore inhibiting Dicer-mediated cleavage of *let-7* [30-32]. In addition, LIN-28 induces the uridylation of *pre-let-7* at its 3' end, blocking its processing by Dicer and leading to destabilization of uridylated *pre-let-7*. Suppression of *pre-let-7* by LIN-28 has been shown to be important for mouse embryonic stem cell programming [33-35].

1.2.3 Mechanisms of actions of animal miRNAs

miRNAs act as post-transcriptional regulators of gene expression. In animals, miRNAs generally interact with target mRNAs via imperfect complementary base pairing to target sites in the mRNA 3' untranslated region (3'UTR).

Over the last 10 years or so, computational algorithms have been developed for the prediction of miRNA targets. In general, factors such as the sequence determinants of the target sites, the thermodynamic stability of the miRNA:mRNA duplex and evolutionary conservation of the site within the 3'UTR sequences form the basis of such prediction programs [31, 45-46]. Based on these criteria, most miRNAs have been predicted to target hundreds of protein-coding genes, while an estimated 30 – 50% of all animal protein-coding transcripts are targeted by at least one miRNA.

While factors such as the thermodynamic stability of the miRNA:mRNA duplex and evolutionary conservation of the site are more straightforward, sequence determinants of miRNA target sites in animals are a bit more complex. In fact, there are three different categories of animal miRNA target sites, namely the 'canonical', the 'marginal' and the 'atypical' sites (reviewed in [36]). The so-called 'seed' region, which refers to nt 2-7, 2-8 or 1-7 of the miRNA, is thought to provide the most specificity in miRNA:mRNA pairing [37]. In fact, the 5' region is the most highly conserved portion of metazoan miRNAs [38]. In canonical miRNA target sites, a 7-mer perfect complementary pairing is formed between the target sequence and sequences within the seed region of miRNA molecule. By contrast, the so-called marginal miRNA sites refer to 6-mer complementary matches to nt 2-7 or 3-8 of the miRNA seed region, which typically have reduced efficiency. In atypical sites, different forms of 3' pairings, including 3' supplementary sites in which complementary pairing at nt 13-16 supplements an existing 5' seed match, and 3' compensatory sites in which 3' pairing compensates a mismatch in the seed region, are thought to contribute positively to miRNA:mRNA interaction [37, 39].

In most cases, formation of miRNA:mRNA duplex within the ribonucleoprotein (RNP) complex, the RNA-induced silencing complex (RISC), results in repression of mRNA expression through destabilization of the target mRNA through deadenylation or cleavage by Argonaute, the core effector protein of RISC, RNase activity, and/or translational repression (reviewed in [36, 40, 41]).

1.2.4 Biological functions of animal miRNAs

miRNA functions have been identified in many biological phenomena; particularly those associated with dynamic cellular and/or developmental processes such as embryonic development and stem cell differentiation. Studies have shown that animals lacking the functions of all miRNA show severe defects at early stages. In *C. elegans*, while *dicer-1* mutants shows defects in germline development [42][51-52], loss of both maternal and zygotic *dicer-1* leads to embryonic lethality. Since Dicer is one of the core proteins required for the biosynthesis of most miRNAs, these studies suggest that, at least, some miRNAs are essential for basic animal survival [43]. Similarly, in *Drosophila*, *dicer-1* mutant germline stem cells display cell division defects and fail to maintain stem cell fate [42, 44]. In zebrafish, *dicer-1* mutants display a general growth arrest and die by 2–3 weeks of age [45]. Conditional knockout of the mouse *dicer* leads to impairment in the ability of embryonic stem cells to proliferate [46], and failures of both embryonic stem cell and T-cell lineages to differentiate [58-59]. Together, these studies demonstrate the importance of miRNAs during animal development.

1.3 Roles of miRNAs in neurogenesis and beyond

Given the complexity of the nervous system and the vast number of genes and signaling molecules required for the proper architecture and wiring of the nervous system, the central nervous system (CNS) development and function are likely to be important targets of miRNA action [60-61]. In addition, the brain is a rich source of miRNAs expression. Recent miRNA expression profiling experiments have revealed that a significant fraction of miRNAs are highly enriched or specifically expressed in the nervous system [31, 62-63]. Furthermore, expression of miRNAs is tightly regulated during brain development [65-66]. Together with the fact that a given miRNA is capable of targeting hundreds of target mRNAs, these initial observations suggest that the neuronal miRNA pathways could provide an additional layer of complexity in the regulation of neuronal gene expression and in the fine tuning of neuronal functions.

Numerous studies reported over the last decade have provided many examples of miRNA functions at various stages of neural development, ranging from the early differentiation of neurons, the development of dendritic spines and dendrites to plasticity in the control of neuronal functions and animal behaviors. Key examples of individual miRNAs with specific roles in the different stages of regulation are listed in Table 1.1.

Table 1.1 List of individual miRNAs with a characterized biological function at various stages of neural development or neural functions.

miRNA	Neuronal function	Target	Organism	Reference
miR-7	Photoreceptor differentiation	Yan	fly	[47]
miR-8	neurodegeneration	Atrophin-1	fly	[48]
miR-9a	SOP specification	Seneseless	fly	[49]
miR-9	Neuronal differentiation	Foxg1	rodent	[50]
miR-9	Neuroadaptation to alcohol	Bk	rodent	[51]
miR-9	neurogenesis	Fgf signalling	Zebrafish	[52]
miR-124	Neuronal differentiation	PTBP1	rodent	[53]
miR-124	Adult neurogenesis	Sox9	rodent	[54]
miR-124	Neuronal differentiation	REST, Ephrin-B1	rodent	[55]
miR-124	Neurite growth	RhoA	P19 cells	[56]
miR-124	Neuronal differntiation	SCP1	chick	[55]
miR-124	Dendritic branching	?	fly	[57, 58]
miR-124	LTF	CREB	Aplysia	[59]
miR-124	Cocaine-induced plasticity	CREB, BDNF	rodent	[60]
miR-132	Dendrite development	Pp250GAp	rodent	[61]
miR-132	homeostasis	MeCP2	rodent	[62]
miR-132	Circadian clock	RFX4	Rodent	[63]
miR-134	Spine development	Limk1	rodent	[64]
miR-134	Dendrite development	Pum2	rodent	[65]
miR-200	Olfactory neurogenesis	?	Rodent/zebrafish	[66]
miR-219	Circadian clock	SCOP	rodent	[67]
miR-273	Chemosensory neuron differentiation	Die-1	worm	[68]
miR-279	Olfactory neuron specification	Nerfin-1	fly	[69]
miR-279	Circadian clock	Upd	fly	[70]
miR-430	Neuronal morphogenesis	Zygotic transcript	zebrafish	[71]

LTF: long term facilitation

?: unknown

SOP: sensory organ precursor

1.3.1 miRNAs and neural differentiation

The first experimental evidence supporting the roles of miRNAs in the nervous system comes from studies involving the genomic ablation of *dicer*, which results in an ablation of almost all miRNAs. For example, in zebrafish, despite the ability to initiate early neuronal differentiation, *dicer-1* mutants display severe defects in terminal differentiation of neuronal subtypes. Interestingly, these early morphogenesis defects can be largely rescued by re-introduction of a single miRNA family, *miR-430* [72]. Similar early embryonic depletion of miRNAs in mouse neocortical progenitors through *Dicer* ablation has no effect on neuronal progenitor proliferation, but results in impaired differentiation of newborn neurons, leading to defective postnatal cortical layering [73]. Specific depletion of *Dicer* in mouse olfactory progenitors gives rise to abnormal terminal differentiation of developing olfactory progenitors in both zebrafish and mouse. Strikingly, this phenotype is phenocopied when a single miRNA family, the *miR-200* family, is inhibited [66]. These studies point towards a role of Dicer, and therefore, miRNAs as a whole, in early development of nervous systems in the model organisms studied.

However, interpretation of *dicer* mutant phenotypes is complicated by two major caveats. Firstly, multiple studies have suggested that loss of *dicer* function, especially at later embryonic stages, results in increased apoptosis [74, 75]. Furthermore, the spectrum of *dicer* mutant phenotypes does not overlap completely with those associated with mutants of other components of the miRNA biosynthetic pathway, such as *dgcr8*, suggesting that there are probably other biological functions of Dicer [76].

While the vertebrate *dicer* mutant studies, such as those mentioned previously, seem to suggest that miRNAs are critically involved in the proper control of differentiation for subpopulations of neurons, they are largely dispensable for early neural cell fate decisions. By contrast, in invertebrates such as *Drosophila* and *C. elegans,* individual miRNAs have been shown to play instructive roles in neuronal specifications [68, 69, 77]. For example, the *Drosophila miR-9* gene has been shown to have an early instructive role in neural patterning by inducing sensory organ precursor formation [78]. However, its mouse counterpart is required in the differentiation of a subpopulation of neuronal cells, called the Cajal-Retzius cells, but not for the induction of its neural progenitors [79].

Another miRNA that is well characterized for its role in differentiation is the miRNA, *miR-124*, which will be discussed in a separate section later on.

1.3.2 miRNAs and dendrite growth

In both vertebrates and invertebrates, a highly organized network of synaptic contacts forms the structural basis for neuronal connectivity. The formation of synaptic contacts involves the outgrowth of axons and dendrites as neurons start to explore their environment for contact information with prospective partner neurons. In particular, the development of dendrites is a highly orchestrated event achieved by the coordination of activity-dependent gene expression. This process is controlled transcriptionally, through new protein synthesis, and post-transcriptionally, through modulations on the local translation of mRNAs stored within neural processes, such as the dendritic shaft and spines [80, 81].

Recent studies have reported the detection of both miRNAs and pre-miRNAs in synaptoneurosomes, which are biochemical preparations of synaptic membranes, indicating a potential role of miRNAs in the post-transcriptional control of dendritically localized mRNAs [82-84]. In addition, a number of miRNA promoter regions were found to be occupied by a master regulator of dendritic growth, the activity-dependent transcription factor CREB [85]. More recently, evidence supporting the significance of miRNAs in the control of dendritogenesis was provided by genetic studies of mutants of the miRNA biogenesis pathway in both vertebrates and invertebrates [74, 86]. In *Drosophila*, a strong genetic interaction was found between components of the miRNA biosynthesis pathway and the fragile X mental retardation protein (FMRP), an RNA binding protein acting as a suppressor of local mRNA translation in the synapto-dendritic compartment [87-89]. For example, several studies reported that the interaction between FMRP and Ago1, a key protein in the miRNA RISC complex, is crucial for synaptogenesis [87].

The first example of a miRNA-mediated local regulation on protein synthesis at the synapse was provided by studies on the roles of a mammalian brain-specific miRNA, *miR-134*. In rat cultured hippocampal neurons, *miR-134* is found to be co-localized with a protein kinase called Limk1, the Lim-domain containing protein kinase 1, in the synapto-dendritic compartment. Limk1 is a positive regulator of actin cytoskeletal dynamics in the dendritic spines, and is involved in control of dendritic spine morphology. *miR-134* acts negatively on the translation of *limk1* mRNA, repressing Limk1 local synthesis. In turn, downregulation of Limk1 leads to reduction in the size of dendritic spines. Since dendritic spines are the postsynaptic sites of excitatory synaptic transmission, this results in a restriction on the development of excitatory

synapse formation. By contrast, extracellular stimuli such as the brain-derived neurotrophic factor, BDNF are released in response to synaptic stimulations. These factors act upon neurons and relieve *miR-134* inhibition on Limk1 translation [64]. This provides a bidirectional switch in the regulation of synaptic plasticity by *miR-134* activity.

Other miRNAs that have been linked to the control of dendritic spine morphology are listed in Table 1.1.

1.3.3 miRNAs and animal behavior

miRNAs has been implicated in the fine-tuning of animal behavior, especially those involving neuroadaptive responses of post-mitotic neurons. The types of animal behaviors shown to be regulated by miRNAs include learning and memory [90], circadian behavior [70, 91, 92] and ethanol tolerance [51]. However, our current knowledge about the roles of individual miRNA in the control of animal behaviors has been largely based on what I would call 'nomination' studies. For example, based on *in silico* correlation analyses on the differential expression pattern of mouse hippocampal miRNA observed in four mouse inbred strains with phenotypic data and mRNA expression obtained in the various strains, the authors in one study postulated potential roles of specific miRNAs in learning and memory, exploration and anxiety behavior [90].

Nevertheless, a handful of *in vivo* studies have provided detailed characterization of the roles of specific miRNAs in various behavior controls. For example, intraventricular infusion of an antagomir against *miR-219,* one of the brain-specific miRNAs found in mammals, results in significant lengthening of circadian period in

mouse, based on wheel-running behavioral rhythm measurements [91]. In *Drosophila, miR-279* has been shown to control rest:activity rhythms of the animal by targeting a component of the JAK/STAT signaling pathway, Unpaired (Upd) [70]. With the identification of a set of conserved miRNAs with cyclical expression pattern in the *Drosophila* brain [93], it is likely that many other miRNAs might be involved in circadian rhythms. However, behavioral and physiological analysis of genetic mutants of these miRNAs will be required for a comprehensive understanding of their physiological functions.

1.4 The conserved *miR-124* gene in animals

1.4.1 Sequence of *miR-124* across species

Among the animal miRNAs implicated in CNS development *miR-124* has been the focus of considerable interest. In *Drosophila* and *C. elegans*, *miR-124* is transcribed from a single genetic locus, whereas in humans (*Homo sapiens*) and mouse (*Mus musculus*), it is encoded by three distinct genes and by six in zebrafish [94-96]. Despite the differences in gene numbers, the mature sequence of *miR-124* is deeply conserved across species, with almost exactly the same nucleotide sequences found from *C. elegans* to *Drosophila* to mouse, and to humans [97] (Figure 1.4).

In addition, unlike many other miRNAs, which share the same or similar seed sequence, the seed sequence (shown in red in Figure 1.4) of *miR-124* is unique among all the known miRNAs in animals.

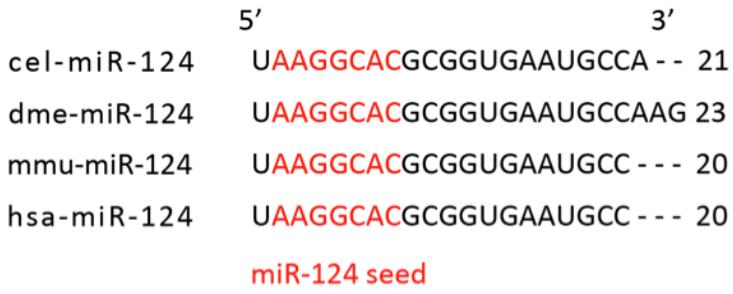

Figure 1.4 Alignment of *Drosophila miR-124* mature sequence with homologues in representative species.

The 21-, 23-, 20- and 20-nt mature transcript sequences of *C. elgans (cel), Drosophila melanogaster (dme), Mus musculus (mms)* and *Homo sapiens (hsa),* respectively are aligned from 5' to 3'. The 5' nt-2-8 representing *miR-124* seed sequences are highlighted in red. Sequences were obtained from the miRBase website [97].

1.4.2 Expression of *miR-124* across species

Expression of *miR-124* across phyla has been highly conserved. To date, most, if not all, studies on *miR-124* expression suggest that *miR-124* is specifically expressed in the CNS of all animal models examined [37, 53, 55, 98-101].

In addition, in all organisms in which it has been studied, *miR-124* is the most abundant miRNA in the CNS, accounting for 25-48 % of all brain-expressed miRNAs in mouse [102, 103], and about 30-40% in *Drosophila* [22].

The subtypes of cells that express *miR-124* are similar across the different organisms. Studies in mouse have reported the expression of *miR-124* in neurons but not in astrocytes, and that the level of *miR-124* increases over time in the developing NS [104-106]. It continues to be expressed into mouse adulthood. Similarly, in *Drosophila*, this miRNA was also reported to be specifically expressed in the neurons but not in glia cells [37]. Additionally, the level of *miR-124* expression increases as neurogenesis proceeds in the developing *Drosophila* embryonic and larval CNS [22]. While the subtypes of neurons expressing *miR-124* have not been identified in most organisms, in *Aplysia californica* and in *C. elegans*, its expression is restricted to sensory neurons [59, 107].

1.4.3 Roles of *miR-124* during NS development and in adult functions

Over the past few years, there have been several reports on the roles of *miR-124* in different model organisms, and depending on the model organism studied, *miR-124* functions have been implicated in various stages of neural development, ranging from

the early differentiation of neurons, the development of dendrites to plasticity in the control of neuronal functions and animal behaviors.

Most studies on *miR-124* functions have been based, largely, on miRNA overexpression or depletion using anti-sense oligonucleotides. They have reached different conclusions, particularly pertaining to the roles of this miRNA in neurogenesis and in the control of dendrite growth and morphology [73-75, 77-78, 119, 124-129].

1.4.3.1 *miR-124* in neurogenesis

To date, analysis of *miR-124* in vertebrates mainly point towards its roles as a positive regulator of neural differentiation and a negative regulator for neural progenitor differentiation via repressing several negative regulators of the neuronal differentiation pathway.

This conclusion has been supported by evidence from several independent studies using both *in vitro* and *in vivo* differentiation models. These studies have identified various molecular targets of *miR-124*, including the RNA splicing regulator PTB1, the SCP1 phosphatase, the transcription factor SOX9 and the EphrinB1 receptor. While the different targets have been shown to be functionally relevant in the various contexts of studies, their underlying molecular and cellular mechanisms diverge on the inhibition of neuronal differentiation [73-75, 115, 125, 130]. However, an independent study using the chick spinal cord as an *in vitro* differentiation model failed to observe consistent findings [99]. Details of these experiments will be re-visited again in Chapter four of this thesis. Nevertheless, whether mammalian *miR-124* promotes neuronal differentiation remains unambiguous at the moment. Studies

performed *in vivo* using genetic mutants that completely remove individual miRNA function may provide the means to further resolve the current ambiguity.

No studies have been reported on the role of *miR-124* in *Drosophila* neurogenesis until the last quartile of the total duration of this thesis work. Again, these will be discussed in the next two chapters of this thesis.

1.4.3.2 *miR-124* in dendrite growth and morphology control

In addition to its role in neurogenesis, *miR-124* has been shown to be involved in neurite and dendrite growth in *Drosophila*. However, results from the literature have been largely inconsistent. In one study, it was demonstrated that ectopic expression of *miR-124* in *Drosophila* sensory neurons led to reduction in dendritic branching [58]. However, the reverse was not observed in *miR-124* loss-of-function analysis. From extensive analysis of a genetic null *miR-124* mutant, Sun *et al.* reported increased dendrite variations instead of increased dendritic branching, as would have been expected from the ectopic expression study [57].

Consistent with the second report, studies in the mouse using model cell lines have demonstrated a growth-promoting role for *miR-124*. The authors have shown that in both differentiating embryonic cell P19 cells and in primary cortical neurons, *miR-124* targets the cell division cycle 42 (Cdc42) mRNA and deactivating ras-related C3 botulinum toxin substrate 1 (Rac1) of the Rho GTPase family. Downregulation of the Rho GTPase family led to reduction in F-actin density and a positive stimulation on tubulin acetylation and cytoskeletal reorganization. The overall effect was positive stimulations on neurite outgrowth [56].

Again, further examination of genetic null mutants in the various model organisms would be required for a better understanding of the reasons behind the apparently conflicting results reported in the literature.

1.4.3.3 *miR-124* and animal behavior

Despite the conservation of high-level neuronal-specific expression across phyla, very few gross behavioral defects related to NS functions have been observed in null mutants from multiple species ([57, 108] and this thesis).

Nevertheless, recently, a role of *miR-124* in activity-driven plasticity has been reported in the marine snail, *Aplysia californica* [59], Similar to its expression in *C. elegans, miR-124* expression in *Aplysia californica* is also restricted to sensory neurons. More specifically, *Aplysia miR-124* was found exclusively presynaptically in the sensory-motor synapse where it targets CREB, an important activity-dependent transcription factor implicated in synaptic plasticity and in learning and memory in many animals. Downregulation of CREB led to reduction in serotonin release, thus constraining serotonin-induced long-term facilitation at the synapse. Strikingly, a coherent feedforward loop appears to exist since the authors have also found an inhibition of serotonin on *miR-124* biogenesis. Repression of *miR-124* production by serotonin would in turn relieve the repression of this miRNA on CREB, leading to an increase in the specificity of the synaptic response. This is the first demonstration of a functional role of *miR-124* in mature neurons physiology across phyla.

A more recent study has identified a role of *miR-124* in learning behavior and social interactions in mouse [109]. In this study, the authors characterized the behavior phenotypes of genetic null mutants for the mouse EPAC proteins, which are guanine

nucleotide exchange factors and intracellular receptors for cyclic AMP, and found that *miR-124* expression was restricted by the expression of EPAC proteins. This was mediated through an activation of mouse *miR-124* promoter by EPAC-induced activation of the Rap1 protein. In *epac* null mice, *miR-124* expression was elevated, which in turn repressed the translation of one of its target, Zif268, an EGF-family transcription factor, leading to severe defects in synaptic transmission, spatial learning and social interactions in these animals. All the phenotypes associated with *epac* null mice were rescued when *miR-124* was depleted simultaneously, demonstrating a role of the mouse *miR-124* in the regulation of these processes.

Given the high level of expression of *miR-124* in the adult NS, it is likely that this miRNA is involved in the control of potentially many other types of behaviors. Careful analysis of genetic null mutants or spatial and temporal-specific *in vivo* manipulations of miRNA level would be required to address such possibilities.

1.5 Neurogenesis in Drosophila melanogaster

In *Drosophila,* the cells in the CNS are produced by neural progenitor cells known as neuroblasts (NBs). There are two separate phases of neurogenesis during *Drosophila* development. The first phase takes place during stage 9-14 of embryogenesis. This involves the specification and delamination of NBs from specialized regions called the neuroectoderm, which subsequently divides in a stem cell-like fashion to generate primary neurons [110]. During late embryogenesis, most of the NBs enter a transient quiescent stage. They re-enter proliferation during the second stage of neurogenesis, which begins at late first instar larval (L1) /early second instar larval (L2) stage and lasts throughout larval stage till early pupal stage. In the second phase, re-activated NBs continues to divide in a stem cell-like manner to generate secondary neurons that make up the bulk of mature neurons in the pupal and adult NS [111] [112].

1.5.1 Asymmetric division of *Drosophila* NBs

Both embryonic and larval NBs utilize the same core mechanisms of asymmetric cell division during proliferation. In both cases, NBs undergo repeated rounds of self-renewing divisions in a stem cell-like manner. Each division generates a larger daughter cell that retains the NB identity and a smaller daughter cell, called the ganglion mother cell (GMC), which divides once to generate two post-mitotic daughter cells that subsequently differentiate into two neurons and/or glia.

As shown in Figure 1.5, the asymmetric division of NBs involves the asymmetric localization of mitotic spindles and cell fate determinants. During late interphase, a molecular complex consisting of the proteins Inscuteable (Insc), the Partition defective (Par) – Bazooka (Baz) - *Drosophila* atypical protein kinase C (DaPKC) signaling cassete and the Partner of Insc (Pins)-containing signaling cassette is

formed at the apical cortex of the dividing NB [113-117]. The maintenance of the apical protein complex leads to displacement of mitotic spindle towards the basal cortex and the establishment of an asymmetric spindle during anaphase-telophase, where the apical half is longer than the basal half. Together, these result in a cell size asymmetry between the larger apical NB and the smaller basal GMC [118-120]. In addition, components of the apical protein complex together with two coiled-coil adaptor proteins, Partner of Numb (Pon, an adaptor for Numb) and Miranda (Mira, an adaptor for Prospero and Brat) are also responsible for the basal localization of cell fate determinants, including Numb, Prospero and Brain tumor (Brat). In addition, basal localization of the RNA binding protein, Staufen (Stau) also results in the basal segregation of *prospero* mRNA [121-127]. As a result, at the end of NB division, these cell determinants are preferentially segregated into the smaller GMC daughter cell.

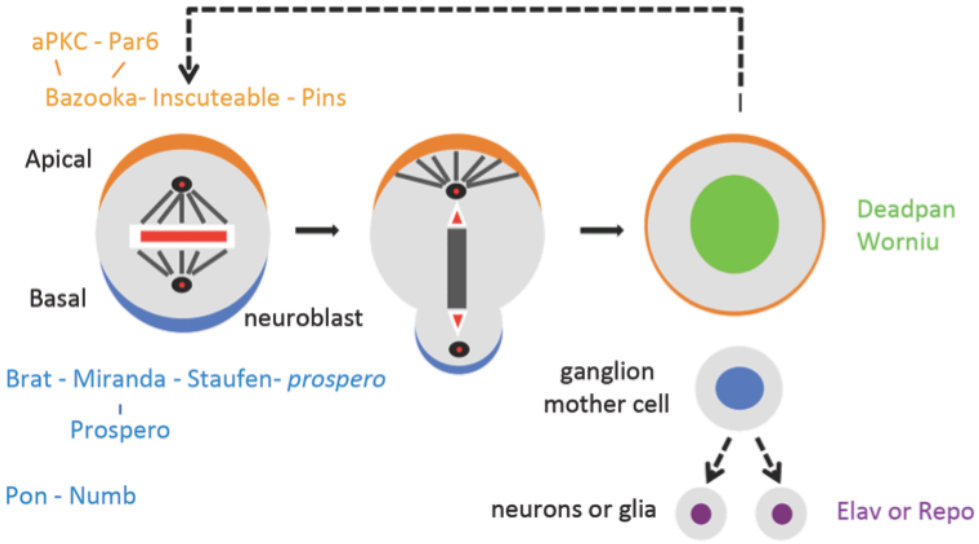

Figure 1.5 Asymmetric division of *Drosophila* NBs.

NBs undergo asymmetric division to generate a larger daughter cell that retains its own identity and a smaller daughter cell, called the ganglion mother cell (GMC). The GMC then divides terminally to produce two smaller post-mitotic cells, which subsequently differentiate into two neurons and/or glia. The asymmetric division of NB is the combined effect of the establishment of a multi-protein complex, including the proteins Inscuteable, the Bazooka-Par6-aPKC complex and Pins; the localization of neural cell fate determinants, including Brat, Prospero and Numb and their adaptor proteins Miranda and Partner-of-Number (Pon). NBs can be identified by the expression of transcription factors such as Deadpan (Dpn) and Worniu (Wor), while GMCs by Prospero, Numb or Pon, mature neurons by ELAV and glia cells by Repo.

1.5.2 The first phase of neurogenesis in *Drosophila*

The early development of insect nervous system is different from that in the vertebrates. In the latter, the primordium of the nervous system, the neural tube, is formed by the centerwards folding of the entire neurectoderm. In *Drosophila*, neural progenitors are scattered, individual cells that segregate from the neurectodermal layer by a process called delamination. This is a feature shared by neurogenesis in all insects. Delamination refers to a morphogenetic movement in which the presumptive neuroblasts constrict apically and lose contact with the neighboring cells before sliding into the interior of the embryos. Neurectodermal cells that remain at the surface do not contribute to the insect CNS, but form the epidermis instead.

The decision to adopt an epidermal or neuronal fate is controlled by two classes of genes, the neurogenic genes and the proneural genes, each with opposing activities. Mutations in the neurogenic genes, such as *Notch, Delta, big brain, shaggy* and components of the *Enhancer of split* gene complex [E(SPL)-C], result in the formation of a highly hyperplastic CNS with the transformation of ectodermal cells into NBs. Death of the mutant embryos is the eventual outcome [111]. By contrast, mutations in the proneural genes, such as *daughterless*, *ventral nervous system condensation defective (vnd)* and components of the *achaete-scute* complex (AS-C), including *achaete, scute, lethal of scute* and *asense*, lead to a hypoplastic CNS with supernumerary epidermoblasts at the expense of functional NBs. The degree of severity of the mutant phenotype varies, depending on the genes that are affected [128, 129].

In addition, equivalence cells within the neurectoderm are clustered in groups of 5-6 cells to form discrete cell populations called pronerual clusters. During delamination, another mechanism known as lateral inhibition ensures that only one cell from each proneural cluster will eventually become a NB. At the initial stage of cell fate acquisition, all the cells in the proneural clusters express both neurogenic and proneural genes. However, positive feedback resulting from the interactions between the neurogenic and proneural genes leads to the reinforcement of proneural gene production in the prospective NB that has initiated neurogenesis. As a result, the increasing concentration of proneural proteins within the prospective NB triggers the transcription of *Delta*. *Delta* encodes the epidermalizing-signaling molecule, which binds to and activates its receptor Notch that is expressed on its adjacent cells. The activation of the Notch pathway in the surrounding cells suppresses transcription of proneural genes in these cells. This reinforces the epidermal cell fate within the cells surrounding the presumptive NBs. Interestingly, despite initial uniform levels of AS-C, Notch or Delta among all the cells within the neurectoderm, the selection of a NB from a proneural cluster is not random and there is always a specific position within the cluster where a NB will arise [130]. Recent studies have suggested possible contributions by the expression of regional specific factors such as the Wingless and the epidermal growth factor receptor (EGFR) pathways in the modulation of neurogenic and proneural protein activities [131].

1.5.3 The second phase of neurogenesis in *Drosophila*

As mentioned earlier on, majority of the embryonic NBs become quiescent at the end of embryogenesis and proliferation is reinstated at the onset of larval development. Similar to embryonic NBs, central brain larval NBs undergo repeated rounds of asymmetric division to maintain the stem cell-like NBs and to generate the

intermediate progenitors, the GMCs. Multiple rounds of NB division produce clonally related populations of neurons and glia. Unlike embryonic NBs, which have a limited self-renewing capacity and become progressively smaller with each round of division, larval central brain NBs grow to their original size at the end of each division and is therefore capable of generating hundreds of daughter cells [136, 156]. This second phase of NB proliferation generates the neurons that make up the bulk of the adult CNS [132]. Larval brain NBs are classified as type I or type II depending on their proliferative characteristics (Figure 1.6). Type I NBs divide repeatedly to produce a series of GMCs that each divides once more to produce two post-mitotic progeny, which differentiate subsequently to two neurons and/or glia cells. Type II NB lineages differ in that the intermediate GMC progenitors, the so-called intermediate neural progenitors (INPs), undergo multiple rounds of asymmetric division to self-renew and produce GMCs that will typically generate two neurons. This transit amplification process produces larger clones from type II NB. Type I NBs are more prevalent in larval central brain while only 8 type II NB lineages per brain lobe, mainly located at the dorsal-medial-posterior region of the central brain, have been identified [133-135]. The difference in type I and type II identities is determined by the differential expression of a subset of transcription factors, which regulate proliferation potential during neurogenesis in these neural progenitor cells [136-138].

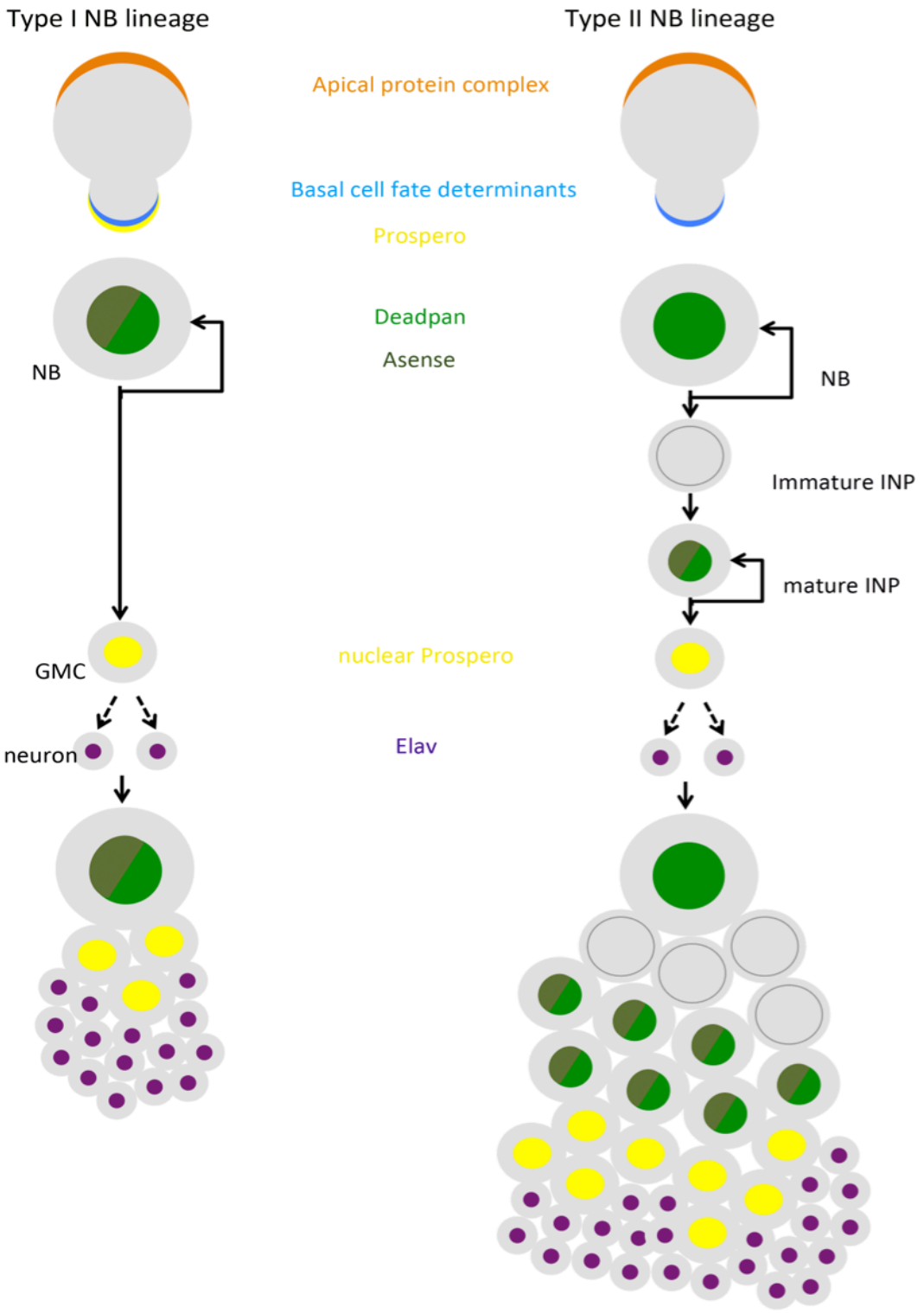

Figure 1.6 Type I and Type II NB lineages in *Drosophila melanogaster*.

During each asymmetric division, a type I NBs divides to produce a larger cell that retains its own identity and one GMC that divides once more to produce two post-mitotic progeny, while a type II NB divides to generate one intermediate neural progenitor (INPs), which divides asymmetrically to self-renew and produce one GMC that generates two neurons. This transit amplification process produces larger clones from type II NB.

1.6 *Drosophila* courtship behavior

Drosophila courtship behavior consists of a series of stereotypical sequence of behavioral steps performed by the males (Figure 1.7). Once a conspecific female is detected, the male quickly orientates towards her abdomen and chases after her as she runs away, extending and vibrating the wing that is nearer to her to generate the so-called courtship song while tapping and licking her genital before curling his abdomen to attempt copulation. Once courtship is initiated, whether to mate or not depends on the female. By contrast, a typical wild-type female makes her decision based on two major factors, whether the male is presenting the species-specific courtship song and whether the male is presenting the proper cocktail of pheromone compounds. If the female is receptive, she will slow down and allow the male to mount (reviewed in [164-165]).

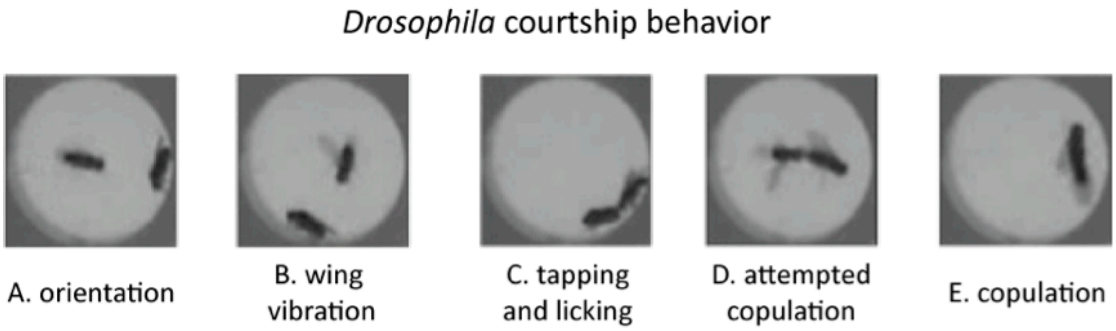

Figure 1.7 *Drosophila melanogaster* courtship behavior.

Video snapshots showing the stereotypical courtship behaviors of the male fly. (A) Abrupt turning of male towards courtship target and circling of male around the target; (B) Unilateral vibration of wing nearest towards the target to generate the species-specific courtship song; (C) Tapping of the target and licking of the target genitalia; (D) Abdominal curling of male to attempt copulation with the target; (E) Mounting of male onto the target to copulate.

1.6.1 Roles of chemical communications in *Drosophila* courtship behavior

Chemical communication between individual *Drosophila* is important for social behaviors required for reproduction and survival, such as courtship and aggression.

With respect to courtship behavior, while it has been shown that *Drosophila* males rely on several chemosensory cues, such as vision, olfaction and gustation, for the initial identification of a potential courtship target, a large body of evidence has suggested pheromonal communication as the forefront signal that induce male courtship behavior [139-142]. Defects in gustatory or olfactory signaling have been shown to hinder male courtship behavior [143, 144]. For examples, males of the *pox neuro* mutants fail to develop gustatory hairs, and as a result, do not court wild-type females in the absence of visual stimuli [145].

Emerging technologies used to characterize chemical signatures have identified key molecules that serve as important chemical cues mediating efficient courtship behavior. Pheromones in *Drosophila melanogaster* are strikingly sexually dimorphic in expression and their effects on male behavior [141, 146]. The vast majority of the cuticular compounds are the hydrocarbons that are synthesized by a set of specialized, segmentally repeated, cells called oenocytes [147] and are presented on the cuticular surface of the abdomen. The pheromone profiles of female flies are largely comprised of *cis, cis*-7, 11-heptacosadiene and *cis, cis*-7, 11-nonacosadiene, both of which are known to serve as aphrodisiacs for male [148]. The cuticular profiles of males consist primarily of hydrocarbons bearing a single double bond (e.g., *cis*-7-tricosene , *cis*-7-pentacosene, and *cis*-9-pentacosene), although these compounds are also produced

by females [149, 150]. Members of the oenocyte-produced pentacosene family can also act as male aphrodisiacs [142, 151].

In addition, *Drosophila* males also produce pheromones in the ejaculatory bulb that are transferred during mating and mediate chemical communication [152, 153]. 11-cis-Vaccenyl-Acetate (cVA), an oxygenated lipid is thought to have an aphrodisiac effect on females, stimulating receptivity towards copulation, and acting as an anti-aphrodisiac on males [141, 143, 154]. CH503 (3-acetoxy-11, 19-octacosadien-1-ol), a second lipid made in the male ejaculatory bulb, also acts as an anti-aphrodisiac for males after being transferred to the female during mating [153, 154].

The blend of chemical signatures present on *Drosophila melanogaster* can be grossly divided into three major functional categories according to their roles in *Drosophila* courtship behavior, namely the ones that confer female appeal, male appeal or male repulsion. Table 1.2 lists the major pheromonal compounds with characterized roles in *Drosophila* courtship behavior.

Table 1.2 Classes of pheromones and their roles in courtship behavior in *Drosophila melanogaster*

Pheromone	Site of Production	Male -> Male Interaction	Male -> Female Interaction	Female -> Male Interaction
7,11-HD	oenocytes	-	-	induces male courtship
7,11-ND	oenocytes	-	-	induces male courtship
7-T	oenocytes	inhibit male-male courtship	promotes female mating	-
7-P	oenocytes	inhibits male-male courtship	unknown	-
9-P	oenocytes	inhibits male-male courtship	unknown	-
cVA	ejaculatory bulb	inhibits male-male courtship	promotes female mating	inhibits courtship *
CH503	ejaculatory bulb	promotes female mating	-	inhibits courtship *

7,11-HD: *cis, cis*-7, 11-heptacosadiene; 7,11-ND: *cis, cis*-7, 11-nonacosadiene;

7-T: *cis*-7-tricosene; 7-P: *cis*-7-pentacosene; 9-P: *cis*-9-pentacosene;

cVA: 11-*cis*-Vaccenyl-Acetate; CH503: 3-acetoxy-11,19-octacosadien-1-ol;

*: compound transferred from male to female during courtship and mating;

-: no known effect

1.6.1.1 The Female Appeal

It has been well believed that the cuticular content of sexually mature virgin female can induce amorous male courtship behavior towards any object that resembles a fly [141]. While *Drosophila* males do not court other mature males, a dummy male that has been stripped off its own cuticular content and 'pasted' with that of a sexually mature virgin female is able to induce courtship behavior from another mature male. Indeed, cuticular hydrocarbon profiling experiments have identified female-specific hydrocarbons, two of the most prominent being *cis, cis*-7, 11-heptacosadiene and *cis, cis*-7, 11-nonacosadiene [148]. Behavior and chemical manipulation experiments have led to the suggestion of these two compounds being the female appeals that act as male aphrodisiacs to turn on male amorous behavior.

However, very recently, it has been shown that females lacking oenocytes, and therefore do not produce any hydrocarbons, are courted upon by wild-type males as much as the latter would towards wild-type females. In fact, such females exhibits a significantly shorter time-to-mating once courtship has been initiated, suggesting that the hydrocarbons present on the females might act as a barrier for mating [147].

1.6.1.2 The Male Appeal

In *Drosophila melanogaster*, once courtship is initiated, whether to mate or not depends on the female. The female makes her decision based on her internal physiological state and the qualities of two major sensory cues she receives from the courting males, that is, the quality of the song made by the wing vibration of the male and the pheromone status of the courtee. Males lacking oenocytes, and therefore do not make any hydrocarbons, take significantly longer time to achieve copulation with

the wild-type females [147], demonstrating the importance of cuticular hydrocarbons for efficient courtship and mating by the males.

A few hydrocarbons have been suggested as male appeals that act as aphrodisiacs for *Drosophila* females. Among them is *cis*-7-tricosene, which has been shown to increase female receptivity. For example, oenocyte-less males that do not express any hydrocarbons are significantly more efficient in achieving copulation when they are painted with synthetic *cis*-7-tricosene [147].

Another chemical that has been implicated as a female aphrodisiac is cVA, a long-chain lipid synthesized by the male ejaculatory bulb. Females that are mutant for *Or67d*, one of the receptors for cVA, are less receptive compared to wild-type females, indicating that activation of the cVA downstream signaling pathway in females is required for female receptivity [154].

1.6.1.3 The Male-Male Repulsion

Sexually mature *Drosophila* males normally do not court other mature males, and this phenomenon is mediated by a group of chemicals that inhibit male-male courtship [155]. Among the compounds implicated in this process are the long-chain hydrocarbons, *cis*-7-tricosene, *cis*-7-pentacosene, and *cis*-9-pentacosene. Males devoid of oenocytes, the cells that make all cuticular hydrocarbons, are courted upon vigorously by other males; and such courtship induction is significantly suppressed when synthetic *cis*-7-tricosene is painted to the target oenocyte-less males, demonstrating the role of *cis*-7-tricosene as a potent male-male courtship inhibitor [147]. By contrast, it has been shown that males of the *Drosophila* subspecies that has higher level of *cis*-7- or 9-pentacosene court males of the subspecies that express

lower of these compounds, indicating a role of these hydrocarbons as potential male courtship inhibitors [142, 151].

Another compound that has been strongly suggested to be potent male-male courtship inhibitor is male-specific lipid, cVA. It has been shown that activation of Or67d, the receptor for cVA, in males reduces courtship behavior towards other males. Males that do not express this receptor show a significantly higher level of courtship towards wild-type males [154]. The observation that the amount of cVA produced by newly born males is negligible and that its production increases as the fly reaches sexual maturity has been suggested to be one of the underlying reasons for the differential level of courtship induction by young and mature males [142].

More recently, using a more sensitive detection method, a novel compound called CH503 has been identified and current studies suggest its role as yet another male anti-aphrodisiac. Similar to cVA, CH503 is made exclusively by the male ejaculatory bulb and transferred to the female during mating and the presence of these compounds in the mated female renders her less attractive to other males. Sexually mature female virgins that have been painted with increasing level of CH503 induce reduced level of courtship activity from wild-type males in a dose-dependent manner as compared to control females. However, unlike cVA which is very highly volatile and therefore do not persist on the mated females for more than 3hrs post mating, CH503 has a higher molecular weight and it remains associated with the mated females up to 10hrs post mating, making it a more potent inhibitor of subsequent mating by other males [153].

1.6.2 Control of courtship behavior and pheromone production by the sex determination pathway

1.6.2.1 *Drosophila* sex determination pathway

In *Drosophila*, somatic sex determination is primarily dependent on the number of sex chromosomes (reviewed in [156]). As shown in Figure 1.8, in diploid XX females, the higher concentration of X-linker signal elements (XSE) activates the early *Sexlethal* (*Sxl*) promoter, giving rise to a spliced form that encodes for a functional early Sxl protein [157]. This early Sxl protein in turn enables the production of a functional late Sxl protein [158]. Positive autoregulation by the late Sxl protein on its own production leads to the maintenance of the female-specific *Sxl* splicing in the late *Sxl* promoter. Expression of the splicing factor Sex-lethal (Sxl^F) in genetically female animals promotes sex specific splicing of the sexually dimorphic *transformer* transcript to produce the female splice form (Tra^F) [159-161]. Tra^F in turn interacts with the non-sex-specific transformer 2 protein (Tra2) which promotes splicing of another sexually dimorphic gene, *doublesex* (*dsx*), resulting in the production of the female form of Doublesex (Dsx^F) [162-165].

In XY male, the low dose of XSE is not sufficient to activate transcription from the early *Sxl* promoter and no early Sxl protein is made. This prevents the establishment of autoregulatory loop for functional late *Sxl* splicing. As a result, the male-specific splicing of *Sxl* mRNA from its late promoter is formed by default, giving rise to a truncated non-functional Sxl protein (Sxl^M). The absence of functional Sxl^F leads to the 'default' splicing of the *tra* mRNA and production of nonfunctional Tra protein, which is expressed non-sex-specifically. In the absence of Tra^F, the default male form of Dsx (Dsx^M) is produced, along with the male form of Fruitless (Fru^M).

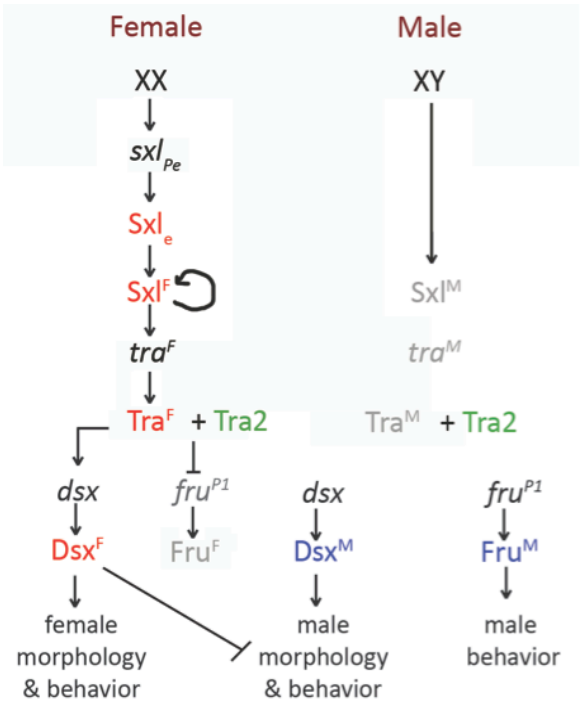

Figure 1.8 The sex determination pathway in *Drosophila melanogaster.*

Shown here are the key components of the sexual differentiation system. Dark grey transcripts are full-lengthed and yield a functional protein. Light grey transcripts contain early in-frame stop condos and give rise to truncated proteins that are nonfunctional. Female-specific functional proteins are in red; male-specific functional proteins are in blue; functional protein that is expressed in both male and female is in green. sxl_{Pe} indicates *sxl* transcript from its early promoter; Sxl_e: early Sxl protein.

1.6.2.2 Control of pheromone production and courtship behavior

Studies in *Drosophila* have shown that sexually dimorphic behavior, including courtship and aggression, and chemical communication is under the control of the sex determination pathway [166-173].

In *Drosophila melanogaster*, genetic experiments have demonstrated the roles of the Dsx proteins, Dsx^M and Dsx^F, in directing male versus female sexual differentiation, including pheromone production [173-176]. Genetic ablation of the *dsx* locus in XX females resulted in failure in the production of all female-specific hydrocarbons, whereas ectopic expression of Dsx^F in XY males caused ectopic production of female-specific diene-hydrocarbons such as *cis*, *cis*-7,11-heptacosadiene and *cis*, *cis*-7,11-nonacosadiene, suggesting that Dsx^F is required in females to ensure the production of female-specific hydrocarbons while suppressing the production of male-specific hydrocarbons and other male-specific pheromones such as cVA [156, 174]. By contrast, genetic ablation that resulted in the loss of the entire *dsx* locus did not affect the production of male-specific pheromones in XY males. However these males express some of the otherwise female-specific hydrocarbons such as *cis*, *cis*-7,11-heptacosadiene. Together, these observations suggest that the *dsx* locus is not required for male pheromone production, but the presence of Dsx^M protein in males ensures that synthesis of female-specific hydrocarbons is suppressed in males [156, 174, 176].

By contrast, the male-specific Fru^M protein is implicated in the control of male sexual behavior but not pheromone production [173, 177, 178]. In the male CNS, Fru^M proteins are expressed from metamorphosis to adult stage [179]. XY males that do

not express the Fru^M proteins perform little to no courtship towards females, generate aberrant courtship song with no pulse song component and never attempt copulation with wild-type females. On the contrary, such males exhibit increased inter-male courtship among their siblings [168, 180]. In contrary, ectopic expression of Fru^M in XX females leads to male-specific courtship behaviors, such as unilateral wing vibration [178]. Together, these observations suggest that Fru^M is necessary for the control of male courtship behavior.

However, the amount of courtship vigor displayed by females with ectopic expression of Fru^M is significantly less than that of wild-type males [204, 207] and the courtship song generated is aberrant, suggesting that Fru^M expression is not sufficient to specify normal male courtship behavior. Other genes are required for a complete male courtship repertoire.

Strikingly, while most research on the functional characterization of the Dsx proteins have been focused on their respective roles in regulating male versus female differentiation including sexually dimorphic pheromone production, an early study examining the courtship behavior of XY males whose *dsx* locus has been genetically ablated, i.e. XY *dsx* males, suggest that the Dsx^M protein could be a potential candidate here. XY *dsx* males are similarly impaired in their courtship vigor and the courtship song generated by those who court is defective [181]. This leads to the hypothesis that Dsx^M is required, in addition to the requirement for the Fru^M proteins, for controlling the full range of male courtship behaviors. Stronger genetics and behavioral evidences have been provided by the recent report by Rideout *et al.* [175]. The authors showed that blocking neuronal function in the cells that endogenously

express the *dsx* transcripts by tetanus neurotoxin light chain expression caused disruptions in the early steps of male courtship behaviors such as orientation and following, and the loss of the later courtship steps such as wing extension, courtship song and attempted copulation. Therefore, there appears to exist a direct and specific contribution of the *dsx* neurons in the control of male courtship behaviors.

Since both Dsx and Fru are under the control of genes more upstream on the sex determination pathway, manipulation of such components of the pathway have also been shown to affect pheromone production and courtship behaviors. For example, genetic feminization of males either by ubiquitous expression of Tra^F or its targeted expression in the adult oenocytes caused feminization of the pheromone compounds produced by otherwise XY males. Such genetically manipulated males displayed abnormal heterosexual courtship behaviors and induced male courtship from other males [182]. Similarly, diploid XX females with hypomorphic alleles for Sxl^F produce high amount of inhibitory, male-specific pheromones and fail to produce the aphrodisiac, female-predominant pheromones. As a result, these females elicit less courtship from mature wild-type males. In addition, a small proportion of these females perform courtship towards other female virgins, suggesting that Sxl^F is required for production of female pheromones and the inhibition of male pheromones production and male courtship behavior [183].

1.7 Outlook – aims and significance of this study

1. While compelling evidence has accumulated that miRNAs are crucial for the various aspects of animal development and function, only a handful of individual miRNAs have been studied functionally *in vivo*. This is largely due to the lack of specific mutants for each miRNA. Therefore, the aim of the global miRNA knockout

project is to generate a miRNA mutant library in *Drosophila melanogaster* so that systematic characterization of each miRNA can be performed *in vivo*.

2. The miRNA, *miR-124*, has attracted considerable interest in the field of miRNA and neurobiology due to its broad conservation and abundant expression in the nervous system throughout the animal kingdom. However, despite an increasing number of reports on its roles in various model organisms, its *in vivo* and physiological roles remain elusive. The aim of the second phase of this thesis is to shed light on the molecular, and ultimately, developmental and functional aspects of the nervous system regulated by *miR-124*, through unbiased and unambiguous characterizations of genetic null mutants of this miRNA.

In the first phase of this thesis, I have made significant improvements to the existing gene targeting strategy in the global *Drosophila* miRNA knockout project, utilizing molecular strategies that increased versatility, scalability and throughput of the method.

In the second phase of the study, I have characterized several phenotypes associated with the *miR-124* genetic null mutants generated using the improved gene targeting strategy. I have used bioinformatics, genetic and molecular biology tools to identity and validate targets of *miR-124* that are functionally important for the roles of this miRNA in neurogenesis and male pheromone production control.

2 Materials and methods

2.1 Molecular work

2.1.1 Recombinant DNA methods

2.1.1.1 Bacterial strains and culture conditions

The *Escherichia coli* strain XL-1 Blue (Agilent) was used for all recombinant DNA procedures unless otherwise stated. For TOPO-TA cloning, TOP10 *E. coli* (Invitrogen) was used. For protein expression in *E. coli*, BL21 Gold chemical competent cell (GE Healthcare) was used. Bacterial strains were cultured in standard Luria-Bertani [LB; 1% (w/v) bacto-tryptone, 0.5% (w/v) yeast extract, 1% (w/v) sodium chloride (NaCl)] broth or grown on agar plates at 37°C. For drug resistance selection in the expression of recombinant plasmids, the culture media was supplemented with the antibiotics ampicillin (100 μg/ml), kanamycin (50μg/ml), or chloroamphenicol (37μg/ml).

2.1.1.2 Preparation of plasmid DNA

QIAprep Miniprep kit (Qiagen) and Plasmid Maxi Kit (Qiagen) were used for small-scale and large-scale preparation of plasmid DNA, according to the manufacturer's instructions, respectively. Plasmid DNA concentration was measured using NanoDrop ND-1000 Spectrophotometer (BioFrontier Technology).

2.1.1.3 Polymerase chain reaction (PCR)

Standard PCR for cloning was performed using the Phusion high-fidelity DNA polymerase (NEB) on a thermocycler (BioRad) according to the manufacturer's protocols, unless otherwise stated. PCR for all the other applications was done with Taq polymerase (TLL home-made).

2.1.1.4 Restriction digestion

Restriction digestion of plasmid DNA was performed using restriction endonucleases (NEB) in accordance with the manufacturer's protocols.

2.1.1.5 Sequencing

Double-stranded DNA sequencing was performed with automatic PCR-based Big-Dye sequencing method. PCR cycling reaction was carried out using the BigDye Terminator v3.1Cycle sequencing kit (Applied Biosystems) in the presence of 100ng of template DNA and 200uM of oligo with the following cycling conditions: 25 cycles of 94°C for 2min,50°C for 30 sec,60°C for 4 min, 60°C for 10min. The reactions were subsequently analyzed using the 3730x1 DNA Analyser (Applied Biosystems; in-house service provided by TLL or IMCB).

2.1.2 Bacterial transformation

Standard chemical transformation by heatshock was used in all bacterial transformations. Briefly, competent cells were thawed on ice and mixed with an appropriate volume of plasmid DNA and incubated on ice for 15min. The mixture was then heatshocked at 42°C using a waterbath for 45sec and placed immediately on ice for 2min. The cells were allowed to recover for 1h in the presence of 1ml of LB without antibiotics in a 37°C shaker at 250rpm. The cells were then plated on LB agar supplemented with the appropriate antibiotics at 37°C overnight.

2.1.3 General cloning strategy

2.1.3.1 Conventional cloning

All DNA fragments, including PCR and restriction digestion products, used in all cloning reaction were isolated using standard agarose gel electrophoresis and recovered from the gel using QIAquick gel extraction kit according to the

manufacturer's protocol (Qiagen). Where necessary, vectors were treated with Calf intestinal phosphatase (NEB) prior to gel electrophoresis, following the manufacturer's instructions. Ligation reaction was set up with a vector:insert molar ratio of 3:1 in the presence of 2U T4 DNA ligase (NEB) and incubated at room temperature for 30min. Typically, half of the ligation volume was used for subsequent bacterial transformation.

2.1.3.2 TOPO TA cloning

Since the Phusion DNA polymerase produces blunt-end PCR products, A-tailing was performed by incubating the purified PCR product with 0.1nM dATP and 3U of Taq polymerase (TLL home-made) at 72°C for 20min.

For TA cloning, the TOPO TA pCRII vector (Invitrogen) and A-tailed insert DNA fragment were mixed in the molar ratio of 1:3 and incubated in the presence of TOPO salt solution for 5min at room temperature. About half of the ligation reaction was used for bacterial transformation. Positive recombinant clones were identified using blue-white selection on LB plate supplemented with 5-bromo-4-chloro-3-indolyl-β-D-galactoside (X-Gal) at 80 μg/ml.

2.1.4 Cloning of constructs used in this study

2.1.4.1 Gene-targeting vectors

Modifications to the existing gene-targeting vector, pW25, were made to incorporate different genetic manipulation elements.

2.1.4.1.1 pW25-RMCE

For the generation of pW25-RMCE targeting vector, a 221-bp fragment for the phage attachment site (attP) was PCR amplified from the pTA-attP plasmid using primer pair 5' GGTACCTCGCGCTCGCGCGACTGACG 3' and 5' GGCGCGCCTGCAG GTACTGACGGACACACCGAA 3', and inverted attP fragments were cloned into *Kpn*I and *Asc*I sites upstream and downstream of the *mini-white* sequence, respectively, in pW25 vector.

2.1.4.1.2 pW25-attB and pW25-Gal4-attB1

For the generation of pW25-attB and pW25-Gal4-attB1 vectors, a 285-bp fragment containing the bacterial phage attachment site (attB) was PCR amplified from the pAT-attB plasmid using primer pair 5' CATATGGTCGACGATGTAGGTCACG 3' and 5' CATATGGTCGACATGCCCGCCGTG 3', and cloned into the *NdeI* site in pW25 and pW25-Gal4 vector backbones respectively.

2.1.4.1.3 pW25-Gal4-attB2

For the generation of the pW25-Gal4-atttB2 vector, the *Gal4* coding sequence was cloned between the 5' *loxP* site and *mini-white* sequence by composite cloning using pW25-attB as the vector backbone. The primer pairs used in the composite cloning were listed in Table 2.1. The primer pairs used were designed to introduce the restriction enzyme sites for *Pac*I and *Fse*I to the multiple cloning sites at the 5' and 3'-end respectively to facilitate directional cloning of 'homology arms'.

Table 2.1 Sequences (5'->3') of primer pairs used in pW25-Gal4-attB2 composite cloning.

Primer	Sequence
p[KpnI_loxP_6bp linker_GAL4(22bp)_F]	GGTACCCATAACTTCGTATAATGTATG CTATACGAAGTTATCATGCCATGAAGC TACTGTCTTCTATC
p[7bplinker_GAL4(22bp)_R]	GTCATGACGGATCCACCAAATAATAA GAC
p[GAL4(11bp)_7bp linker_HSP70(20bp)_F]	TGGTGGATCCGTCATGACCCGTTATTC TCTATTCGTTT
p[AflII_mini-white_R]	CTTAAGATGTATGCACATGTACTACTC A

2.1.4.2 Gene-targeting constructs for KO generation

2.1.4.2.1 Gene-targeting constructs for global miRNA KO project

For the generation of most of the gene-targeting constructs in the global miRNA knockout project, about 2.5-4kb homology sequences flanking the miRNA of interest were cloned into the selected vector using one of the multiple cloning sites depicted in the vector maps.

DNA for the homology arms was amplified from wild-type Oregon R genomic DNA by PCR using Phusion High-Fidelity DNA Polymerase. PCR products were run on agarose gels to confirm their sizes and DNA recovered by standard gel extraction procedures. The PCR fragments were cloned by the TOPO TA cloning strategy depicted in 2.1.3.2. Positive TOPO clones were then sequenced to check for mutations that might have occurred during the PCR amplification step and the clone without any mutations was then selected for subsequent cloning. Single nucleotide polymorphisms that might have been present in the lab strain used as template genomic DNA was differentiated from PCR-induced mutation errors by comparing the sequences of independent PCR reaction using batches of wild-type genomic DNA.

Nucleotide deviations from the reference genome that were consistent among independent PCR sequences were regarded as true polymorphisms in the lab strain and clones with such deviations accepted for subsequent cloning.

Flanking homology fragments were cloned into the selected targeting vector using standard cloning strategy depicted in 2.1.3.1. The ends of both flanking homology arms in the final gene-targeting construct were sequenced using oligos that recognize the vector ends of the multiple cloning sites to confirm the orientation of the insertions.

2.1.4.2.2 Gene-targeting constructs for *miR-124*

Three independent gene-targeting constructs were made for *miR-124*, using the pW25, pW25-Gal4 and pW25-RMCE vectors. The sets of flanking homology fragments used in the three constructs were similar but not identical and the sequences of the primers used for PCR amplifications of these fragments were listed in Table 2.2.

Table 2.2 Sequences (5'->3') of primer pairs used for *miR-124* KO constructs generation.

Primer	Sequence
miR-124_5'_NotI_F	GCGGCCGCAGAGGACAGATGGGTTTTTGAA
miR-124_5'_NotI_R	GCGGCCGCCGAGAATATCCTTGACCGAATC
miR-124_3'_SbfI_F	CCTGCAGGGTGGAATCATTGTAACCAACAAAAA
miR-124_3'_SbfI_R2	CCTGCAGGGCCGTTCATTAAGATAAAAGGAGA
miR-124_3'_AscI_F	GGCGCGCCGTGGAATCATTGTAACCAACAAAAA
miR-124_3'_AscI_R	GGCGCGCCGCCGTTCATTAAGATAAAAGGAGA

2.1.4.3 UAS constructs

The *UAS-miR-124* lines were made by cloning a 250 base pair genomic fragment containing the miRNA hairpin into the 3'UTR of dsRed in pUAST, as described in [184].

2.1.4.4 UTR reporter constructs

The *ana* 3'UTR and *tra* 3' UTR luciferase reporters were made by cloning, respectively, the 900bp *ana* 3'UTR, 989bp *tra-RB* 3'UTR and 320bp *tra-RA 3'UTR* after luciferase, under the control of the tubulin promoter [185]. *ana* 3' UTR reporter with mutated *miR-124* sites was generated by PCR using primers designed to change the seed region from GTGCCTT into GTACATG. The *tra* 3'UTR reporter mutant was generated by overlapping PCR that deleted a 20nt sequence, 5' UAUUUACAUUCGUGUGUUUU 3', containing the first *miR-124* target site. PCR products were verified by sequencing. The primers used to amplify all the other UTR reporters used in this study were listed in Table 2.3.

Table 2.3 Sequences (5'->3') of primers used in cloning of UTR reporters.

Primer	Sequence
ana_3'UTR_XbaI_wt	GATCGCGTGGTAATTCTAGAAAGCAGGAATAGATGCCACAAT
ana_3'UTR_XhoI_wt	GTGGTATGGCTGATTATGATCTAGCTCGAGAGGTTGCCAATCGTAATTCTGT
ana_3'UTR_mut_up_R	AGATTTAGCAGACATGTACTTTAAACCTAG
ana_3'UTR_mut_dn_F	AATAAGTCACTAGGTTTAAAGTACATGTCTG
tra_RB-3'UTR_XbaI_wt	ACCGTCTAGAGAAGCTAGGACAATAGGACTCTCAA
tra_RB-3'UTR_XhoI_wt	ACCGCTCGAGACCATGAGTGTATGTGTAAATGTGC
tra_RA-3'UTR_XbaI_wt	ACCGTCTAGACATATTGAACATACTCCATTCGACA
tra_RA-3'UTR_XhoI_wt	ACCGCTCGAGCTCGAAACCATGAGTGTATGTGTAA

2.1.4.5 RMCE-related constructs

The piB-miR-124 plasmid was generated by replacing the GFP reporter in piB-GFP [15] with a 430bp genomic fragment containing the miRNA hairpin in the center, using the *Sal*I and *BamH*I restriction enzyme sites. The primer pair used to amplify the genomic fragment was p[piB-miR-124_F_*Sal*I]: 5' ACCGTCGACAGGATATTCTCGCCATTGGATA 3' and p[piB-miR-124_R_*BamH*I]: 5' ACCGGATCCTGAAAGCTTTTACGGTTTAGCA 3'.

2.1.5 Genomic DNA preparation from fly tissues

2.1.5.1 Small-scale genomic DNA extraction

Small-scale genomic DNA was prepared by mashing 1-10 flies in 50µl of ice-cold squishing buffer [10 mM Tris pH8.0, 25 mM NaCl, 1 mM EDTA, and 200 µg/ml freshly diluted proteinase K (Sigma)] for 5-10sec with a pipette tip. The buffer containing fly debris was incubated at 37°C for 30min, followed by inactivation at 95°C for 2min and stored at 4°C or -20°C for further use.

2.1.5.2 Large-scale genomic DNA extraction

Large-scale genomic DNA extraction was performed using the DNaeasy blood and tissue kit (Qiagen) following the manufacturer's protocols. Approximately 20 flies, snap-frozen in liquid nitrogen, were used in each extraction unless otherwise stated.

2.1.6 Molecular verification of loss of miRNA in knockout mutants

2.1.6.1 PCR verification of heterozygous mutants

Verification of heterozygous mutants was done through the molecular confirmation of the presence of the *mini-white* reporter at the targeted locus. Genomic DNA was extracted from about 15-20 heterozygous adult flies following the method depicted in

section 2.1.5.2. PCR was performed using the oligo Pflank, which recognizes the flanking genomic region located outside the homology arm, and another oligo Pwhite, which recognizes the *mini-white* marker, as depicted in Figure 2.1. The pair of oligos was designed to amplify a fragment of about 4kb. Two sets of oligos were designed for each locus so that amplification at both ends of the *mini-white* gene was confirmed.

Figure 2.1 Illustration of primer design in molecular verification of heterozygous mutants.

A forward primer (Pflank_F) in the flanking region located outside the homology arm is paired with a reverse primer (Pwhite_R) in the *mini-white* sequence for amplification of left homology arm. Similarly for the right arm, a forward primer (Pwhite_F) in the *mini-white* sequence and a reverse primer (Pflank_R) in the flanking region located outside the homology region are used for amplification.

2.1.6.2 PCR verification of homozygous mutants

Viable homozygous mutants were verified molecularly by the absence of the targeted miRNA loci. Single fly genomic DNA was extracted following the protocol of small-scale genomic DNA extraction protocol depicted in section 2.1.5.1. PCR was performed using a pair of oligos that recognize sequences within the targeted locus, as illustrated in Figure 2.2.

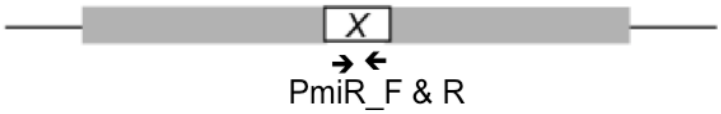

Figure 2.2 Illustration of primer design in molecular verification of viable homozygous targeted mutants.

A pair of primers (PmiR_F and PmiR_R) recognizing sequences in the deleted region results in a small amplicon in wild-type or heterozygous mutants but not in homozygous mutant flies.

2.1.7 RNA extraction

Total RNA was extracted using TRlzol® Reagent with Phase Lock Gel Heavy (Qiagen). Briefly, fly tissues used for total RNA extraction were snap frozen in liquid nitrogen and homogenized in 0.2ml TRIzol reagent using a pellet pestle with a cordless motor (Sigma-Aldrich). After homogenization, 0.8ml of TRIzol Reagent was added to top up the total volume of the TRIzol to 1ml and the total cell lysate added to eppendorf tubes containing pre-spun Phase Lock Gel-Heavy. After a 5min room temperature incubation, 0.2ml of chloroform per 1ml TRIzol Reagent was added and the mixture shaken vigorously for 15sec before being centrifuged at 12,000g for 10min at 4°C. The aqueous phase containing total RNA was then decanted into fresh

eppendorf tubes and total RNA precipitated by adding 0.5ml isopropyl alcohol per 1ml of TRIzole Reagent used. The mixture was then mixed thoroughly by repeated inversions and allowed to incubate at room temperature for 10min, after which, the sample was centrifuged at 12,000g for 10min at 4°C. The RNA pellets obtained were then washed twice in 1ml of 75% ethanol and allowed to air dry at room temperature for about 5min and dissolved in appropriate volume of DEPC-treated water.

For RNA extracted for subsequent reverse transcription and quantification using real-time rtPCR, the total RNA sample extracted was further purified using the RNeasy kit and treated with on-column DNase treatment for 60min (Qiagen) to eliminate DNA contamination, following the manufacturer's protocols. RNA concentration was estimated using a NanoDrop ND-1000 Spectrophotometer (BioFrontier Technology) and standardized by adjusting with DEPC-treated water.

2.1.8 Reverse transcription (RT)

Reverse transcription was done with 1-10μg of DNase-treated total RNA using oligo(dT)15 and Superscript III reverse transcriptase (Invitrogen) following the manufacturer's protocol. A negative control reaction without reverse transcriptase was prepared for each RNA sample. The newly synthesized first strand DNA was normalized and checked for genomic DNA contamination by performing PCR with *actin42A* and *rp49* primers.

2.1.9 Quantitative PCR

2.1.9.1 mRNA RT-qPCR

Quantitative real-time PCR was performed using the SYBR green system (Applied Biosystems) in an ABI7500 real time thermal cycler (Applied Biosystems) following

the manufacturer's protocol. Measurements were normalized to *actin42A* or *rp49* mRNA.

All RT-qPCR primers were designed using the web-based Primer3 program (http://frodo.wi.mit.edu/primer3). The optimal parameters were set as follows: primer length 24nt, product length 80-250nt, annealing temperature 60°C, GC content 50%, no predicted primer dimers. The sequences of the primer pairs used are listed in Table 2.4.

Table 2.4 Sequences (5'->3') of primer pairs used in qRT-PCR.

Primer	Sequence
rp49_F	AATTATGCATTAGTGGGACACCTT
rp49_R	CATCAGATACTGTCCCTTGAAGC
actin 42A_F	GCTTCGCTGTCTACTTTCCA
actin 42A_R	CAGCCCGACTACTGCTTAGA
ana_F	ATGGAGCGTTTACCGAACAG
ana_R	ATCGTGGGTGAGTTGGATGT
tra^F_F	GGAACCCAGCATCGAGATTC
tra^F_R	ATCGCCCATGGTATTCTCTTTC
tra^M_F	GCGCCAAACACTATGCGTTA
tra^M_R	GAGCCACGGGAATCTATGTGA
dsx^F_F	TCAACACGTTCGCATCACAAA
dsx^F_R	TAGACTGTGATTAGCCCAAT

2.1.9.2 miRNA RT-qPCR

For miRNA qRT-PCR, 20ng of total RNA extracted directly by TRIzol® Reagent with Phase Lock Gel Heavy (Qiagen) was used for reverse transcription. Primer sets designed to amplify mature *miR-124* were obtained from Applied Biosystems. Mature *miR-124* levels were calculated relative to reference genes snoR442 and 2S rRNA (Applied Biosystems), after having confirmed that the levels of these two small RNAs remain constant in the relevant fly strains.

2.2 Fly genetics

2.2.1 Fly husbandry and stocks

Drosophila melanogaster stocks were maintained on standard yeast-cornmeal-agar medium (1.2% agar, 1.8% dry yeast, 1% soy flour, 2.2% turnip syrup, 8% malt extract, 8% corn powder, 0.24% methyl-4-hydroxybenzoate) at 25°C unless otherwise stated. Canton-S (CS) flies were used as the wild-type control, unless otherwise specified. w^{1118} flies were used cases when w^- control flies were required. Balancer flies used for general fly genetic crosses were *FM6, If/CyO* and *TM2/TM6B* for first, second and third chromosome respectively. Fly stocks generated/used for different purposes were listed in tables or descriptions under each section.

2.2.2 Generation of transgenic flies

All transgenic flies generated in this study were listed in Table 2.5.

Table 2.5 Transgenic flies generated in this work.

Strain	Source/Creator	Description
miR-124$^{\Delta 4}$	J.S. Karres	miR-124 knock-out allele
miR-124$^{\Delta 177}$	R. Weng	miR-124 knock-out allele (RMCE)
miR-124$^{\Delta 177\text{-RMCE}}$	R. Weng	miR-124 RMCE-rescued allele
UAS-miR-124	N. Bushati	Transgene expressing miR-124
miR-124-Gal4	N. Bushati	Gal4 under control of miR-124 promoter
Fluc-ana 3'UTR	R. Weng	Fluc reporter transgene
Fluc-ana 3'UTR mut	R. Weng	Fluc reporter transgene
GFP-ana 3'UTR	R. Weng	GFP reporter transgene
GFP-ana 3'UTR mut	R. Weng	GFP reporter transgene
Fluc-tra 3'UTR-1	R. Weng	Fluc reporter transgene
Fluc-tra 3'UTR-1 mut	R. Weng	Fluc reporter transgene
Fluc-tra 3'UTR-2	R. Weng	Fluc reporter transgene

2.2.2.1 Strategies used for transgenesis

Transgenes were inserted into the *Drosophila* genome using either the *P* transposable element system or the *ϕC31* integrase.

For *P*-element-based transformation, the *P*-element ends present in the respective (pCaSpeR4, pW25 and pUAST plasmids) vectors flank the transgene and its regulatory regions. Plasmids were injected into blastoderm embryos expressing the *P*-element transposase, *delta 2-3*, (Kah-Junn Tan, TLL, and Genetic Services, Inc.), which lead to a random but stable integration of the transgene into the germline genome.

For *ϕC31* integrase-mediated transformation, transgenic constructs were injected into blastoderm embryos expressing germ cell-specific *ϕC31* integrase and the bacterial phage-landing site, the *att*P site, on desired chromosomal position. The following landing sites were used in this study. Landing site on chromosome *2* with *ϕC31* integrase on *X* chromosome: y^{1}, *M{vas-int.Dm}*[186]*ZH-2A*, *w**; *M{3xP3-RFP.attP'}ZH-22A*, landing site on chromosome *2*: y^{1}, w^{67c23}; $P\{y^{+t7.7}$ = *CaryP}attP16,* landing site on chromosome *3* with *ϕC31* integrase on chromosome *4*: y^{1}, *w**; *M{3xP3-RFP.attP}ZH-86Fb*; *M{vas-int.B}ZH-102D*, and landing site on chromosome *3*: y^{1}, w^{67c23}; $P\{y^{+t7.7}$ = *CaryP}attP2.*

The *mini-white* reporter gene was used as a selection marker in both strategies. Emerging injected animals were crossed to appropriate balancer flies and their progeny screened for the presence of the transgene based on the expression of the *mini-white* gene in the eyes. For *P*-element-based transposition, red-eyed flies were

crossed to balancer flies and the transgene mapped to a specific chromosome. For *ϕC31* integrase-based transposition, red-eyed progeny was stocked by crossing to balancers to the targeted chromosome.

2.2.2.2 Generation of fly mutants by ends-out homologous recombination

Gene targeting by ends-out homologous recombination was carried out as previously described. The constructs used for gene targeting were made as depicted in 2.1.4.2. The fly strains used in the general gene targeting strategy were obtained from Bloomington Stock Centre and are listed in Table 2.6.

Table 2.6 Fly strains used in gene targeting

Strain	Description
w1118	Mutant strain for white locus for detecting transgenes with the mini-white reporter by eye color
y^1, w*, lethal/FM6	Balancer stock for chromosome X
w*; Kr $^{If-1}$, Slbo-lacZ(1310)/CyO	Balancer stock for chromosome 2
w*; TM3, Sb, Ser/TM6B, Tb	Balancer stock for chromosome 3
w*; Bl/CyO; TM2, Ubx/TM6B, Tb	Double-balancer stock used for chromosome mapping
y1, M{vas-int.Dm}ZH-2A, w*; M{3xP3-RFP.attP'}ZH-22A	Site-specific landing strain used for integrase-mediated transformation with landing site on chromosome 2 and *ϕC31* integrase on X chromosome
y^1, w*; M{3xP3-RFP.attP}ZH-86Fb; M{vas-int.B}ZH-102D	Site-specific landing strain used for integrase-mediated transformation with landing site on chromosome 3 and *ϕC31* integrase on chromosome 4
y^1, w^{67c23}; P{$y^{+t7.7}$ = CaryP}attP2	landing site on chromosome 3
y^1,w^{67c23}; P{$y^{+t7.7}$ = CaryP}attP16	landing site on chromosome 2
y^1, w*; P{$ry^{+t7.2}$ = 70FLP}11, P{$v^{+t1.8}$ = 70I-SceI}2B, nocSco/CyO, S2	Strain providing expression of FLP recombinase and *I-SceI* endonuclease with FLP and *I-SceI* on chromosome 2
y1, w*; P{$ry^{+t7.2}$ = 70FLP}23, P{$v^{+t1.8}$ = 70I-SceI}4A/TM6, Ubx	Strain providing expression of FLP recombinase and *I-SceI* endonuclease: FLP and *I-SceI* on chromosome 3
w*; Kr^{If-1}, Slbo-lacZ(1310)/CyO; hs-Cre^{w+}/TM3, Ser	Strain providing expression of *Cre* recombinase: *Cre* on chromosome 3
w*, hs- Cre^{w+}/FM6; Sb/TM3, Ser	Strain providing expression of *Cre* recombinase: *Cre* on chromosome X
y^1, M{3xP3-RFP.attP}ZH-2A, w*; +; +; M{eGFP.vas-int.B} ZH-102D	*ϕC31* integrase on chromosome 4 which is used for RMCE

2.2.2.2.1 Generation of transgenic donor lines

The introduction of the gene-targeting construct into the fly genome was the first step in a typical gene targeting strategy. As depicted in 2.2.2, different approaches can be used to get these transgenic "donor" flies, depending on the choice of vector. For the constructs generated using gene-targeting vectors that do not carry the *attB* site, conventional *P*-element-mediated transgenesis was used. In such cases, the insertions were mapped, using the strategy depicted in 2.2.2, to determine on which chromosome they were located before the crosses for the targeting event. A balanced stock for each insertion was then established and one to two independent insertions, preferentially not on the same chromosome as the targeted miRNA, were then selected for subsequent homologous recombination.

2.2.2.2.2 Gene targeting by homologous recombination

Several genetic crosses were involved in a typical gene-targeting strategy adopted in this study and an example of crossing scheme is provided in Figure 2.3

The donor construct was mobilized from its integration site by crossing 3–5 males of the 'donor' transgenic flies to 15–20 virgin females of the transgenic flies that express the FLP recombinase and the *I-SceI* endonuclease, under the control of a heatshock promoter. Concurrent induction of both enzymes was done by heatshocking the 24hr AEL embryos of this cross at 38°C for 1hr. The cross was flipped every 24hrs for 1 week to collect sufficient embryos for heatshock induction.

Emerging female adult flies carrying mosaic pattern of white and pigmented ommatidia in the eyes, depicting the excision of the 'donor' DNA carrying the *white* marker, were crossed to males from a suitable balancer stock, with a *white*$^{-}$

background. Typically, 400 independent crosses were set up to ensure a reasonable likelihood of success for homologous recombination.

Candidates carrying the expected targeting event were then selected as progeny with *white*$^{+}$ eyes in the next generation. Normally only male progeny was selected in this step, and typically, only one male was selected from each cross unless males with different eye colors were found in the same vial. In such cases, independent crosses were set up for each male. The candidates were then crossed to female virgins of chromosome balancer stock. Chromosomal mapping for the *white*$^{+}$ transgene was performed to ensure that targeting event has taken place at the expected chromosome.

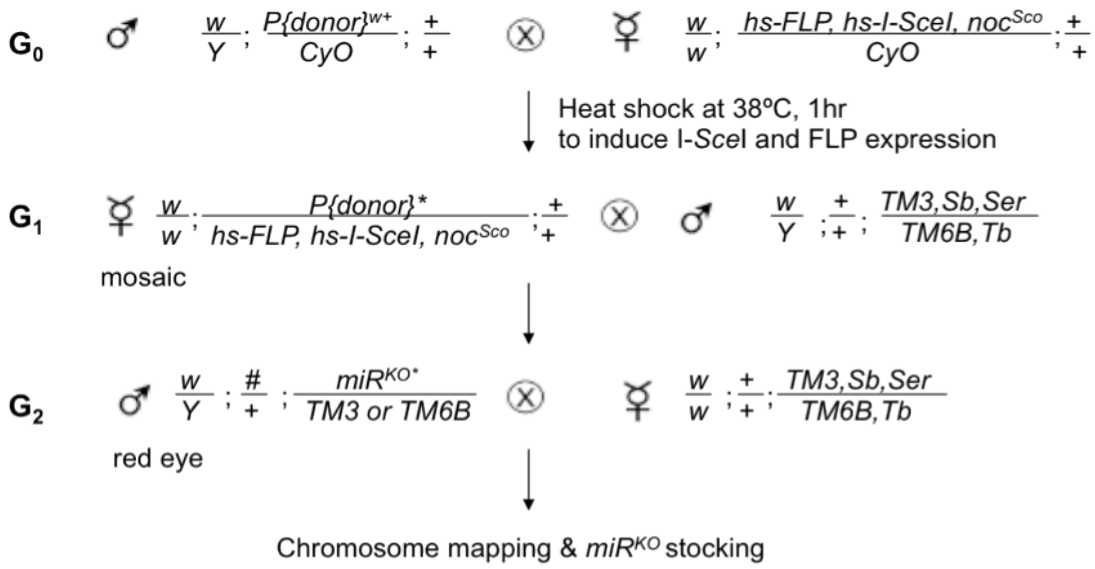

Figure 2.3 Illustration of genetic crosses in ends-out gene targeting for a gene on chromosome 3.

Donor flies are crossed to *hs-FLP,hs-I-SceI* flies. Set up 10 crosses and flip them every day to a new tube for 5 consecutive days. Heat shock tubes on the third day at 38°C for 1 hour. Next generation, set up 400 crosses of individual female with mosaic eyes to balancer males. Screen for red eye males at G_2 generation. Red eye flies are further crossed to balancer flies to determine which chromosome it is on by marker segregation.

2.2.2.3 Cassette exchange by RMCE

The steps involved in the induction of cassette exchange by RMCE are outlined in Figure 2.4. Briefly, flies carrying the locus to be retargeted by RMCE were crossed to flies expressing *φC31* integrase in the germ line. Microinjection was done to introduce the donor *att*B plasmid into the resulting embryos containing the integrase. The adult flies that have emerged from these injected embryos were crossed individually to a *white* mutant strain, w^{1118} to allow identification of flies from which the *mini-white* marker was successfully excised. Putative RMCE candidates were screened by the loss of eye pigment. Individual candidate RMCE event was crossed to appropriate balancer flies to establish balanced stocks. The RMCE candidates were then verified individually by PCR. Candidates with the RMCE cassette inserted in the expected orientation were kept for subsequent experiments while at least one candidate with the reverse orientation of cassette integration was kept as a control. PCR design to screen for orientation for cassette integration is illustrated in Figure 2.4.

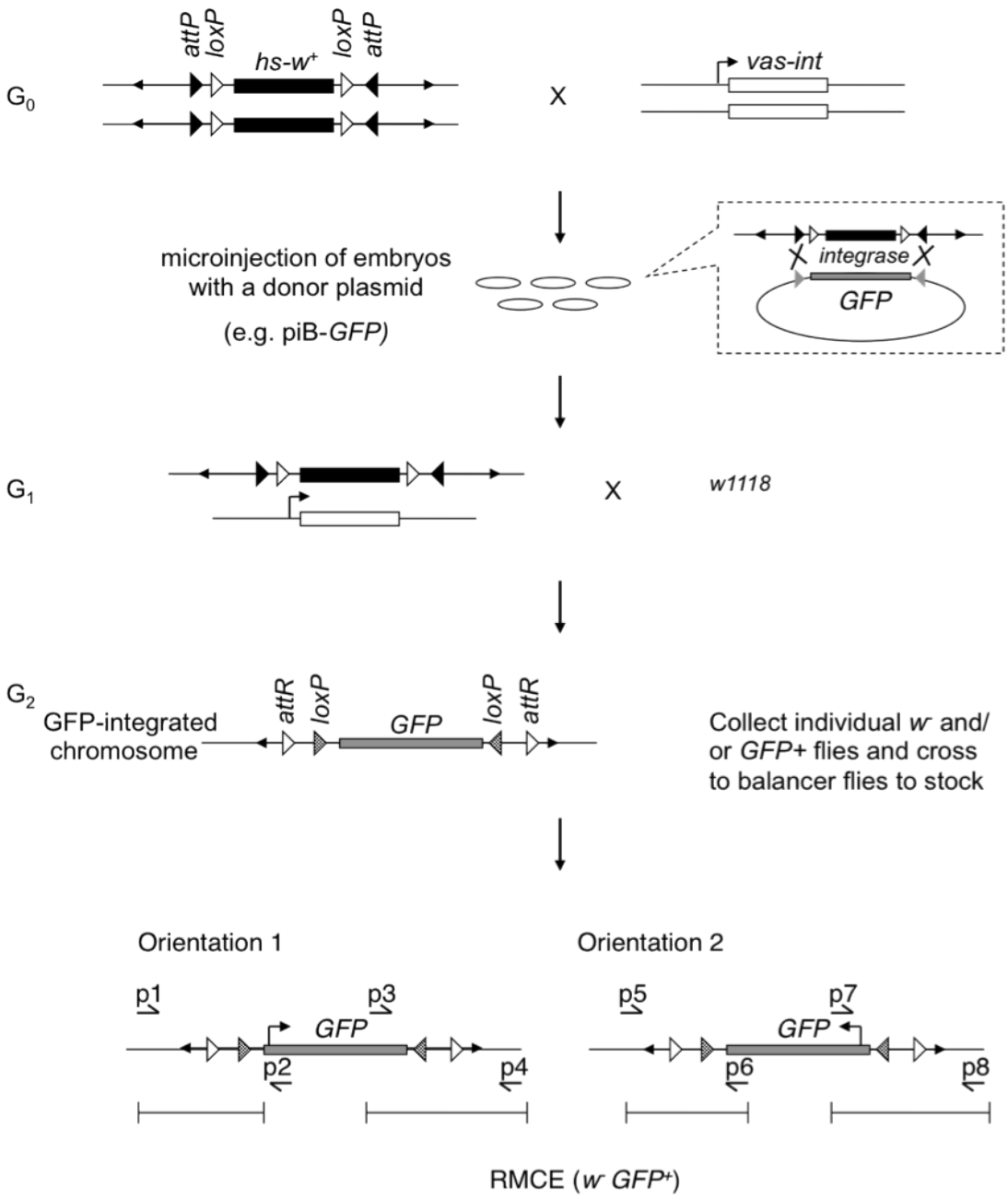

Figure 2.4 Illustration of cassette exchange strategy by RMCE.

Flies carrying the targeted locus, marked by *mini-white*, are crossed to transgenic flies expressing *φC31* integrase. Embryos obtained from this cross are injected with a donor plasmid expressing genetic sequence of interest flanked by inverted *attB* sites, such as piB-GFP donor plasmid, which expresses *GFP*. Double crossover between the two *attP* and *attB* sites would lead to a clean exchange of *mini-white* by *GFP*. Emerging adults are mated individually with w^{1118} partners and putative RMCE events were identified by the loss of *mini-white* expression in the eyes. Molecular genotyping by PCR is used to determine the orientation of *GFP* insertion.

2.2.2.4 Removal of *mini-white* marker by *Cre* recombinase

There are two scenarios in which removal of the *mini-white* marker in the targeted mutants is essential. The first case involves mutants for miRNAs located in the introns of protein-coding genes while the second concerns miRNA mutants used in behavioral analysis. In both cases, the *mini-white* marker was removed by the expression of the *Cre* recombinase following the scheme depicted in Figure 2.5.

Briefly, flies carrying the targeted allele were crossed to transgenic flies expressing the *cre* recombinase, whose expression was controlled by an upstream heat shock promoter. Induction of *Cre* expression was done by a 10 minutes heat shock of the first instar larvae from this cross at 37°C(i.e. at 24-48 hours AEL).

Male mosaic flies with partial to complete loss of eye pigmentation indicating the excision of *mini-white* marker were collected and crossed with balancer flies. A balanced stock for the desired progeny with white eyes from this cross was established by backcrossing to an appropriately marked balancer strain.

The excision of the complete cassette and the loss of the miRNA sequences were confirmed by molecular verification using the PCR strategy described in section 2.1.6.

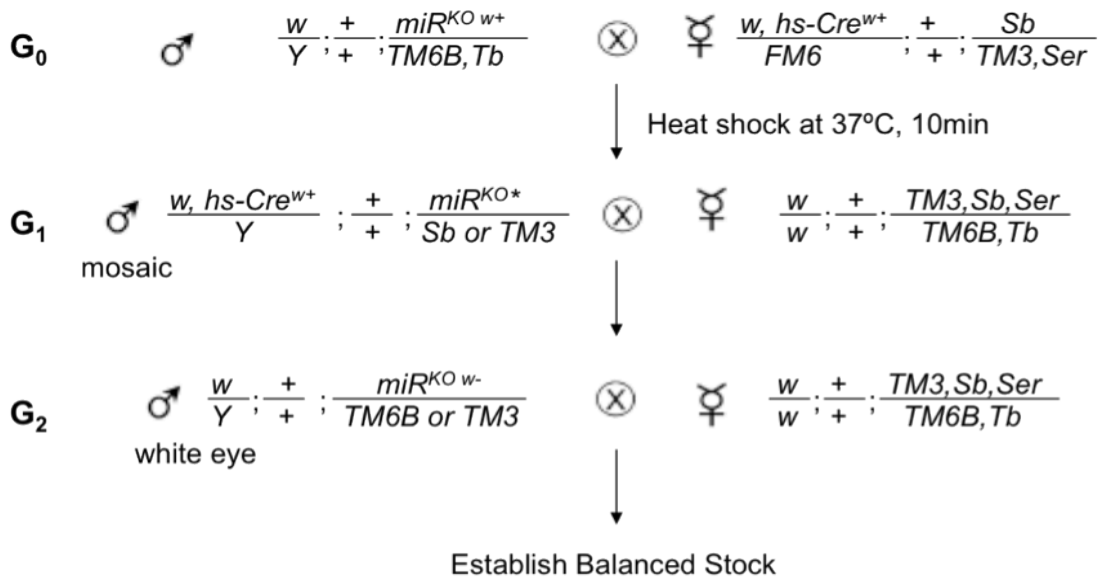

Figure 2.5 Illustration of a genetic cross for the removal of *mini-white* in miRNA KO flies by *Cre* recombinase.

Shown here is an example of miRNA knockout mutant ($miR^{KO\ w+}$) on chromosome *3*, using an *X* chromosome source of *hs-Cre*. Knockout flies are crossed to flies carrying $hs\text{-}Cre^{w+}$, which is also marked by red eye. Next generation, select males with mosaic eyes on an orange background, and cross them to balancer flies individually. In G_2 generation, white-eye males are selected for crosses and stocking.

2.3 Viability test

F_0 adult flies were collected and aged in groups of 20-30 flies per vial for 3 days. 60 F_0 female virgins and 40 males were crossed on apple juice plate with fresh yeast paste. The cages and apple juice plate were changed every day for 3 days. Embryos used for viability test were collected at 4hrs interval on the 4th day and newly hatched L1 larvae were collected about 24hrs later and seeded on the surface of food vial in groups of 20. Multiple vials were prepared to ensure sufficient number of progeny could be scored. The total number of progeny for each genotype, identified by the presence or absence of GFP, reaching the late L3, early pupae, pupae and adult stage was recorded and the percentage of each genotype at each stage was calculated.

2.4 Fertility test

Single 5-day old CS or *miR-124* mutant male was paired with two 5-day old CS female virgins overnight with the adults being transferred to a fresh vial 24hrs post pairing. The first vials with the eggs laid on the surface were kept under standard fly culture conditions. The cross that resulted in viable progeny was scored as fertile and the number of such crosses was recorded. The total number of pupae obtained from each fertile cross was recorded.

2.5 Cell Transfection And Luciferase Assays

S2 cells were transfected in 24-well plates with 250ng of miRNA expression plasmid or empty vector, 25ng of firefly luciferase reporter plasmid, and 25ng of Renilla luciferase DNA as a transfection control. Transfections were performed in triplicate in at least three independent experiments. At 60hrs after transfection, Dual luciferase assays (Promega) were performed according to the manufacturer's instruction. For luciferase assays on larval CNS, tissues were dissected and immediately lysed in passive lysis buffer (Promega). Luciferase activity was normalized to total protein content, measured on the same sample using the Bradford method (Bio-Rad).

2.6 TU tagging

TU tagging was performed as described [187], with the following modification. Larvae of the indicated genotypes were collected in groups of 20 at 72hrs ALH, transferred to food vials with 4-TU containing yeast paste at 29°C for 16hrs before CNS dissection.

2.7 MARCM analysis

MARCM clonal analysis was done according to the general strategy reported previously [188] with the following modifications. Embryos were collected over a 4hrs time window, and subjected to a 60min heat shock treatment at 37°C at 0hr ALH and a second heat shock treatment of 60min at 37°C at 24hr ALH for all experiments unless otherwise specified. The treated L1 larvae were cultured on fresh yeast paste added to the surface of standard food vial at 18°C until dissection. Unless otherwise stated, all larvae were dissected and processed for immuno-histology analysis at late wandering third larval stage. The genotypes of the stocks used for the clonal analysis were listed in Table 2.7.

Table 2.7 Fly strains used in MARCM clonal analysis

Strain	Description
hsFLP, elav-Gal4, UAS-mCD8::GFP; FRT40A, tubP-Gal80/Cyo	MARCM ready stock
w*; P[ry^{+} neo FRT]40A / w*; P[ry^{+} neo FRT]40A	Stock for wild-type clone generation
w*; P[ry^{+} neo FRT]40A, miR-124$^{\Delta 177,w+}$ /Cyo	Stock for *miR-124* mutant clone generation
w*; P[ry^{+} neo FRT]40A, miR-124$^{\Delta 177,w+}$ /Cyo; UAS-miR-124	Stock for *miR-124* clonal rescue
w*; P[ry^{+} neo FRT]40A, miR-124$^{\Delta 177,w+}$, ana^{1} / Cyo	Stock for *ana* functional rescue; ana^{1}: Bloomington Stock 8926
w*; P[ry^{+} neo FRT]40A, miR-124$^{\Delta 177,w+}$ /Cyo; UAS-ana[RNAi]	Stock for *ana* functional rescue; UAS-ana[RNAi]:Bloomington Stock 27515
w*; P[ry^{+} neo FRT]40A / w*; P[ry^{+} neo FRT]40A; UAS-ana / TM6B	Stock for clonal ana overexpression; UAS-ana: Bloomington Stock 22173

2.8 Immunocytochemistry and imaging

Larval CNS tissues were dissected and fixed in 4% formaldehyde in PBS with 0.1% Triton-X100 for 20min on ice. DNA stain used was DAPI (Sigma). Samples were mounted in Vectashield (Vector Laboratories). Quantification of mitotic neuroblasts was done using projections of confocal sections.

Primary antibodies used were rat anti-ELAV (Developmental Studies Hybridoma Bank), 1:50; mouse anti-Pros (Developmental Studies Hybridoma Bank), 1:50; mouse anti-Repo (Developmental Studies Hybridoma Bank), 1:50; mouse anti-Mira (Developmental Studies Hybridoma Bank), 1:20; guinea pig anti-Deadpan (J. Skeath), 1:2000; chicken anti-GFP (Abcam), 1:3000; rabbit anti-Pon (Y.N. Jan), 1:500; rabbit anti-Ase (Y.N. Jan), 1:1000; rabbit anti-Phospho-histone H3 (Cell Signalling), 1:300; chicken anti-β-gal (Abcam), 1:2000.

Secondary antibodies were conjugated to either Alexa Fluor 405, Alexa Fluor 488, Alexa Fluor 555, or Alexa Fluor 633 (Invitrogen), and used at 1:500, 1:1000 and 1:300 respectively. DNA stain used was DAPI (Sigma), 1:2000 and samples were mounted in Vectashield (Vectashield, Innovative Biotech Pte Ltd).

2.9 Fluorescent *in situ* hybridization

The *miR-124* locked nucleic acid probe was from Exiqon. Anti-DIG-POD primary antibody (1:200) was used and detected using the Tyramide Signal Amplification kit (cyanine 3) from Perkin Elmer following standard protocols.

2.10 Behavior Assays

In all courtship assays performed, test flies were collected at late pupal stage and aged individually to 5-day-old in standard food vial; target flies were collected at late pupal

stage and aged to 5-day-old in groups of 20 flies per vial. Flies used for aggression assay were collected at late pupal stage and aged individually to 5-day-old in standard food vial. All behavioral assays were performed between 2-4hrs before lights off, at 25°C, 60% relative humidity under normal ambient light, unless otherwise stated. All fly behavior movies were recorded using a Sony Camcorder, unless otherwise mentioned.

2.10.1 Male-female courtship assay

The male-female courtship assay was carried out in a round chamber of 10mm diameter and 4mm height as described previously [178]. 5-day-old Canton-S virgin females served as mating targets. 5-day-old socially naïve males of Canton-S, *miR-124* mutants or *miR-124*^{RMCE} rescue flies serve as test flies. Courtship behavior was videotaped for 45 min after a virgin female and a test male were introduced into the courtship chamber by gentle aspiration.

2.10.2 Female Receptivity Assay

Male-female courtship assays were carried out in a round chamber of 10mm diameter and 4mm height as described previously [178]. 5-day-old socially naïve Canton-S males were paired individually with either 5-day-old Canton-S or 5-day-old *miR-124* virgin females. Courtship behavior was videotaped for 45 min after fly pairing. The percentage of females that accepted copulation by CS males was recorded for each genotype.

2.10.3 Male-male courtship assay

Test and target males were collected and aged as above. On the day of the experiment, target males were briefly anesthetized on ice and decapitated with a razor blade before being introduced into round chambers of 10mm diameter and 4mm height.

Individual intact test male was gently aspirated into the chamber containing a decapitated target and the courtship behavior, if any, of the test males recorded for 45min.

2.10.4 Female choice assay

Round chambers of 10mm diameter and 4mm height were used for the mating competition assay. Mutants and wild-type male flies were collected at late pupal stage and isolated in standard food vials. On the fourth day post eclosion, mutants and controls were anaesthetized briefly and marked with acrylic paint at the back of the thorax. On the fifth day, a mutant and a wild type with different colors were introduced into a courtship chamber containing a Canton-S virgin female and were videotaped for 70min. The percentage of copulation success for both mutants and controls was measured.

2.10.5 Aggression assay

The size of the fighting chamber was 14mm in diameter and 10mm in height. A food patch was introduced by pipetting 50ul of melted standard fly food in the center of the chamber and allowed to solidified at RT.

In the aggression assay, pairs of socially naïve 5-day-old male flies were aspirated gently into the fighting chamber. Behaviors were recorded for the next 45min. Experimental and control groups were taped simultaneously under the same camera.

Fighting behavior of male flies was measured using two indices: latency and frequency. Latency measures the number of encounters between the fly pair from introduction of the males into the chambers until the initiation of the first agonistic

encounter. Frequency describes the number of fighting behaviors, including lunging and fencing, over the first 30 minutes of observation.

2.10.6 Locomotion assay

5-day-old socially naïve CS or *miR-124* mutant males were individually aspirated into the courtship chamber used for the male-female courtship assay as described above. The activity of the fly was videotaped for 15min by a Sony Camcorder and analyzed by ImageJ (Rasband WS. ImageJ, U.S. National Institutes of Health, Bethesda, Maryland, USA, imagej.nih.gov/ij/, 1997—2012). Locomotion was defined as the velocity of the fly in the first 10min of observation.

2.11 Cuticular hydrocarbon extraction

Flies used for CHC extraction were raised in the same conditions as the ones used for behavior assays. Flies were aged in groups of 15-20 flies per vial. Three replicates of 15 five-day-old male flies were briefly anaesthetized on ice and placed into 1.8mL glass microvials with Teflon caps (s/n 224740; Wheaton). 120µl of hexane containing 10µg/mL of hexacosane (Sigma-Aldrich) standard was added into each vial and incubated at room temperature for 20min. 100µl of the solvent was then transferred into a new vial and evaporated under a gentle stream of nitrogen under a chemical hood, leaving the compounds coating the surface of the bottom. Extracts were stored at –20°C and redissolved in 30µL of heptane prior to GC/MS analysis.

2.12 Analysis of cuticular hydrocarbon profiles

2.12.1 Gas chromatography–mass spectrometry (GC-MS) analysis of cuticular hydrocarbon profiles

Extracts were redissolved in 60µL of hexane and transferred into GC-MS vials (Supelco). Analysis was run in a 5% phenyl-methylpolysiloxane (DB-5, 30m length, 0.32 i.d., 0.25µm film thickness, Agilent) column and GCMS QP2010 system (Shimadzu) with an initial column temperature of 50°C for 2min and increased to 300°C at a rate of 15°C/min in splitless mode. The relative signal intensity for each hydrocarbon species was calculated by dividing the area under the chromatography peak by the total area under all of the peaks. The values from 3-6 replicate measurements were averaged.

2.12.2 Analysis of perfumed flies using Direct Analysis in Real Time Mass Spectrometry (DART MS)

The atmospheric pressure ionization time-of-flight mass spectrometer (AccuTOF-DART™, JEOL USA, Inc.) was equipped with a DART interface and operated in positive-ion mode at a resolving power of 6000 (FWHM definition). Mass accuracy is within ±15ppm. The DART interface was operated using the following settings: the gas heater was set to 200°C, the glow discharge needle was set at 3.5kV. Electrode 1 was set to +150 V and electrode 2 was set to +250 V. He_2 gas flow was set to 2.5 L/min. Under these conditions, mostly protonated ($[M+H]^+$) molecules are observed. Using clean forceps, an anaesthetized fly was picked up by both wings, making sure not to damage the fly. The fly was placed in a stream of charged helium gas until peaks of triacylglycerides start to appear. All fly samples were placed approximately in the same location in the DART source for the same amount of time in order to obtain reproducible spectra. 6 flies of each genotype were measured. Polyethylene

glycol (Sigma-Aldrich) was used as the calibrant. Relative quantification of compound abundance was performed by normalizing the areas under the signals corresponding to cVA ($[M+H]^+$ 311.29) and CH503 ($[M+H]^+$ 465.43) to the tricosene signal ($[M+H]^+$ 323.36). DART MS is unable to differentiate isoforms of tricosene therefore the tricosene signal represents the summed signal intensity from 5, 7, and 9-Tricosene. Tricosene was selected as the normalization peak due to the unaltered levels in mutants compared to CS controls in GC-MS.

2.12.3 Analysis of cuticular hydrocarbon extracts using DART MS

CHC extractions from groups of 15 flies were performed as described above and stored on ice. Immediately before DART anaylsis, 30µl of hexane was added into prepared extracts and vortexed briefly and gently. Vials were placed on ice before sampling. Borosilate glass capillaries (World Precision Instruments, Inc) were used for sampling, placing a finger over the end of the capillary to prevent uptake of solvent. The capillary was placed in the DART stream for 5secs. Six technical replicates from the same vial were performed using new capillaries and placing the capillaries in approximately the same position each time. Relative quantification of compound abundance was performed as mentioned in the above section.

2.13 Pheromone perfuming

For application of synthetic compounds to target flies, 9µg of synthetic cVA (Cayman Chemical Company Ann Arbor, Michigan, USA) was diluted in 200µL of hexane and introduced into a 1.8-mL glass microvial. The hexane was evaporated under a gentle flow of nitrogen, leaving the compound as a residue coating the bottom of the vial. Flies were briefly anaesthetized on ice, transferred to coated vials in groups of seven, and subjected to three vortex pulses lasting 20secs each, with 10secs pauses between each pulse. The perfumed flies were allowed to recover for about 1hr in fresh vials

with standard food. Six flies from each group were used for behavioral tests and the remaining fly was subjected to hydrocarbon analysis by Direct Analysis in Real Time mass spectrometry (DART-MS) to monitor effective transfer of the test compound to the flies.

2.14 Statistics

Statistical analysis of experimental data was done using either paired or unpaired 2-tailed Student t-test, unless otherwise stated. Statistical analysis for behavior assays and hydrocarbon quantification was done using Prism 4 (GraphPad Software). For behavioral data, a nonparametric Mann-Whitney test was used to compare two samples while Kruskal-Wallis test followed by Dunn's post-test was used to compare multiple samples. For hydrocarbon analysis, a multi-way ANOVA followed by Tukey HSD post-test was performed.

3 RESULTS

3.1 Establishment of a *Drosophila* miRNA mutant library

Rigorous investigation in the past 10 years or so has shown that the miRNA machinery is involved in many biological phenomena, particularly those associated with dynamic cellular and/or developmental processes such as embryonic development. To perform a global study of the *in vivo* functions of miRNAs in *Drosophila melanogastor*, a few members of the lab and I have initiated a global knockout project targeting many of the *Drosophila* miRNAs. The aim was to establish a comprehensive *Drosophila* miRNA mutant library, which would allow a global survey of miRNA functions using assays specific to biological processes of interest in the lab.

At the time when I joined the project, there were all together 152 miRNAs discovered in *Drosophila melanogaster* by a combined effort of deep sequencing and computational prediction. Of these 152, no Northern blot evidence was obtained for four miRNAs while the sequences of 21 miRNA genes were not conserved among the 12 *Drosophila* species. Therefore, the initial phase of the global miRNA project aimed to create a mutant library for the remaining 127 miRNAs that are conserved at least among the different *Drosophila* species. Of the 127 miRNAs chosen, mutants covering 33 miRNAs had already been made in the lab or by others. Therefore, the remaining 94 miRNAs were targeted for the first phase of the global miRNA project (overviewed in Figure 3.1).

During the course of this study, the number of miRNAs in *Drosophila melanogaster,* together with many other model organisms, has expanded tremendously thanks to improvements in the methods used in miRNA identification. At the time of writing of this thesis, miRBase [189] has reported a total of 426 mature miRNAs. Some miRNA genes are clustered on a single genetic locus and transcribed as one pre-miRNA transcript. Additionally, some miRNAs can make two distinct gene products if transcripts from both the 5' and 3' strands are produced. Therefore, these 426 mature miRNAs are processed from 238 pre-miRNAs, representing 238 individual genetic loci encoding miRNAs. Some of these have been incorporated into the mutant library project subsequently. Nevertheless, these will not be mentioned in this thesis.

A strategy using ends-out gene targeting via homologous recombination was used for the generation of targeted miRNA null mutants, as outlined in Figure 1.2. This gene targeting strategy allows the production of targeted deletions to make loss of function mutations. More specifically, straightforward sequence replacement with modified variants, for example epitope-tagged coding sequence, can be achieved using the "ends-out" homologous recombination approach [10, 12].

As the project progressed, improvements were made to the ends-out gene targeting strategy to increase the efficiency of the method. As a result, different gene-targeting vectors were used for the generation of the miRNA mutants at different stages of the project. This will be highlighted again in the next section when results from the improved gene targeting strategy are presented.

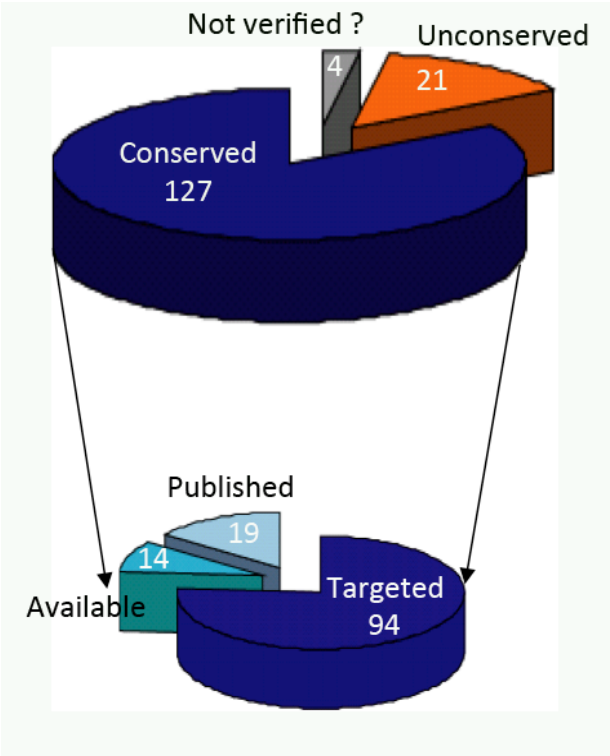

Figure 3.1 Overview of global miRNA KO project.

At the time when I joined the KO project, 152 miRNAs have been discovered in *Drosophila melanogaster*. Among these, deep sequencing findings for 4 miRNAs were not confirmed by Northern Blot while the sequences of 21 miRNAs were not even conserved among the 12 *Drosophila* species. Therefore, only the remaining 127 miRNAs were included for the first phase of the project. Of these 127, mutants for 33 miRNAs have either been published or were available. Thus, this phase of the KO project aimed to generate mutants for the remaining 94 miRNAs.

3.1.1 Improvements of the existing ends-out gene targeting vectors

As the global mutagenesis project demands a great deal of time and effort, it is important to optimize the mutant generation pipeline, particularly the gene targeting strategy used in the generation of the miRNA mutants. Furthermore, since the ultimate aim of the project was to perform a systematic study of miRNA functions *in vivo*, it is also crucial that the strategy should also allow flexible genetic manipulation of the mutants for phenotypic characterization. Therefore, my initial goal was to optimize the existing gene targeting strategy used in the miRNA knockout project.

A major drawback of the existing homologous recombination-based gene targeting vectors was that none of these vectors has the capacity to allow repeated targeting of a single locus for the creation of variant alleles. Each targeted genetic variant requires starting with a new targeting vector. In addition, the frequency of successful gene targeting events varies, ranging from 1 in 200 to 1 in 350,000, depending on factors such as the size of the deletion or the targeting locus [177, 190]. Therefore, my aim was to design a series of gene-targeting vectors to improve the versatility, scalability and throughput of the current gene targeting strategy.

3.1.1.1 Adopting the RMCE strategy to improve versatility of gene targeting

To improve the versatility of the gene-targeting vector, I made use of the bacteriophage φC31 integrase-mediated cassette exchange strategy. Recombinase-mediated cassette exchange (RMCE) allows directional site-specific recombination between a plasmid ‘donor cassette’ and a chromosomal ‘acceptor cassette’, resulting in the replacement of the target cassette at frequencies of 5-20% [15]. To add this capability to the gene-targeting repertoire, I introduced an acceptor cassette into

pW25 by flanking *mini-white* with inverted *attP* sites (pW25-RMCE; Figure 3.2). Successful gene targeting with this vector would lead to the specific replacement of the targeted locus by the *mini-white* marker. The inverted *attP* sites flanking the *mini-white* gene in the pW25-RMCE vector would then serve as chromosomal 'acceptor' sites to allow for subsequent RMCE events. Exchange of the acceptor cassette would allow replacement of the *mini-white* marker at the targeted locus with any desired sequence.

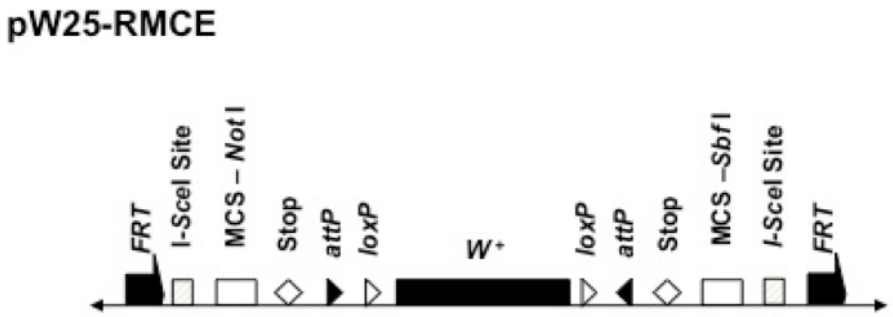

Figure 3.2 Schematic showing the pW25-RMCE ends-out gene-targeting vector.

A 221-bp fragment for the phage attachment site (*attP*, denoted by black triangles,) was PCR amplified from the pTA-*attP* plasmid and inverted *attP* fragments were cloned into *Kpn*I and *Asc*I site upstream and downstream of the *mini-white* sequence respectively.

3.1.1.1.1 Demonstration of site-specific integration via RMCE

To test the versatility of the RMCE system for subsequent genetic manipulation on the mutant, I knocked out the *Drosophila* miRNA *miR-31b* by ends-out homologous recombination with a construct based on pW25-RMCE. *miR-31b* is located in the second intron of the protein coding gene *CG01962*. Targeted knockout of *miR-31b* introduced the *mini-white* reporter into the intron of *CG01962* (Figure 3.3A). I verified the replacement both by the gain of *mini-white* expression in the eyes and by the use of quantitative RT-PCR, which confirmed the loss of the miRNA mature transcript in the mutant (Figure 3.3B).

To enable cassette exchange, I injected embryos obtained from a cross between flies carrying the targeted *miR-31b* locus and those expressing φC31 integrase [191] with the piB-*GFP* donor plasmid, in which *GFP* is flanked by inverted *attB* sites [15]. When the injected animals reached adulthood, I crossed them individually with w^{1118} partners and identified putative RMCE events by the loss of *mini-white* expression in the eyes. To determine the orientation of *GFP* insertion, I performed molecular genotyping by standard PCR (Figure 3.3C). In two separate trials, I observed an efficiency of ~25% of injected embryos with successful RMCE events, with 50% of events having the GFP reporter inserted in the same transcriptional orientation as *miR-31b*.

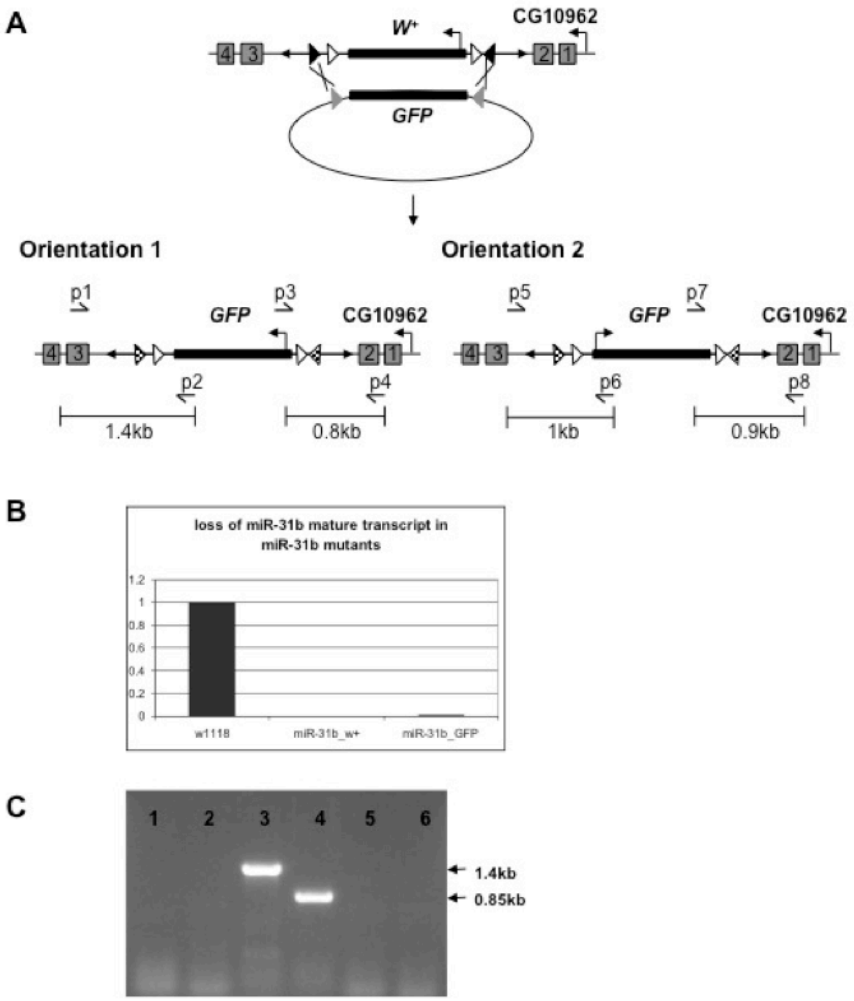

Figure 3.3 Site-specific integration via φC31 integrase-mediated RMCE.

(A) Schematic representation of the targeting event replacing miR-31b with *mini-white*, flanked by *att*P and *lox*P, in the intron of CG10962. Exchange of *mini-white* with *GFP* by cross-over between the two inverted *attP* and *attB* sites leads to clean exchange of *mini-white* by *GFP*, resulting in new *attR* site, denoted by checkered triangles. RMCE can occur in both orientations. Primer pairs (arrows) were designed to distinguish the two outcomes. (B) Quantitative miRNA PCR to measure the level of miR-31b in total RNA from control flies (w^{1118}), mutants carrying the *mini-white* targeted allele ($miR\text{-}31^{w+}$) and mutants carrying the GFP replacement allele ($miR\text{-}31^{GFP}$). (C) Determination of orientation of GFP insertion by PCR genotyping. Absence of GFP in orientation 2 (lane 1 and 2: failure to amplify with primer pairs p5/p6 and p7/p8); presence of GFP in orientation 1 (lanes 3 and 4: the product amplified by primer pairs p1/p2 and p3/p4); demonstration of the specificity of primer pairs p1/p2 and p3/p4 using initial *mini-white*-containing mutant genomic DNA as the template.

3.1.1.1.2 Demonstration of other utilities of RMCE

Another problem with the existing ends-out gene-targeting vectors was the potential for disruption of proper splicing of the targeted locus. This can occur because the *mini-white* reporter is a shortened genomic version of the *white* gene that contains introns [192]. As a result, mini-white can serve as a 'gene trap' when located in an intron (illustrated in Figure 3.4A). The potential for mis-splicing is a concern in the generation of mutants for intronic miRNAs. However, this could be resolved by replacing the *mini-white* sequence with an intronless reporter such as coding sequence of the GFP reporter using the RMCE strategy.

To demonstrate the utility of the RMCE strategy in the 'curing' of such a gene trap generated by the *mini-white* marker, I checked the splicing pattern of the host gene of *miR-31b*. The *Drosophila miR-31b* gene is located in the second intron of the gene CG10962. In the wild-type chromosome, endogenous splicing of the four exons of CG10962 results in a functional transcript (Figure 3.4A, A' and D). However, flies homozygous for the *miR-31b* allele with the *mini-white* cassette showed reduced levels of correctly spliced *CG01962* transcript (Figure 3.4B, B' and D). Exchanging the *mini-white* locus with intron-less GFP restored *CG01962* mRNA levels (Figure 3.4C, C' and D). This example illustrates the utility of RMCE to produce an intronic mutant with minimal disruption of the flanking locus.

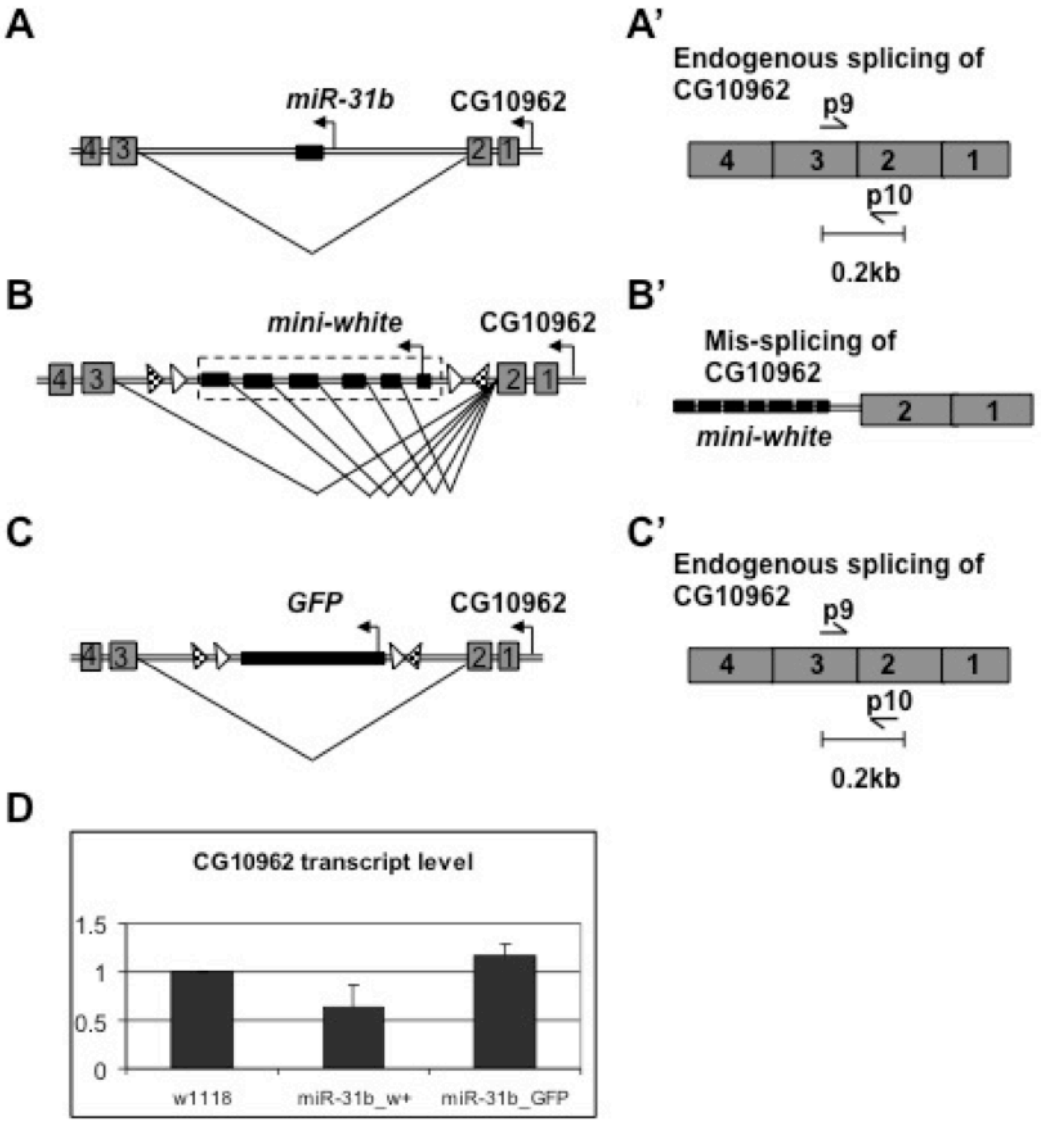

Figure 3.4 The 'curing' of a gene trap by the use of RMCE.

(A-C') Illustration of possible splicing patterns of CG10962 in various *miR-31b* mutants. (A) *CG10962-RA* has 4 exons, denoted by grey boxes 1-4. *miR-31b* is present in the second intron. (A') Endogenous splicing of CG10962 results in a functional transcript consists of exon 1 to 4. (B) The *mini-white* marker in the targeting vector contains introns and exons of the *white* locus and could interfere with splicing of *CG10962*, resulting in mis-splicing of this host gene (B'). (C) Replacement of *mini-white* with an intron-less GFP cassette restores the endogenous splicing of CG10962 (C'). Primers p9/p10 amplify a product spanning the exon2 and exon3 junction (A' and C') and can be used in quantitative RT-PCR to measure the efficiency of removal of intron 2 using total RNA from flies with the respective genotypes (D).

3.1.1.2 Improvements to increase scalability and throughput of gene-targeting

Yet another problem associated with the existing ends-out gene targeting vectors was that the production of the initial donor fly relies on conventional *P*-element mediated transformation. The use of two 2.5-3.5kb homology fragments in the generation of a gene-targeting construct unavoidably results in a relatively large plasmid, usually about 17-18kb. This reduces the efficiency of genetic transformation by microinjection of the KO plasmid. In addition, since the conventional *P*-element mediated transformation results in random insertion of the KO plasmid, additional genetic crosses are required to map the chromosomal insertion site, lengthening the gene targeting procedure. Therefore, one of the bottlenecks was to obtain a suitable donor fly to initiate gene targeting.

To improve the efficiency of donor transgenic strain generation, I again made use of the φC31 integrase-mediated site-specific transformation. To implement this modification, I cloned the *attB* site into the backbone of pW25 (pW25-*attB*, Figure 3.5A). Injection of targeting constructs in this vector into embryos expressing φC31 integrase and containing the bacterial phage-landing site, *attP*, at a known genomic location (e.g. [191]) would result in the insertion of the transgene at the desired chromosomal locus, which would greatly facilitate the crossing schemes needed for targeting.

One point worth mentioning, though, is that the use of φC31 integrase-mediated site-specific transformation to obtain the initial donor flies means that the RMCE strategy could not be used to allow cassette exchange at the targeted locus. Therefore, use of

the pW25-*attB* vector increases the overall throughput of the gene targeting strategy, at the cost of forgoing the versatility provided by RMCE retargeting.

To optimize for both scalability and versatility, I decided to incorporate the UAS/GAL4 system to the pw25-*attB* vector. This would allow the use of Gal4 at the targeted locus as a driver for miRNA expression study or for genetic manipulations.

Two versions were made. In the first case, I cloned the *attB* site into the backbone of pW25-*Gal4* vector generated by Dr. Natascha Bushati, a former member of the lab. In this vector, the *Gal4-VP16* sequence was upstream of the *lox*P site in pW25-*attB* (pW25-*Gal4-attB*1, Figure 3.5B). Targeting with this vector would produce alleles that direct *Gal4* expression from the endogenous regulatory elements at the targeted locus. However, since *Gal4* is upstream of the *lox*P site, it would not be possible to remove the *Gal4* sequence once the initial KO mutant was generated. Again, this would create some kind of the 'gene trapping' problem similar to *mini-white* should the targeted miRNA locus was located in the intron of some host gene. To overcome this problem, I made a second modification by introducing the *Gal4* sequence in between the 5'-*lox*P site and *mini-white* gene (pW25-*Gal4-attB*2, Figure 3.5C). This would then allow removal of *Gal4* with *mini-white* by the *Cre-lox*P recombinase system, resulting in a 'clean' knock out.

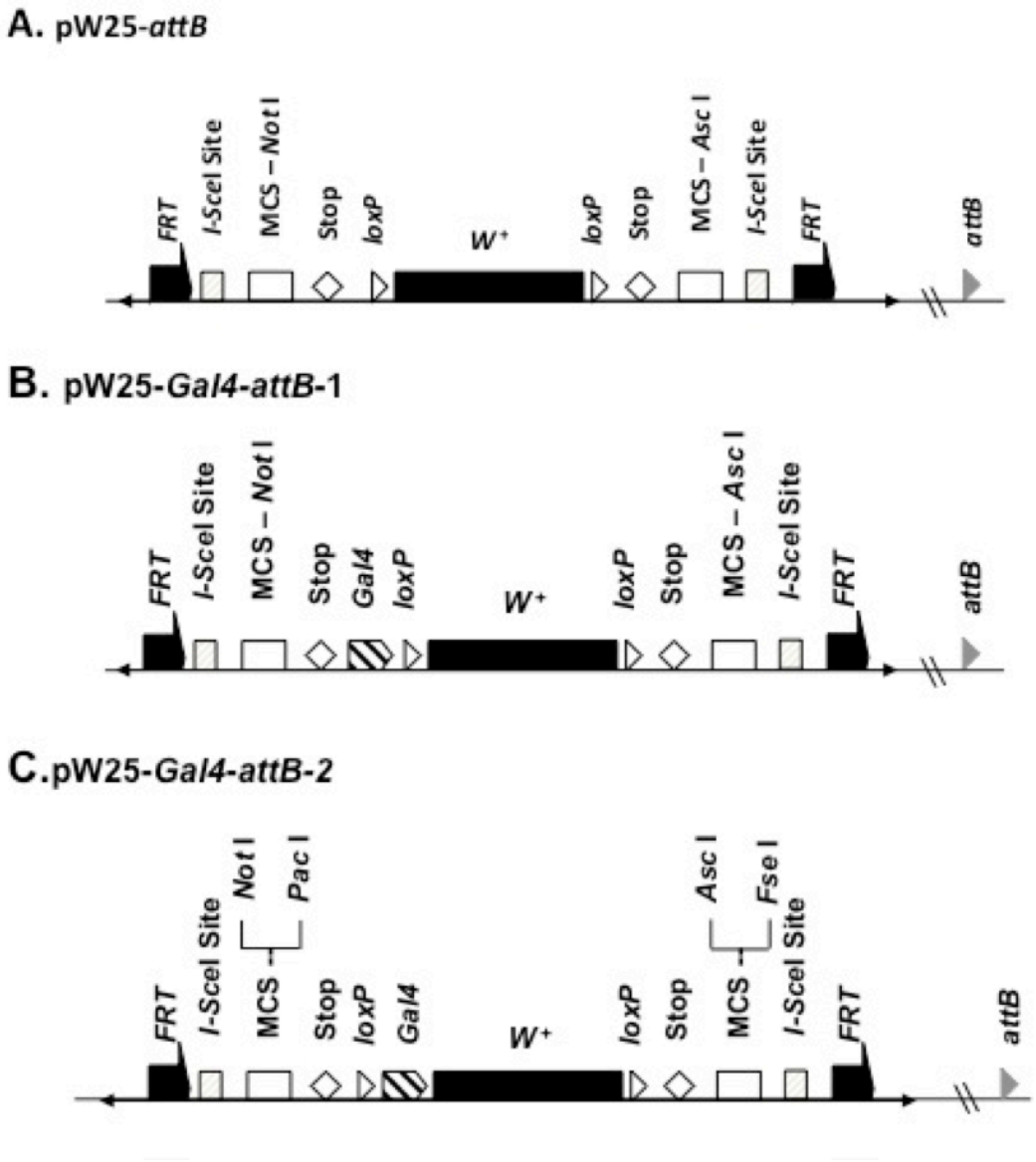

Figure 3.5 Schematics showing pW25-*attB* and pW25-*Gal4-attB1* and pW25-*Gal4-attB2* ends-out gene targeting vectors.

(A) pW25-*attB* and (B) pW25-*Gal4-attB1* vector. A 285-bp fragment containing the bacterial phage attachment site (attB, denoted by gray triangles) was cloned into pW25 and pW25-*Gal4* vector backbones at the NdeI site. (C) pW25-*Gal4-attB2* vector. The *Gal4* coding sequence was cloned between the 5' *loxP* site and *mini-white* by composite cloning using pW25-attB as the vector backbone. This allows removal of *Gal4* driver together with *mini-white* marker using the Cre-LoxP recombinase system. Restriction enzyme sites for *Pac*I and *Fse*I were introduced to the multiple cloning sites at the 5' and 3'-end respectively to facilitate directional cloning of 'homology arms'.

3.2 Characterization of *Drosophila miR-124* functions

3.2.1 Characterization of *miR-124* expression

3.2.1.1 *miR-124* expression in the developing nervous system

Previous studies using *in situ hybridization* and tissue-specific sequencing approaches have shown that *miR-124* is expressed in the CNS from early embryonic stages to adulthood in *Drosophila melanogaster* [37, 193]. To further characterize the neuronal expression pattern of *miR-124*, I have used several genetic and molecular means, including the use of a *miR-124* promoter-driven GFP reporter, fluorescent *in situ* hybridization analysis and *miR-124* nuclear GFP sensor characterization in this study.

3.2.1.1.1 *miR-124* expression following *miR-124-GFP* reporter expression

As a first approach, I used a 4.7 kb genomic region upstream of the *miR-124* locus, likely covering the promoter region for *miR-124* expression, to drive expression of a GFP reporter using the GAL4/UAS system [194]. (Figure 3.6A). In the developing embryonic CNS, this reporter showed GFP expression in both the embryonic brain and ventral nerve cord (VNC) (Figure 3.6B, C as reported earlier [37]. Using markers for the various cell types within the CNS, I observed co-expression of *miR-124-GFP* with neuroblast (NB) markers, such as the transcription factor Worniu (Wor), and with the post-mitotic neuronal marker, Embryonic Lethal Abnormal Vision (Elav) (Figure 3.6D, E) in the embryonic CNS. This suggested that *miR-124* is expressed in both the neuronal precursors and the mature post-mitotic neurons.

Furthermore, in mature third instar larvae, GFP expression was high in the central brain, and ventral nerve cord, and detectable but somewhat lower in the optic lobes (Figure 3.6F). Similar to its expression at the embryonic CNS, *miR-124-GFP* was co-

expressed with NB markers, Deadpan (Dpn), and with the post-mitotic neuronal marker, Elav *(*Figure 3.6G) in mature larval CNS. In addition, projection from a series of optical sections shows *miR-124 GFP* in most Dpn-positive cells (Figure 3.6H) in the larval CNS and this has led me to the conclusion that *miR-124* is expressed in most of the neuronal precursors of the developing larval brain.

By contrast, when I used an antibody against the transcription factor, Reverse Polarity (Repo), which labeled most of the larval brain glia cells, I did not observe co-expression of *miR-124-GFP* in these cells (Figure 3.6I, J), suggesting the absence of miR-124 expression in the glia population within the CNS.

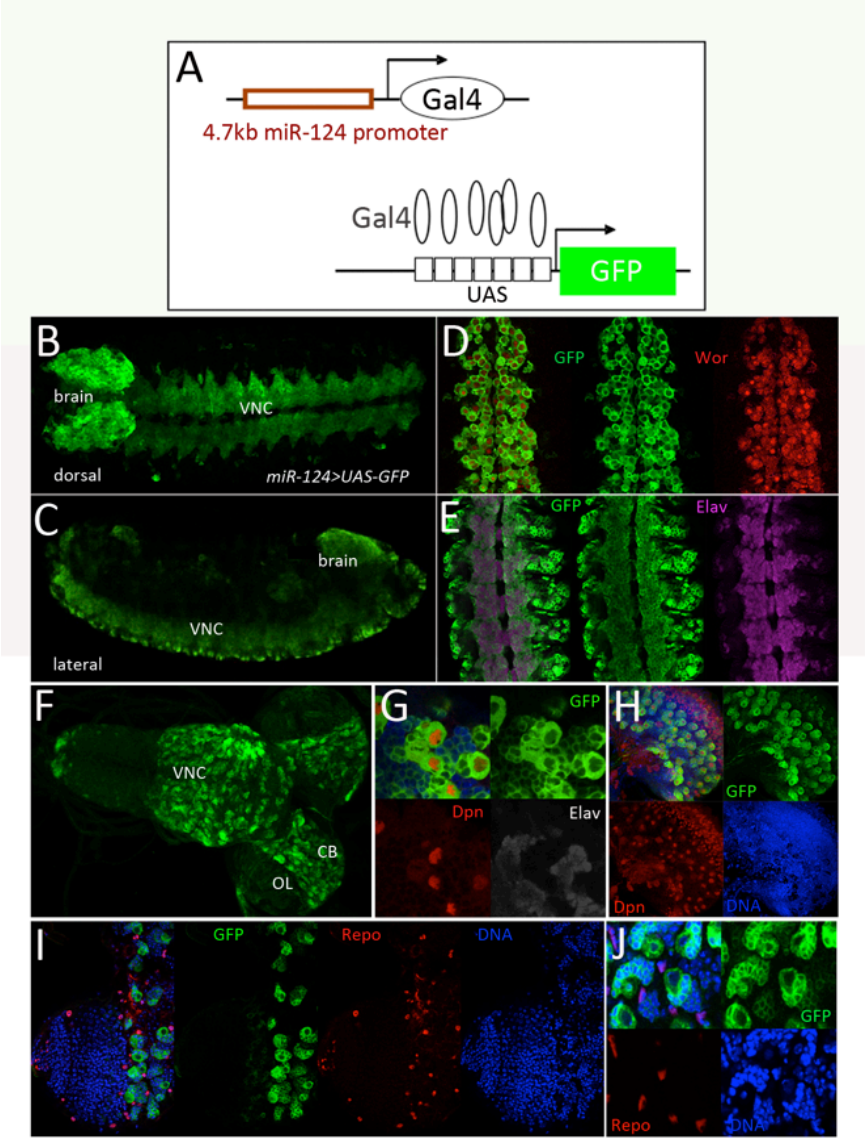

Figure 3.6 Expression of *miR-124-GFP* reporter in the developing CNS.

(A) Schematics showing design of *miR-124-GFP* reporter. GFP expression expression is driven by a 4.7kb *cis*-regulatory element from the *miR-124* locus. (B, C and F) Dorsal (B) and lateral (C) view, respectively, of GFP expression (green) in stage 16 embryos, and ventral view of 3rd instar larval brain (F), from a projection of optical sections. Central brains (CB), optic lobes (OL) and ventral nerve cord (VNC). (D and E) Single optical section showing many neuroblasts labeled with anti-Wor (red) near the surface of the VNC (D) and mature neurons deeper into the cortex labeled with anti-Elav (megenda) (E). (G) Single optical section near the surface of the cortex, showing several neuroblasts labeled with anti-Dpn(red) and neurons labeled with anti-Elav (blue/gray). (H) Dorsal view showing a projection of optical sections for one brain hemisphere. Most central brain NB (identified by Dpn expression, red) express miR-124 GFP (green). miR-124-GFP was detected at lower levels in the NB of the optic proliferation center (upper right). (I) Single optical section near the surface of the ventral cortex showing glia cells labeled with anti-Repo (red). (J) Single optical section at higher magnification (40x) showing the non-overlapping pattern of miR-124-GFP and Repo staining in I.

3.2.1.1.2 *miR-124* expression by fluorescent *in situ* hybridization

The caveat of using a promoter construct to study the expression of a gene was that this reporter might not fully recapitulate the endogenous expression pattern of the gene. This is because distal enhancer element might have been lost in the artificial promoter construct. In addition, there could be positional effect on expression due to the site of insertion of the promoter construct.

Therefore, as an independent means to visualize *miR-124* expression I used fluorescent *in situ* hybridization (FISH). I made use of the MARCM strategy [188, 195] to compare clones of genetically marked *miR-124* mutant cells with control clones. As a control for the specificity of the protocol, I performed the FISH experiment on brain samples containing *miR-124* mutant clones. Since no signal was detected in the *miR-124* mutant tissue, I was confident about the specificity of the probe (Figure 3.7A). In the wild-type control clones, I observed the presence of mature *miR-124* in post-mitotic neurons but extremely low levels in NB (Figure 3.7B).

To increase the sensitivity of the FISH method, I used a longer probe directed against the primary transcript of *miR-124*. Primary transcript FISH detected pairs of dots in the nuclei of NB in the central brain of wild-type 3rd instar larvae (Figure 3.7C). Such dots correspond to sites of transcriptional activity, confirming that nascent *miR-124* transcripts are being generated in the NB of the larval brain. These observations confirmed that *miR-124* is expressed in proliferating neuronal progenitors as well as in differentiating post-mitotic neurons.

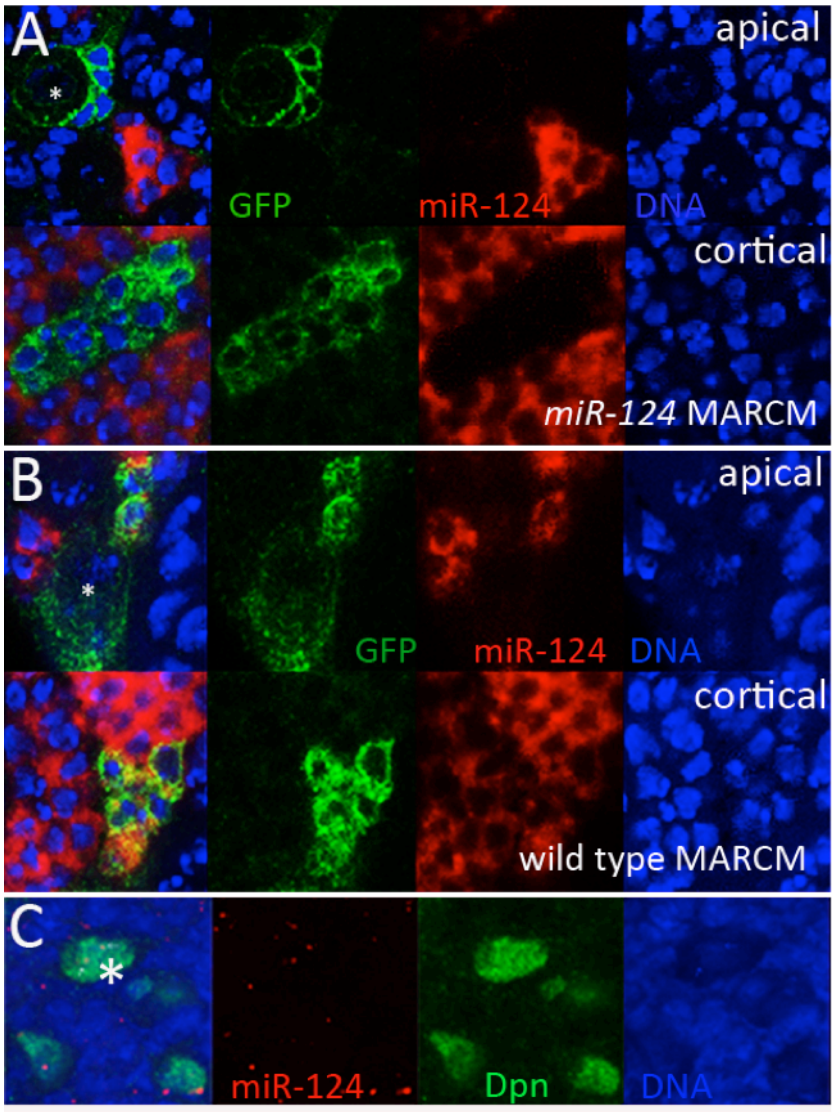

Figure 3.7 *miR-124* expression in larval central brain using fluorescent *in situ* hybridization.

(A and B) *miR-124* mutant MARCM clone (A, green) and wild-type MARCM clone (B, green) showing a single NB lineage. Expression of mature *miR-124* miRNA transcript detected by a *in situ hybridization* probe against sequence of mature *miR-124*(red); DNA is stained with DAPI (blue). Upper panel: superficial optical section. Lower panel: deeper optical section showing differentiating neurons. (C) Wild-type central brain showing the presence of *miR-124* primary transcript as pairs of nuclear dots on the DNA. NB are labeled with anti-Dpn (green) and DNA is stained with DAPI (blue). NB are marked with * in all panels.

3.2.1.1.3 *miR-124* expression following *miR-124* nuclear GFP sensor expression

As an independent means of visualizing *miR-124* activity, I have created a transgenic fly expressing a nuclear GFP sensor for *miR-124*. In this sensor fly, nuclear GFP was driven by a constitutive promoter, *tubulin*. One copy of perfect recognition site for *miR-124* was introduced to the 3'UTR of the GFP reporter (Figure 3.8A). As a result, cells that express *miR-124* would express low level of GFP whereas cells with low or no *miR-124* expression would show high level of GFP expression. Therefore, *miR-124* activity would be inversely correlated with the expression of the GFP sensor.

As shown in Figure 3.8, in 3rd instar larval brain, GFP expression was almost undetectable in large apical cells in the central brain and VNC. These cells are the NB of the brain based on their apical position and the smooth, round cellular morphology. Similarly, no GFP expression was detected in the cluster of small mature neurons residing deeper into the cortex in the central brain, optic lobes and VNC. However, strong GFP expression was readily detectable in cells scattered around the cortex as well as the surface of the entire brain and VNC, with monopolar, bipolar or multipolar morphologies. Based on the location and morphology, these are the glia cells in the larval CNS. Since the level of GFP expression is inversely proportional to the level of miRNA expression, these observations confirm the results obtained from the *miR-124-GFP* reporter study described above, and further support the conclusion that *miR-124* expression is neuron specific.

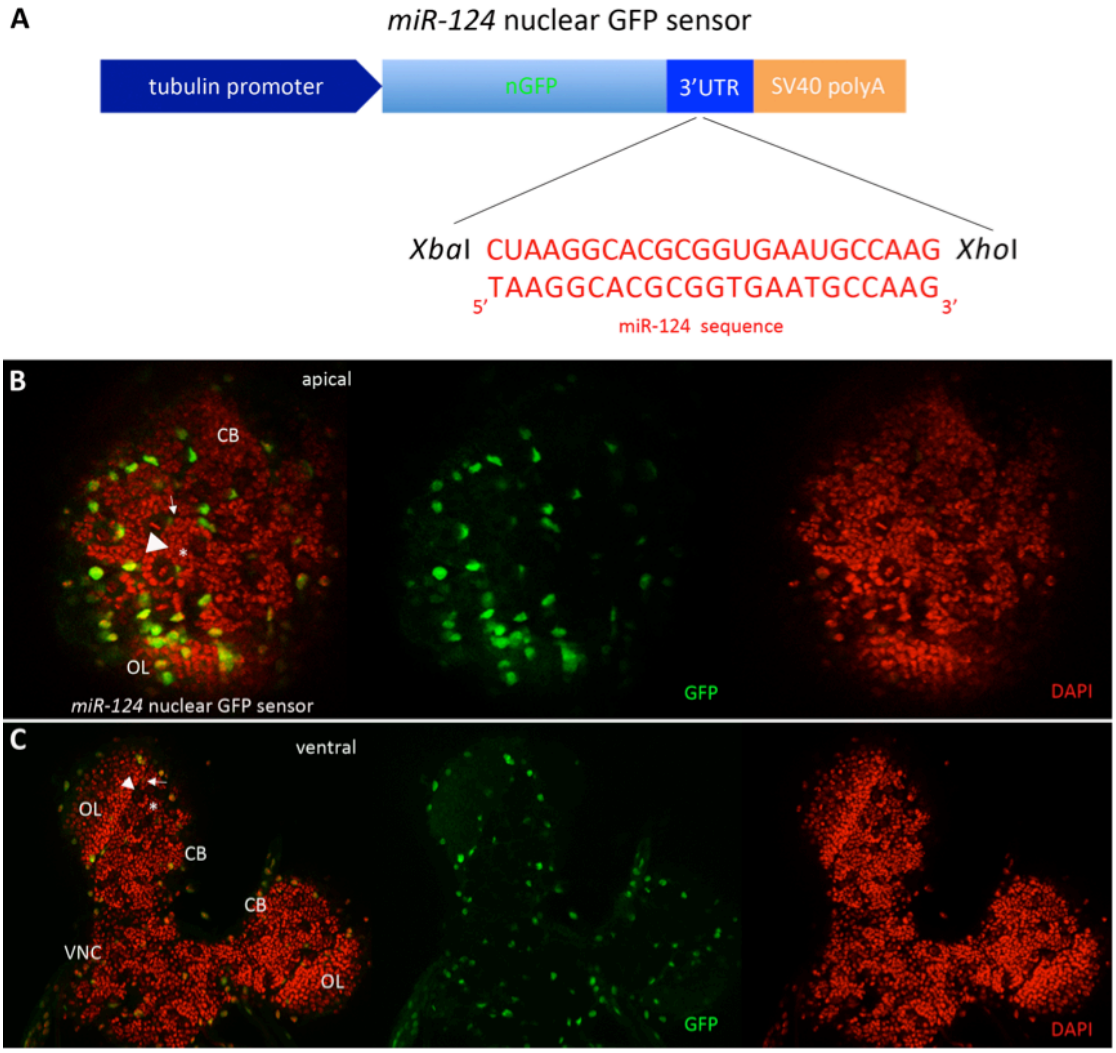

Figure 3.8 *miR-124* expression in the larval CNS using *miR-124* nuclear GFP sensor.

(A) Schematics showing the design of the *miR-124* nuclear GFP sensor. Nuclear GFP expression is driven by a constitutive tubulin promoter. A copy of complementary mature *miR-124* sequence (sequence shown in red characters) is cloned into the 3' UTR of GFP using the *Xba*I and *Xho*I restriction enzyme sites. (B-C) Single optical section showing the expression of nuclear GFP, costained with DAPI for the nuclei, in 3rd instar larval brain from apical (B, at 40x magnification) and ventral view (C, at 20x magnification). The NBs, indicated by white arrowheads, are identified by their apical position, the large size and the smooth, round morphology. Post-mitotic neurons, labeled with asterisk, are identified based on their cortical position and the small round morphology. Glia cells, indicated by white arrow, are identified by their scattered position within the larval brain and surrounding the brain surface.

3.2.1.2 *miR-124* expression in the adults

Having established that the *miR-124-GFP* reporter construct mostly recapitulated the endogenous expression pattern of *miR-124*, as validated by both FISH and *miR-124* sensor expression analysis, I continued to characterize the expression of *miR-124* in the adult flies using this reporter construct.

3.2.1.2.1 *miR-124* expression in the adult brain

Similar to the high level of expression of *miR-124* in the larval CNS, results from deep sequencing effort shows extremely high number of sequencing reads for the mature sequence of this miRNA in the adult head [22]. To confirm this, I analyzed expression of *miR-124-GFP* reporter in the adult brain. High level of GFP expression was readily detectable in the adult central brain, particularly in the mushroom bodies, regions of the central complex and the periesophageal neuropils centre (Figure 3.9).

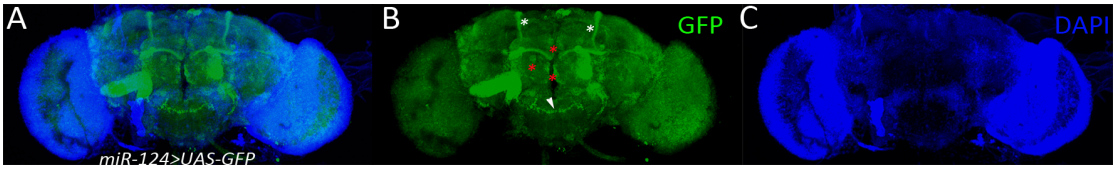

Figure 3.9 Expression of *miR-124-GFP* reporter in the adult brain.

(A) GFP expression following the *miR-124-GFP* reporter in 5day-old adult brain. High level of GFP expression in adult mushroom bodies (white asterisks), regions of the central complex (red asterisks) and perioesophageal neuropils centre (white arrow head) (B). DNA is labeled with DAPI (C). Images taken at 20x magnification.

3.2.1.2.2 *miR-124* expression in the male reproductive system

Interestingly, while all past studies on *miR-124* studies have reported a nervous system specific expression pattern of this miRNA in all the model organisms, including *C. elegans* [107], *Drosophila Melanogaster* [45, 77] and mice [53, 54, 196], I observed notable miR-124-GFP reporter expression in the reproductive system in the male flies.

As shown in Figure 3.10, within the male reproductive system, GFP was readily detectable in the anterior ejaculatory duct (eda), the base of the accessory gland (ag), at the tip of the testis as well as the ejactulatory bulb. To ask if the cells that express GFP are part of the peripheral nervous system, I co-stained the tissues with the antibody against neurons, anti-ELAV. GFP expression was found to partially overlap with ant-ELAV staining, indicating that *miR-124-GFP* reporter is expressed in both cells of the peripheral nervous system that innervate the male reproductive system as well as some other cell types within these tissues. More detailed characterization using antibodies to recognize the other cell types of the male reproductive system will be required to determine the nature of these GFP-expressing cells.

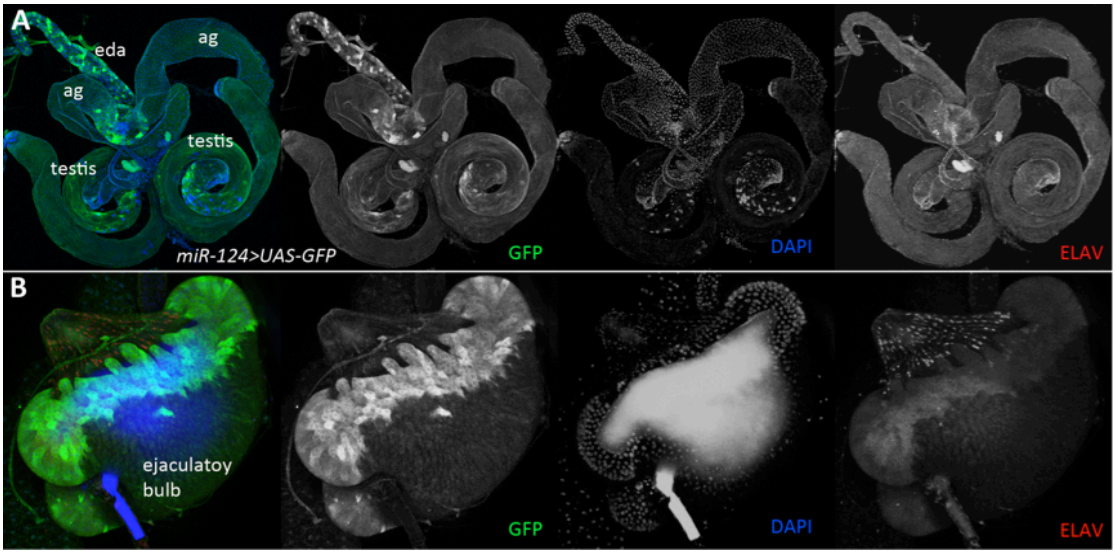

Figure 3.10 Expression of *miR-124-GFP* reporter in the male reproductive system.

GFP expression following the *miR-124-GFP* reporter at the anterior ejaculatory duct (eda), the base of the accessory gland (ag), at the tip of the testis (A, at 20x magnification) and the ejaculatory bulb (B, at 40x magnification). DNA is labeled with DAPI (blue) and neurons labeled with anti-ELAV (red).

3.2.2 Generation of *miR-124* knock-out mutants

I am interested in the functions of miRNAs in the development and functions of the nervous system in the fly. Since *miR-124* has been the focus of considerable interest among the animal miRNAs implicated in CNS development, I focused on the analysis of *miR-124* function(s) in the second phase of my study.

In order to explore *miR-124* function *in vivo*, a previous graduate student in the lab had generated a *miR-124* mutant via homologous recombination using the standard ends-out gene-targeting vector, pW25. In this mutant, named *miR-124*$^{\Delta 4}$, the *miR-124* locus of 300bp was replaced with a *mini-white* reporter. (Figure 3.11 *Δ4*).

To facilitate further genetic analysis, I decided to generate an independent mutant allele using an RMCE vector [197]. In this mutant, which I named *miR-124*$^{\Delta 177}$, I deleted 264 bp encompassing the *miR-124* hairpin and introduced the *mini-white* reporter flanked by inverted *attP* sites at the locus of the miRNA to permit subsequent genetic rescue by RMCE (Figure 3.11 *Δ177*).

I confirmed that the targeted *miR-124* loci were deleted in both mutant alleles by using a pair of primers that amplify the genomic region spanning the overlapping region of the two independent targeted loci. As shown by Figure 3.12A, single fly PCR amplifies a PCR product at the expected size of about 150bp using genomic DNA from control flies but not from homozygous of *miR-124*$^{\Delta 177}$ / *miR-124*$^{\Delta 4}$.

Together with the other co-workers in the generation of the global knockout library, I have observed a low frequency of re-insertion of the targeted genomic fragment into

some other random genomic loci after it was deleted from its endogenous locus [198]. Therefore, it is possible that mutants that have been verified to be deficient for the targeted loci using the single PCR method mentioned above might not be a true genetic null for the miRNA hairpin. Therefore, quantitative microRNA-PCR was used to test for the loss of *miR-124* production in both knockout alleles. As shown in Figure 3.12B, a pair of qRT-PCR oligos designed to amplify the mature sequence of *miR-124* detected the presence of the miRNA mature transcript in WT and heterozygous, $miR\text{-}124^{\Delta 4}$ / *WT* or $miR\text{-}124^{\Delta 177}$ / *WT* control flies but not from trans-heterozygous $miR\text{-}124^{\Delta 177}$ / $miR\text{-}124^{\Delta 4}$, demonstrating the complete genomic ablation of *miR-124* mature transcript from the KO alleles created.

To create a genetic rescue animal that expresses *miR-124* under its endogenous promoter, a 350bp DNA fragment containing *miR-124* hairpin was re-introduced into the targeted locus in the *Δ177* allele using the RMCE strategy depicted in the previous section. As shown in Figure 3.12B, quantitative RT-PCR has verified that the expression of mature *miR-124* transcript in this rescue animal, $miR\text{-}124^{RMCE}$ / $miR\text{-}124^{RMCE}$, was restored to almost its wild-type level. The rescue fly thus created this way would be useful for the confirmation of the specificities of *miR-124* loss-of-function phenotypes in the characterization of the *miR-124* mutants.

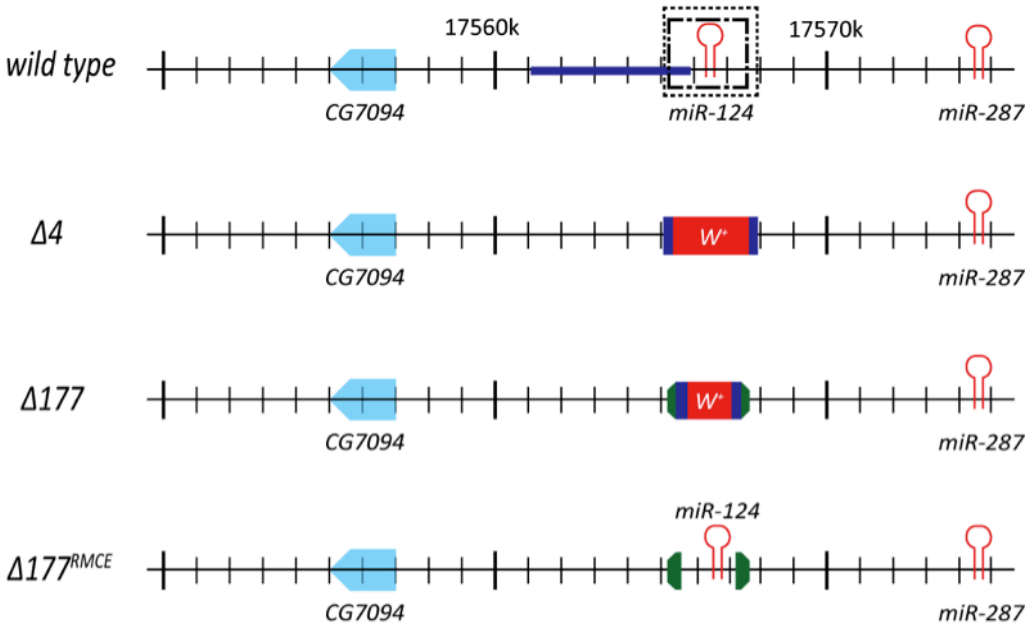

Figure 3.11 Schematics showing the genomic loci of various *miR-124* alleles used in this study.

miR-124 is located on Chr 2L in the WT flies, relatively distant, about 10kb and 8kb away respectively, from the neighboring genes, *CG7094* and *miR-287*. The *miR-124*$^{\Delta 4}$ allele has a 300-bp genomic fragment covering the miRNA mature transcript sequence replaced by the *loxP-mini-white-loxP* cassette from the pW25 gene-targeting vector. The *miR-124*$^{\Delta 177}$ allele has a 264-bp genomic fragment covering the miRNA mature transcript replaced by the *attP-loxP-mini-white-loxP-attP* RMCE cassette from the pW25-RMCE gene-targeting vector. In the *miR-124*^{RMCE} allele, the *attP-loxP-mini-white-loxP-attP* RMCE cassette from the initial *miR-124*$^{\Delta 177}$ allele has been replaced with an *attL-350bp mature miR-124 sequence-attL* fragment using the RMCE strategy. Inner dotted square represents genomic region deleted in the *miR-124*$^{\Delta 4}$ allele; outer dotted square represents genomic region deleted in the *miR-124*$^{\Delta 177}$ allele; red hairpin represents *miR-124* and nearby *miR-287* hairpin structures as indicated; red square represents the *mini-white* reporter used in the gene-targeting vector; bar represents *loxP* sites; green bar represents *attP* or *attL* sites.

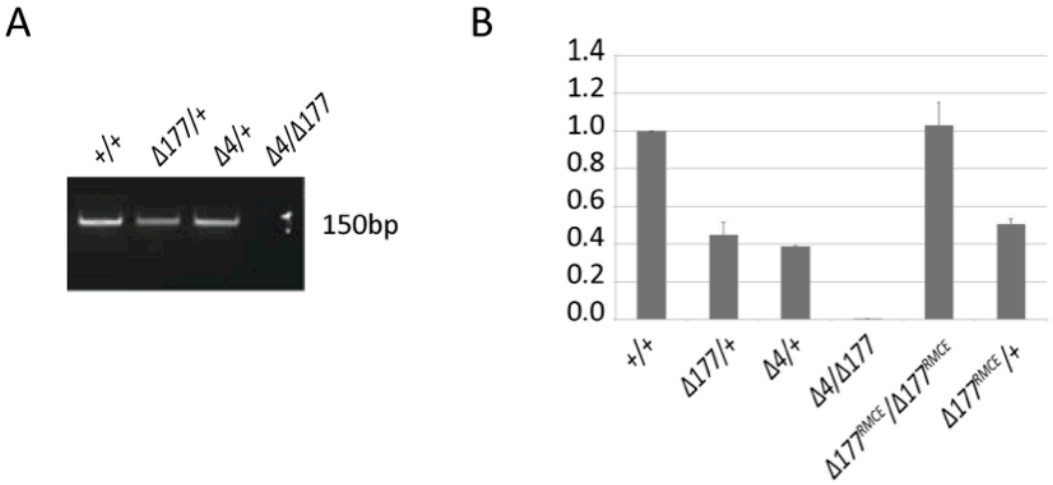

Figure 3.12 Verification of loss of *miR-124* in *miR-124* alleles by single fly PCR and qRT-PCR experiments.

(A) Detection of PCR fragment covering the targeted *miR-124* hairpin sequences in wild-type and heterozygous mutant of either KO allele over wild-type but not in trans-heterozygote of both alleles; (B) miRNA qRT-PCR using oligos directed against the mature transcript of *miR-124* detected ~ 40-50% wild-type level of its mature transcript in heterozygous mutant of either KO allele over wild-type and transgenic flies with a single copy of the rescue allele, close to 0% in trans-heterozygote of both alleles and close to 100% wild-type level in transgenic flies containing two copies of the rescue alleles.

3.2.3 *miR-124* is not required for basic survival of the fly.

3.2.3.1 Presence of background lethality mutation(s) in *miR-124* KO alleles

No homozygous adults were obtained in stocks of either knockout allele of miR-124 balanced with chromosome balancer, *CyO*, suggesting that the *miR-124* LOF mutants were homozygous lethal. However, when crossed over a deficiency (Df) strain containing a genomic deletion uncovering the *miR-124* locus, adults trans-heterozygous for the Df and each of the KO alleles were obtained. This suggested that the lethality observed in the two KO stocks were due to other lethal mutation(s) on the chromosomes that were not located at the *miR-124* locus.

I was unable to remove the background lethality in these alleles after six generations of backcrossing with the Canton-S (CS) wild-type strain, suggesting that the lethal mutations associated were in close proximity with the targeted *miR-124* loci (although not included in the Df used). However, trans-heterozygous mutant for these two alleles was viable, suggesting that the lethal genetic background associated with two KO alleles are independent. Consequently, only trans-heterozygotes between the two independent KO alleles or between either allele and the genomic deficiency line were used for further characterization of the mutant phenotypes; and in the following discussion, the term '*miR-124* mutant' always refers to the trans-heterozygous combination of $miR\text{-}124^{\Delta 177}$ / $miR\text{-}124^{\Delta 4}$.

3.2.3.2 *miR-124* is not required for viability of the fly

Results from whole genome deep sequencing analysis have shown that *miR-124* is expressed at a high level from early embryonic stages of the fly development [22], suggesting that it might play an important role in early fly development.

As a first approach to address this question, I asked if *miR-124* is required for the viability of the fly during development. To do this, I scored the percentage of trans-heterozygous *miR-124*$^{\Delta 177}$ / *miR-124*$^{\Delta 4}$ adult flies emerging from the progeny obtained from a cross between these two independent knockout alleles. Progeny from the crosses, regardless of their genotypes, were raised in groups of 20 per standard food vial from early embryonic stages onwards. Under such controlled culturing conditions, trans-heterozygotes of *miR-124*$^{\Delta 177}$/*miR-124*$^{\Delta 4}$ flies emerged as adults at the expected Mendelian genetics ratio (Figure 3.13). This suggests that *miR-124* is not required for the survival of the animal when growth conditions were optimal.

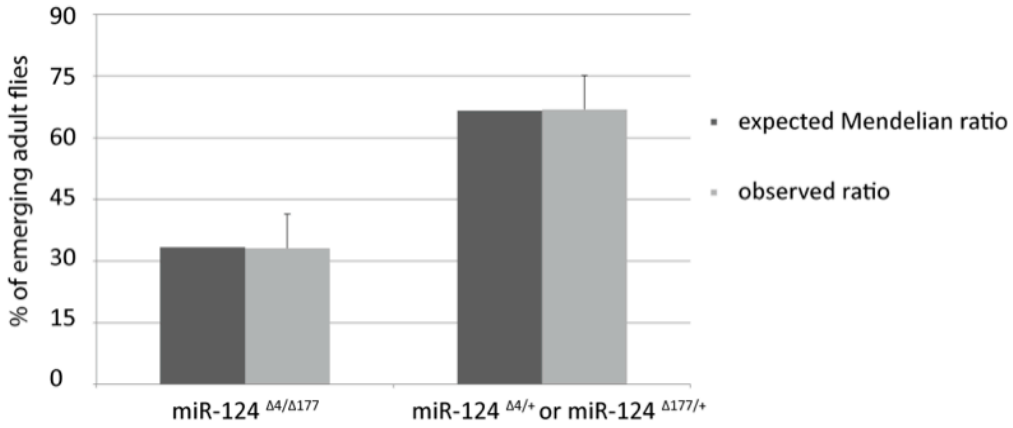

Figure 3.13 Viability of *miR-124* mutants.

Percentage of emerging adult flies with the indicated genotypes, as observed in viability test and as expected from the Mendelian ratio.

3.2.3.3 *miR-124* is not required for reproduction of the fly

To ask if *miR-124* is required for reproduction, I carried out single pairing fertility tests crossing sexually mature males or females of *miR-124* mutants to flies of the opposite sex and quantified the fertility of the mutant using two scoring parameters. The first parameter compared the percentage of individual fly pairings that resulted in viable progeny and the second parameter measured the number of progeny produced in each reproductive pairing. As shown in Figure 3.14, no significant changes in either parameter were observed for male or female mutants of *miR-124*.

When individual mutant males were paired with two CS female virgins for 48hrs, close to 95% of the crosses resulted in viable progeny. This was very similar to the percentages of fertile single pairings between CS or *miR-124* heterozygous control males and CS female virgins (95% and 100% respectively, Figure 3.14 A). This indicated that *miR-124* LOF did not compromise the reproduction capability of the male fly. The same was true when individual mutant females were paired with two CS males (Figure 3.13B). Similarly, the total number of progeny obtained from the single pairing fertility tests did not deviate significantly between crosses of mutant male with CS females and of control males and CS females, and vice versa (median number of progeny = 75 vs 74 in the male test, $P>0.05$ and 45 vs 50, $P>0.05$, in the female test, Figure 3.14C and D). This suggested that *miR-124* LOF did not affect the reproductive capacity of young sexually mature flies of either sex. Together, these results indicated that *miR-124* was not required for reproduction of the fly.

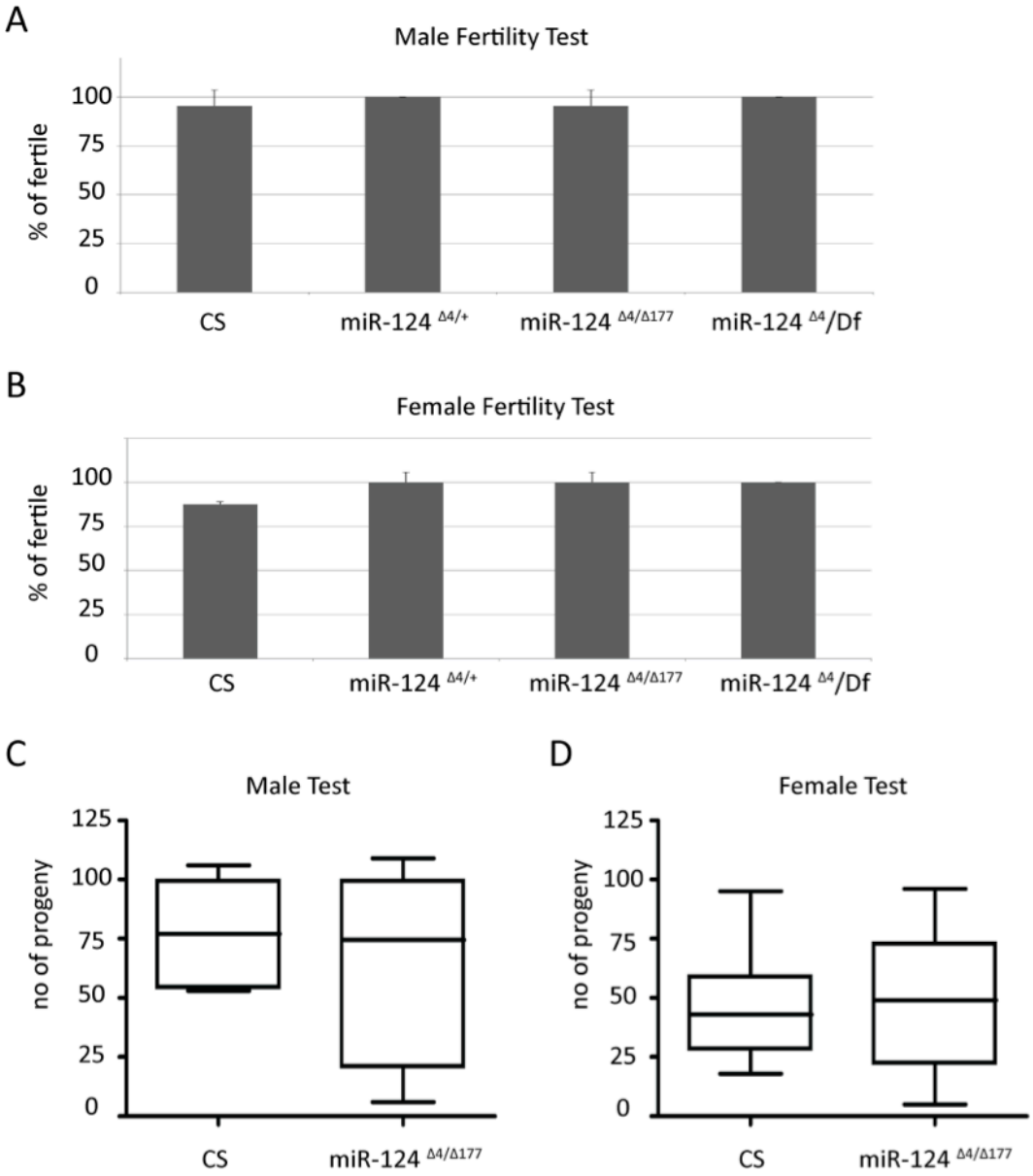

Figure 3.14 Fertility of *miR-124* mutants.

(A-B) The percent of fertile crosses was scored. Control CS or *miR-124* mutant males were paired with CS female virgins (A) and Control CS or *miR-124* mutant female virgins were paired with CS male overnight (B). The presence of progeny in the vial was later scored. Data represent average of 3 independent experiments (n= 20 single pair matings per experiment). Error bars represent SEM. There was no significant significance. (C-D) The total number of progeny resulting from each fertile cross between control CS or *miR-124* males with control CS female virgins (C), and between control CS or *miR-124* female virgins with control CS male (D). Pupae were counted. Box plot showing median, upper and lower quartiles. There was no significant difference between the samples.

3.2.4 *miR-124* function in CNS development

3.2.4.1 *miR-124* is not required for gross CNS early development

Since *miR-124* is expressed at a high level in the developing embryonic and larval CNS, I asked if this miRNA played a role in development of the fly CNS.

To ask if *miR-124* LOF affects the development of the embryonic nervous system, I analyzed homozygous mutants at late embryonic stage, stage 16 using a subset of neuronal markers. I did not observe gross morphological changes in *miR-124* LOF embryos at stage 16. For example, anti-Eve antibody, which labels the neuronal progeny of four embryonic NB, revealed a similar pattern and number of labeled neurons in the *miR-124* LOF mutant embryos (Figure 3.15 A and B). This suggested that *miR-124* LOF unlikely affects the specification of cell fate in the embryonic nervous system. In addition, staining with the anti-BP102 antibody, which labels embryonic CNS axons revealed no gross morphological defects with axon scaffolding in the stage 16 *miR-124* mutant embryos compared to that of the wild-type.

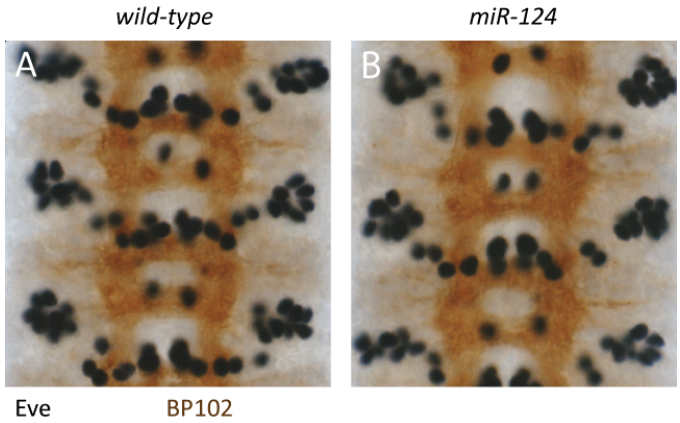

Figure 3.15 Gross morphology of the embryonic nervous system is not affected in miR-124 LOF.

Anti-BP102 (brown) shows no gross morphological defects with axon scaffolding in the stage 16 *miR-124* mutant embryos compared to that of the wild-type. Anti-Eve antibody (black) labels a subset of 9-12 neurons per hemisphere in stage 16 wild-type embryos, which does not seem to deviate significantly in *miR-124* mutant embryo.

3.2.4.2 *miR-124* is not required for asymmetric division of larval NBs

Since *miR-124* is expressed in NB lineages of the larval central brain, I wondered if its presence is important for the development of these central brain NB lineages. To test this, I made use of the mosaic analysis of a repressible marker (MARCM) technique and compared genetically marked NB clones that were normal or mutant for *miR-124*.

More specifically, I induced randomly positioned MARCM clones in early first instar larvae when the NBs start to reenter proliferation and analyzed these clones in late third instar larval brains. All labeled control and *miR-124* mutant type I NB lineages contained one large cell, the NB, which expressed Deadpan (Dpn; Figure 3.16 A and B) as well as many smaller cells. GMC were identified by expression of the differentiation marker, Prospero (Pros, Figure 3.16C and D) and by Partner of Numb (Pon, Figure 3.16E and F), which is segregated to the GMCs during asymmetric NB division. Pros and Pon were detected in wild type and mutant GMCs. GMC were found clustered directly adjacent to the large apical NB in both control and mutant clones (Figure 3.16C and F). In addition to the NB and GMC precursors, control and *miR-124* clones contained many smaller cells that expressed Elav, representing the neuronal progeny of the GMCs (Figure 3.16A and F). The presence of the labeled NB and GMC together with many post-mitotic progeny in each clone reflects the successive rounds of asymmetric NB division to produce many GMC.

To visualize mitotic cells, I made use of an antibody specific for the phosphorylated form of histone-H3 (pH3). Histone-H3 Ser-10 phosphorylation is known to coincide with chromosome condensation [199]. Therefore, the presence of pH3 indicates that

the cell has entered mitosis. As shown in Figure 3.16 G and H, a subset of NB and GMC were labeled with anti-pH3 in control and *miR-124* mutant clones, indicating that NB and GMC were mitotically active. Comparable observations were made for marked *miR-124* mutant type II NB clones. Therefore, *miR-124* is not required for neuronal cell fates in type I nor type II larval brain NB lineages.

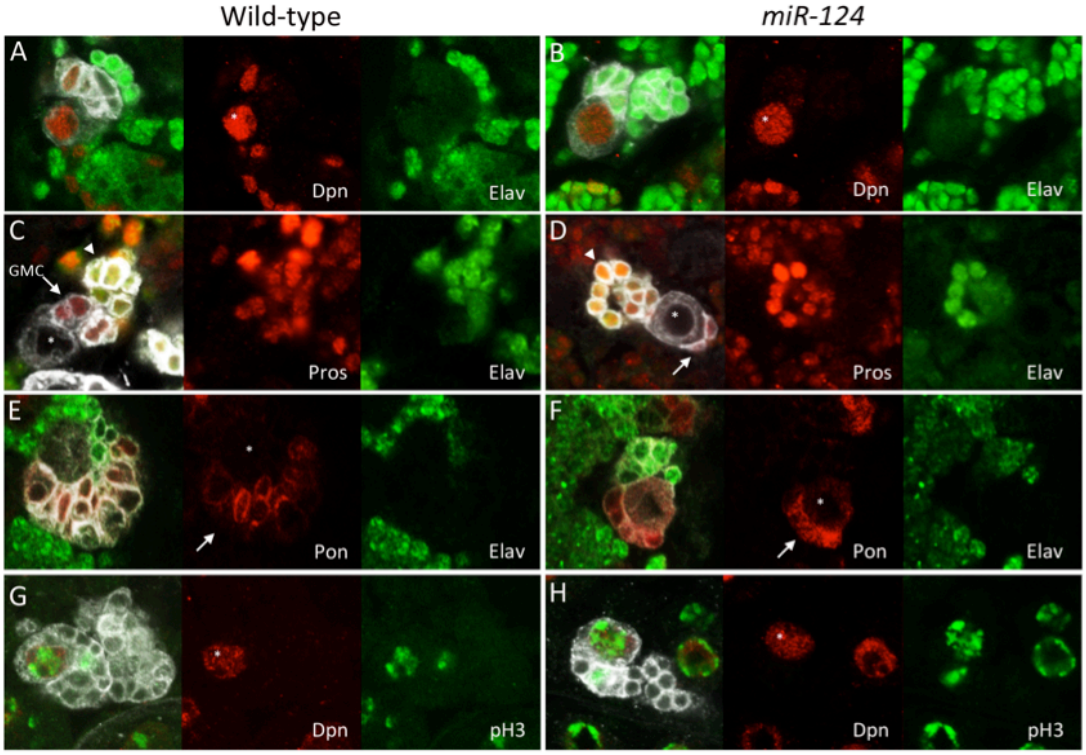

Figure 3.16 Cell types in the NB lineages are not altered in *miR-124* mutant clones.

(A-F) Single optical sections showing GFP labeled MARCM clones of the indicated genotypes. MARCM clones (GFP: grey); (A, B) NB labeled with anti-Dpn (red). Postmitotic neurons were labeled with anti-Elav (green). (C, D) GMC (arrows) were identified by labeling with anti-Pros (red) and by the absence of the postmitotic marker anti-Elav (green). Arrowheads indicate Elav-positive postmitotic neurons. (E, F) NB and GMC labeled anti-Pon (red) and neurons labeled with anti-Elav (green). (G, H) NB labeled with anti-Dpn (red) and with anti-phospho-Histone H3 (green).

3.2.4.3 *miR-124* is required for NB proliferation in larval central brain

3.2.4.3.1 *miR-124* LOF led to reduction in the size of central brain NB lineages

Although loss of *miR-124* did not compromise the ability of type I NB to undergo asymmetric division, upon closer examination, I observed a reduction in the number of post-mitotic neurons in the NB clones that are mutant for *miR-124* (Figure 3.17).

As part of the MARCM analysis, I determined the average number of GFP-labeled, Elav-positive cells for control and mutant type I NB clones by counting the total number of these cells in the confocal images obtained. Control clones contained an average of 85 cells (±5), while *miR-124* mutant clones contained an average of 66 cells (±9), cells per clone (Figure 3.17, * $P<0.05$). To confirm that this difference was due to the absence of *miR-124*, I carried out a clonal rescue experiment. In the MARCM experiment, I have made use of *Elav-Gal4* to direct *UAS-GFP* expression to positively label clones. It is worth noting that the *Elav-Gal4* driver is expressed in all cells of the NB lineage, in contrast to Elav protein, which is limited to post-mitotic neurons. To perform clonal genetic rescue, I co-expressed a *UAS-miR-124* transgene along with *UAS-GFP* in control and *miR-124* mutant MARCM clones. This restored mutant type I NB clone size to normal control levels (Figure 3.17, $P=0.44$ for control vs rescued mutant). These findings indicate that *miR-124* is required in the NB lineage to generate the normal number of post-mitotic neurons.

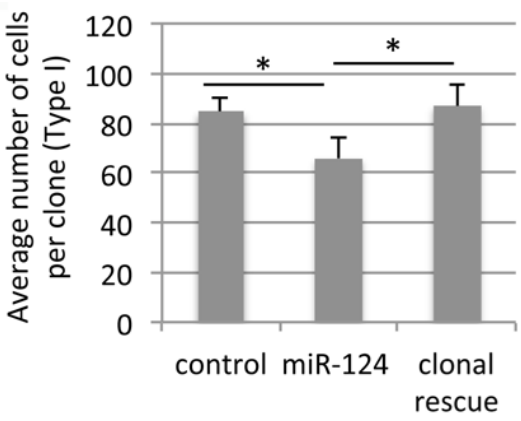

Figure 3.17 *miR-124* LOF leads to reduction in size of central brain NB lineages.

Average cell number in wild-type control type I NB MARCM clones, compared with *miR-124* mutant and rescued *miR-124* clones. SD = 5 (control), 9 (*miR-124*) and 8 (clonal rescue). One asterisk: $P<0.05$; two asterisks $P<0.01$ using two-tailed unpaired Student's t-test ($n > 100$ for each genotype).

3.2.4.3.2 *miR-124* LOF led to reduced proliferation of NB in larval central brain

The reduction in cell number observed in *miR-124* mutant NB clones suggests that mutant cells either divide less or that some of them die during postembryonic development.

To explore the possibility that the reduction in clone size in *miR-124* mutant as a consequence of alteration in NB proliferative capacity, I scored the number of MARCM clones containing type I NB labeled with the mitotic marker pH3. I observed that only 35% of NB in *miR-124* mutant clones was pH3-positive while 46% of control clones had pH3-positive NB (Figure 3.18, ** $P<0.01$). Performing the genetic clonal rescue experiment described above, I observed restoration of the mitotic index to its normal level in the rescued *UAS-miR-124* clones (Figure 3.18, $P=0.28$ for control vs rescued mutant; * $P<0.05$ for mutant vs rescued mutant). Since post-mitotic neurons within a NB lineage are generated by successive rounds of NB asymmetric cell divisions, the reduction in the progenitor NB proliferation could contribute to the overall reduction in size of the *miR-124* mutant clones.

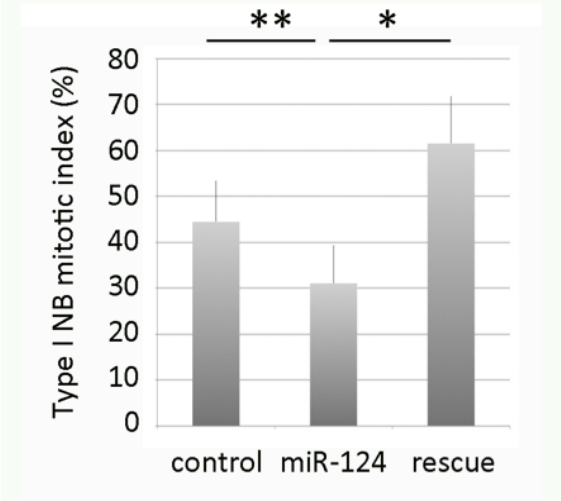

Figure 3.18 Proliferative status of *miR-124* mutant type I NB clones.

Mitotic index of type I NB in wild-type, *miR-124* mutant and rescued *miR-124* MARCM clones, shown as the percentage of NB that expressed phospho-histone H3 in late wandering third instar larval brains. SD = 12% (control), 4% (*miR-124*) and 13% (clonal rescue). One asterisk: $P<0.05$; two asterisks $P<0.01$ using two-tailed unpaired Student's t-test ($n > 100$ for each genotype).

3.2.4.3.3 Blocking cell death did not rescue reduction in *miR-124* clone size

As mentioned earlier, a second possible mechanism for the reduction in overall clone size is cell death in the postembryonic larval brain. To test this, I performed a similar experiment using targeted mis-expression of the pan-caspase inhibitor, P35, to block apoptosis in the *miR-124* mutant MARCM clones. Blocking cell death by *p35* overexpression did not restore the mitotic index of the mutant NB (Figure 3.19), indicating that the reduction in *miR-124* clone size could not have been due to elevated cell death within the NB lineages.

Taken together, these experiments suggest that reduced proliferative activity could account for the reduction in mutant clone size, and suggests that *miR-124* is required for the proliferation of neuronal progenitors in the developing CNS.

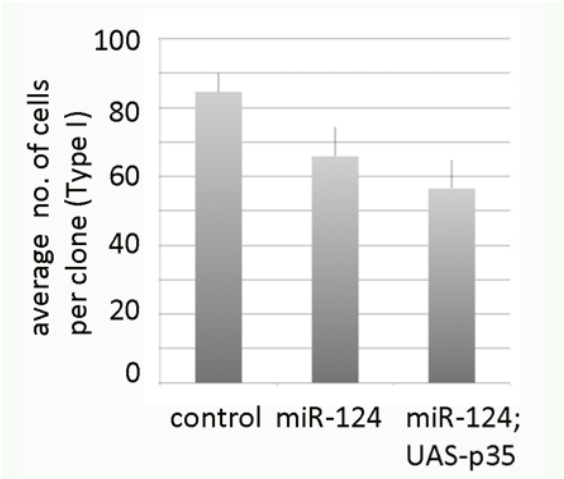

Figure 3.19 Blocking cell death does not rescue reduction in *miR-124* clone size.
Average cell number in wild-type control type I NB MARCM clones, compared with *miR-124* mutant and *miR-124* mutant clones expressing *UAS-p35*. SD = 5 (control), 9 (*miR-124*) and 4 (*miR-124; UAS-p35*).

3.2.4.4 Elevated *ana* level contributes to the *miR-124* NB proliferation phenotype

Computational predictions have suggested that *miR-124* targets mainly epithelial-specific or non-neuronal genes, including the glial-specific genes *repo* and *gliotactin* [37]. Intriguingly, the list of predicted targets of *miR-124* includes *anachronism* (*ana*), which has been reported to encode a negative regulator of NB proliferation that is expressed specifically in a subset of glial cells [200]. As a first step to determine whether *ana* might be a functionally important target of *miR-124*, I examined *ana* transcript levels by quantitative RT-PCR in RNA samples from dissected third instar brains of control and *miR-124* mutants. I observed an elevated level of *ana* transcript in the mutant brains, which were restored to normal level in the RMCE rescued mutant (Figure 3.20A, ** $P<0.01$). This indicates that the endogenous *ana* transcript is affected in a manner consistent with regulation by *miR-124*.

If *ana* over-expression was the cause of *miR-124* mutant clone phenotype, increasing *ana* level in cells of the NB lineages should phenocopy *miR-124* mutant phenotypes. As a first step to assess whether elevated *ana* expression contributes to the *miR-124* mutant phenotype, I made use of the MARCM system to generate clones of cells overexpressing *ana* in the neuronal lineage. This resulted in a reduced proliferative index (Figure 3.20B, * $P<0.05$). This experiment shows that upregulation of *ana* is sufficient to mimic the effects of *miR-124* LOF on NB proliferation.

As a more direct and rigorous functional test of whether *ana* overexpression contributes to the reduced NB proliferation observed in *miR-124* mutants, I asked if limiting *ana* levels could suppress the mutant phenotype. As a first approach, I

examined proliferation of *miR-124* mutant clones in flies heterozygous for a null allele of *ana* [201]. Limiting the capacity to overexpress *ana* in this way restored the proliferative activity of *miR-124* mutant NB to near normal levels (Figure 3.20C, * $P<0.05$). Together these experiments suggest that the elevated level of *ana* transcript in the *miR-124* mutant brain contributes to *miR-124* clonal phenotypes.

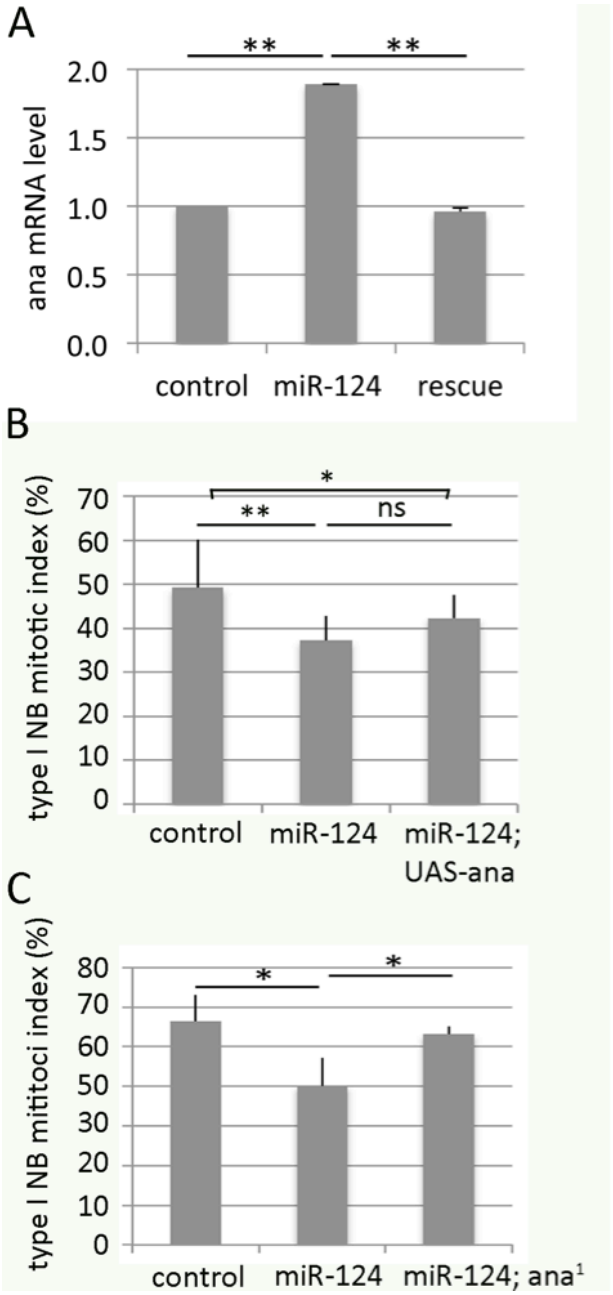

Figure 3.20 *miR-124* regulates *anachronism* expression.

(A) Normalized *ana* mRNA levels measured by qRT-PCR in RNA from late wandering third instar larval brains of the indicated genotypes. Data are presented as mean ± SD based on six independent biological replicates. Two Asterisks: $P<0.01$ using the Wilcoxon two-sample test. (B and C) Genetic evidence that *miR-124* acts via regulation of *anachronism*. Histograms showing the percentage of type I NB MARCM clones that expressed phospho-histone H3 in late wandering third instar larval brains. One asterisk: $P<0.05$ using two-tailed unpaired Student's t-test ($n > 100$ for each genotype). (A) Genotypes: control denotes Canton S, *miR-124* mutant and Canton S flies that coexpressed the *UAS-ana* transgene to over-express *ana* mRNA selectively in the marked NB clones. SD = 11% (control), 6% (*miR-124*) and 5% (*UAS-ana*). (B) Genotypes: control denotes Canton S, *miR-124* mutant, *miR-124* mutant clones that carrying 1 copy of the ana^1 mutant allele. SD = 7% (control), 7% (*miR-124*) and 2% (*miR-124*, $UAS\text{-}ana^1$).

3.2.4.5 *miR-124* negatively regulates the expression of anachronism

As a first approach to address if *miR-124* regulates *ana* directly, I scanned through the 3'UTR of *ana* and found two potential *miR-124* binding sites (Figure 3.21A). To validate the functionality of the *miR-124* binding sites on *ana* 3'UTR, I generated luciferase reporter constructs carrying the full length *ana* 3'UTR or a mutant version in which 3 nucleotides of one of the predicted *miR-124* sites were mutated to compromise pairing to the miRNA seed region (grey, Figure3.21B). When I co-expressed the UTR reporters with *miR-124* in S2 cells, I observed a significant reduction in luciferase activity from the reporter carrying the intact target site but not on the mutant form of the *ana* reporter (Figure 3.21C, ** $P<0.01$). This suggests that *miR-124* can act directly via this target site to repress *ana* expression.

To further assess the functionality of the *miR-124* target site *in vivo*, I generated transgenic flies expressing the *ana* 3'UTR luciferase reporter. I then compared luciferase activity levels in brains dissected from late third instar control larvae to that from *miR-124* mutant, and observed elevated luciferase activity in *miR-124* mutant brains carrying the intact *ana* reporter transgene, compared to the level of expression of this transgene in the control brains (Figure 3.21D, * $P<0.05$). I did not observe statistically significant upregulation of the UTR reporter carrying the mutated version of *miR-124* site in *miR-124* mutant brains.

Based on these observations, I concluded that *miR-124* can act directly via the site identified in the 3'UTR to regulate *ana* mRNA levels *in vivo*.

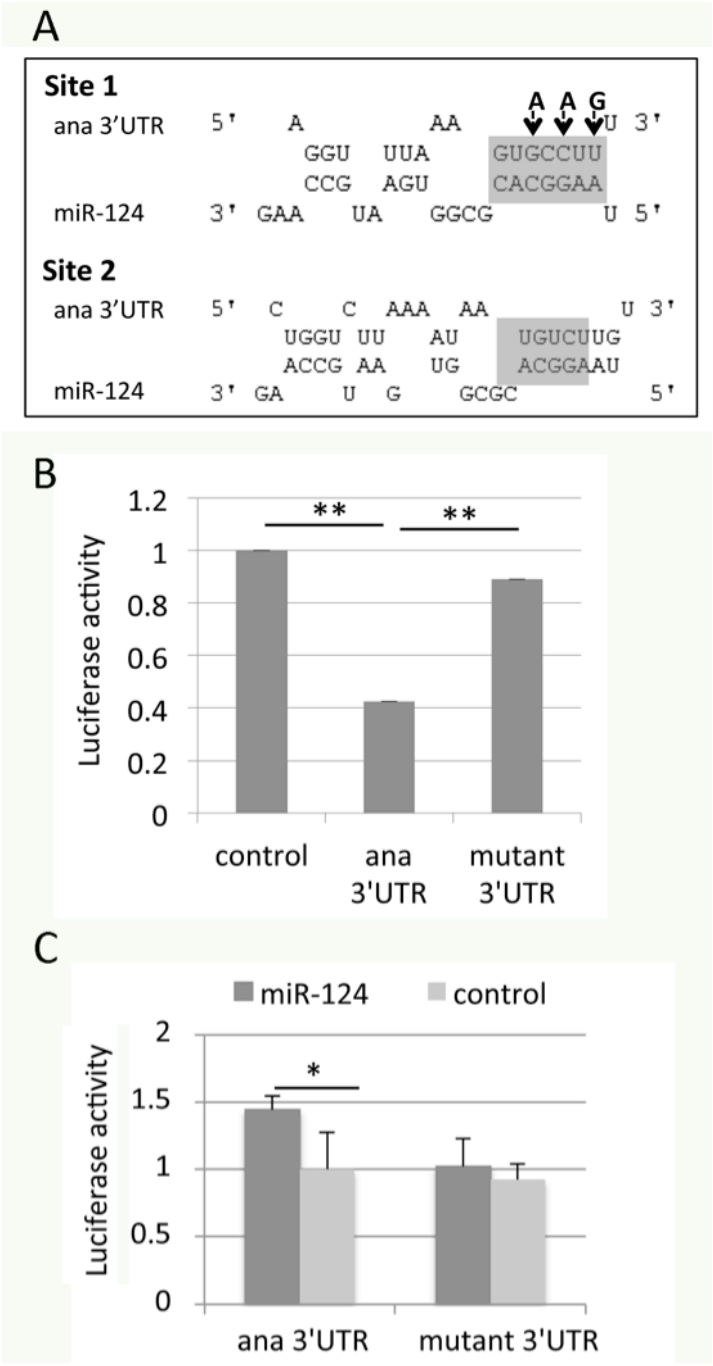

Figure 3.21 *miR-124* target sites on *ana* 3'UTR are functional.

(A) Predicted *miR-124* target sites in the *ana* 3'UTR. Arrows indicated residues changed in the site 1 mutant. (B, C) Luciferase assays showing regulation of a firefly luciferase reporter containing the *ana* 3'UTR or a version of the *ana* UTR with site 1 mutated as indicated in panel B. Data show the ratio of firefly to Renilla luciferase activity and represent mean ± SD based on three independent biological replicates. One asterisk: $P<0.05$; two asterisks: $P<0.01$ using two-tailed unpaired Student's t-test. (B) S2 cells were transfected to express the *ana* 3'UTR reporter or the site 1 mutant version of the reporter. Cells were cotransfected to express *miR-124* or a vector-only control, and a Renilla luciferase reporter as a control for transfection efficiency. (C) Normalized luciferase activity from the *ana* 3'UTR reporter transgene in control or *miR-124* mutant larval brain lysates.

3.2.4.6 *miR-124* controls *ana* level in NB lineages

3.2.4.6.1 Low level of *ana* expression in the NB lineages of the larval brain

What I have observed suggested that *ana* is a functionally significant target of *miR-124 in vivo*. However, this conclusion would result in an apparent conundrum in that *miR-124* is neuronal specific in its expression whereas earlier reports have suggested that *ana* is expressed only in glia [200].

To explore the possibility that the *ana* transcript might in fact be present at low levels in the neuronal lineage, I made use of the TU-tagging method [187] to selectively label and purify RNA from neuronal cells of the NB lineage. The method is based on cell-type specific expression of the uracil phosphoribosyltransferase (UPRT) enzyme, which permits incorporation of a 4-thiouracil base into newly synthesized mRNA. I made use of the *elav*-Gal4 driver to direct expression of UAS-UPRT in all neuronal cells of the larval brain. As a positive control for neuronal mRNA, I performed RT-PCR for *elav* mRNA. The glial-specific transcript *repo* was used as a control for glial cell mRNA. *elav* mRNA was recovered in the *elav-Gal4* samples, whereas *repo* transcript was not detectably recovered (Figure 3.22A). *ana* mRNA was detected using primers specific for the mature spliced form of its transcript, indicating that *ana* was synthesized in the *elav-Gal4* expressing cells of wild-type neuronal lineages (Figure 3.22A).

Next, I used quantitative RT-PCR to measure *ana* transcript levels by TU tagging RNA from *miR-124* expressing cells, using *miR-124-Gal4* to direct *UAS-UPRT* expression. Samples were prepared from control brains and *miR-124* mutant brains and PCR was normalized to the level of actin mRNA. The level of *elav* transcript was

unchanged, but *ana* transcript was increased by ~2 fold in the *miR-124* mutant cells (Figure 3.22B). Again, *repo* transcript was not detected, confirming the absence of glial cells in this population. Based on these findings, I concluded that (1) that *ana* transcript is, in fact, expressed in neuronal cells and (2) that the level of *ana* transcript increased in *miR-124*-expressing cells in *miR-124* mutant.

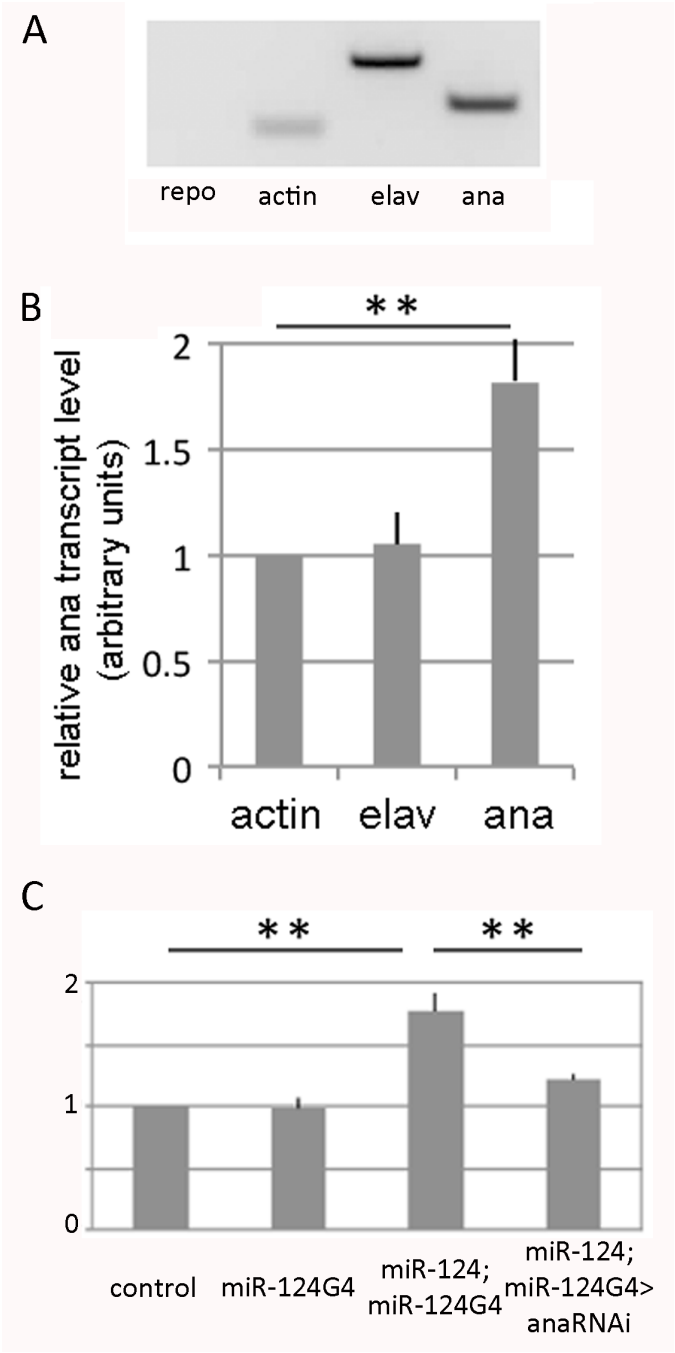

Figure 3.22 *anachronism* expression *miR-124*-expressing neuronal lineages.

(A) Normalized mRNA levels of the indicated genes measured by qRT-PCR in neuronal RNA isolated from *elav (c155)-Gal4* driving *UAS-UPRT*. Data are presented as mean ± SD based on three independent biological replicates. Two Asterisks: P<0.01 using the student t-test. (B) Changes in mRNA level of the indicated genes measured by qRT-PCR in neuronal RNA isolated from *miR-124-Gal4* driving *UAS-UPRT* in *miR-124* mutant background, normalized to RNA sample isolated from wild-type larvae. Data are presented as mean ± SD based on three independent biological replicates. Two Asterisks: P<0.01 using the student t-test. (C) Quantitative PCR to assess the efficacy of the RNAi transgene at depletion of *ana* transcript in *miR-124*-expressing cells. Genotypes: control denotes Canton S, *miR-*

124 mutant, *miR-124* mutant expressing *miR-124-Gal4* and *UAS-ana-RNAi* transgene to deplete *ana* mRNA selectively in *miR-124*-expressing cells.

3.2.4.6.2 Upregulation of *ana* within NB lineages contributes to *miR-124* NB phenotype

Seeing that *ana* transcript levels were elevated in the *miR-124* expressing cells in the *miR-124* mutant, I then asked if the elevated *ana* level in these cells contributed to the *miR-124* mutant clone phenotype. To do this, I used the MARCM system to selectively reduce *ana* levels in these cells. I first monitored the efficacy of depletion of *ana* transcript in *miR-124* expressing cells. The level of *ana* transcript was compared by quantitative RT-PCR in RNA from *miR-124* mutant brains expressing *miR-124-Gal4* alone or together with a *UAS-ana-RNAi* transgene. *ana* transcript levels in the mutant were reduced to near normal control levels by the RNAi treatment (Figure 3.23A, ** $P<0.01$), indicating *ana* depletion by *ana* RNAi was efficient.

Next, as a functional test for the effect of *ana* depletion in *miR-124* mutant clones, I induced *miR-124* mutant MARCM clones in the presence or absence of the *ana*RNAi transgene, and assayed for NB proliferative capacity. I found that selectively lowering *ana* levels in the *miR-124* mutant NB clones was sufficient to restore proliferation to near normal levels (Figure 3.23B, * $P<0.05$). This provides the direct evidence that the upregulation of *ana* transcript due to the loss of *miR-124* suppression contributes to the *miR-124* NB proliferation phetnoypes.

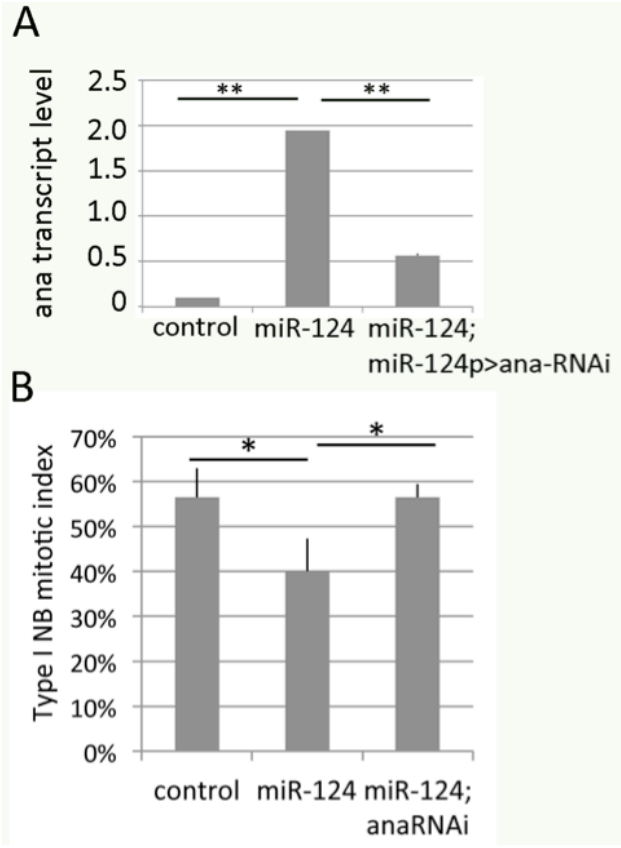

Figure 3.23 ANA functions in *miR-124* expressing neuronal lineages.

(A) Efficiency of *ana* knockdown by *UAS-ana-RNAi* driven by *miR-124-Gal4* activity. Normalized mRNA levels of *ana* measured by qRT-PCR in total RNA samples of 3rd instar larval brain of the indicated genotypes. Data are presented as mean ± SD based on three independent biological replicates. Two Asterisks: $P<0.01$ using the student t-test. (B) Functional test for the effect of *ana* depletion in *miR-124* mutant clones. Genotypes: control denotes Canton S, *miR-124* mutant, *miR-124* mutant clones that carrying 1 copy of the *UAS-ana-RNAi* allele. SD = 7% (control), 7% (*miR-124*) and 3% (*miR-124*;*UAS-ana -RNAi*).

3.2.4.6.3 *miR-124* limits *ana* expression in the NB lineages to functionally inconsequential level

Given that *ana* and *miR-124* are coexpressed in the NB lineage, I next asked whether the role of *miR-124* was to tune *ana* expression to optimal levels in the NB. Tuning relationships have been shown previously: in *miR-430* regulation of nodal activity [202]; in *miR-8* regulation of Atrophin in the CNS [48] and in *miR-14* regulation of Sugarbabe in the insulin-producing neurosecretory cells [203]. In the latter two cases, it was shown that the level of target expression that remained after miRNA-mediated downregulation was functionally significant in the miRNA-expressing cells. To address this issue I performed an experiment similar to that in Figure 3.23, except that the MARCM system was used to express the *UAS-ana-RNAi* transgene along with the *UAS-GFP* marker in wild-type control NB clones that expressed *miR-124* at normal levels. RNAi-mediated depletion of *ana* in these clones did not alter NB clone size (Figure 3.24). Thus, further reduction of *ana* levels below that achieved by *miR-124* appears to be without consequence on NB proliferation. On this basis I dismiss the possibility of a tuning relationship between *miR-124* and *ana* expression in the NB lineages. Instead, I propose that at least one of the roles of *miR-124* in the developing larval central brain was to limit the expression of *ana* to functionally insignificant levels in the NB lineage.

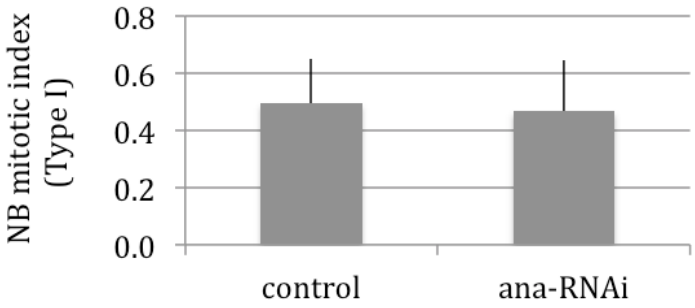

Figure 3.24 *miR-124* limits *ana* expression in NB lineages to optimal level.

Type I NB mitotic index for clones with the following genotypes: Canton S control, and Canton S flies that coexpressed the *UAS-ana-RNAi* transgene to deplete *ana* mRNA selectively in the marked NB clones. SD = 11% (control) and 5% (*UAS-ana-RNAi*).

3.2.5 *miR-124* function in adult fly behavior

3.2.5.1 *miR-124* loss of function reduces male courtship success

miR-124 is abundantly expressed in the adult brain of *Drosophila*. To explore the potential functions of *miR-124* in the adult brain, I examined a set of adult behaviors and observed a defect in the mating behavior of *miR-124* mutant males.

As mentioned in the introduction, *Drosophila* males engage in a complex set of courtship behaviors to induce receptiveness of females to mating. To ask if mating behavior is affected by *miR-124* loss of function, I used the classical male-female courtship assay. A sexually mature wild-type Canton S (CS) or *miR-124* mutant male was paired with a mature wild-type CS female virgin in a 10mm observation chamber. Behavior was quantified using a series of courtship parameters. *miR-124* mutant males exhibited a normal repertoire of behaviors, including orientation toward the female, courtship song, tapping, licking, abdomen curling, and attempted copulation. However, *miR-124* mutant males showed significantly lower levels of successful copulation than CS controls during the 30-minute observation period. While almost 90% of control males achieved copulation, less than 20% of *miR-124* males managed to do so (Figure 3.25A, ** $P<0.01$). This defect was rescued when *miR-124* expression was restored in the miRNA expressing cells of the mutant using the RMCE strategy. By contrast, when I paired 5-day old socially naïve CS males individually with 5-day old CS or *miR-124* virgin females and scored the number of females that accepted copulation over an observation period of 20 minutes, I did not observe

a significant difference in the receptiveness of *miR-124* mutant females and CS females to courtship (Figure 3.25B), suggesting that the defect was specific to males.

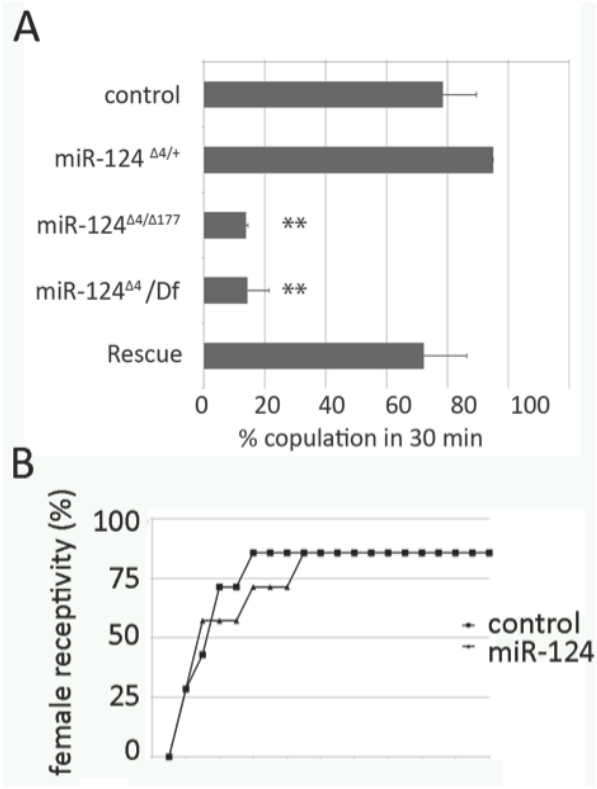

Figure 3.25 Performance of *miR-124* mutants in classical male courtship assay.

(A) Percentage of males achieving copulation in a 30 min observation period. Genotypes as indicated. Control males were CS. Rescue indicates the *miR-124* RMCE allele with miR-124 reintegrated at the endogenous locus (34). Data represent the average of 5 independent experiments ± SEM. ** = P<0.01 compared to heterozygous control. (B) Percentage of females that accepted copulation over an observation period of 20 minutes was scored. No significant difference was observed in receptivity of 5-day old control (CS) or *miR-124* virgin females towards 5-day old socially naïve CS males.

Reduced success at mating could be due to an inability to initiate courtship or to perform courtship behavior at all. To examine if there was a problem with courtship initiation, I scored for the initiation latency, which measures the amount of time taken by the male to recognize the female and begin courtship. As shown in Figure 3.26, I did not observe significant difference in initiation latency between mutant and control males, suggesting that the reduced copulation of the mutant is not due to an inability to initiate courtship.

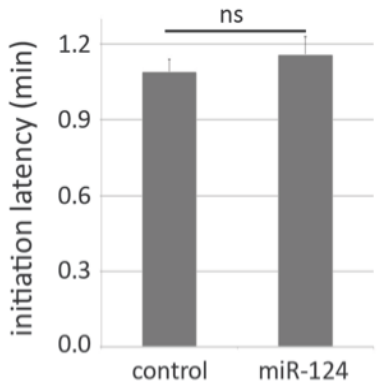

Figure 3.26 Performance of *miR-124* mutant males in courtship initiation.

Courtship initiation latency measures time (in min) to initiate copulation for CS control and *miR-124* flies. Data represent the average of 4 independent experiments ± SEM. ns: no significant difference.

Similarly, a possible contribution of reduced vigor of *miR-124* males in the courtship performance was ruled out when I scored for the courtship index, which measures the amount of time a male spends courting a target female. Since progression from courtship to copulation involves behavioral input from female flies [22, 204], I used decapitated female virgins as target flies to remove female behavioral response from the assay. Under these conditions, *miR-124* males showed levels of courtship activity comparable to the CS control males (Figure 3.27, the difference was not statistically significant). Therefore, the reduced mating success of mutant males is unlikely due to a reduced effort of the mutant in courtship performance.

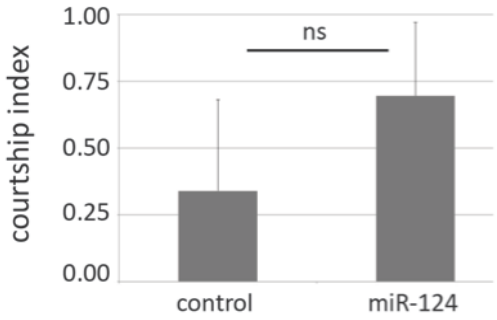

Figure 3.27 Performance of *miR-124* mutant males in maintaining courtship drive.

Courtship index compares the proportion of the measurement period males spent courting. CS control and *miR-124* mutant males were tested using decapitated CS females as targets. Data represent the average of 4 independent experiments ± SEM. ns: no significant difference.

Drosophila males use a courtship song produced by wing vibration as one means of communication to elicit receptivity in female flies. Therefore, another possible cause of the poor mating success of *miR-124* mutant males could be a defective courtship song generated by *miR-124* mutant males. If this was the cause, taking away the contribution of the courtship song from both genotypes should eliminate the difference in receptivity of females to control and mutant males. To investigate this possibility, I surgically removed the wings from control and mutant males and compared their performance with that of their intact siblings. Under these conditions, *miR-124* mutants were also less successful in mating than control males (Figure 3.28). Thus, courtship song does not appear to be an important contributor to the difference between control and mutant males.

Based on the detailed analysis of the courtship performance of *miR-124* mutant males, I conclude that the observed delayed onset of copulation therefore likely reflects rejection of the *miR-124* mutant male's advances by the female.

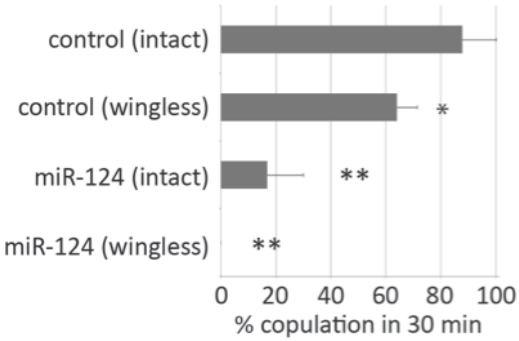

Figure 3.28 Effect of wing removal on copulation success.

Percentage of males achieving copulation in 30 min, comparing CS control and *miR-124* mutant flies before and after removal of the wings. Data represent the mean of more than 20 movies per genotype ± SD.*= P<0.05, **= P<0.01 compared to control.

3.2.5.2 *miR-124* mutant males induce aberrant behavior in other males

Very interestingly, I have occasionally observed males of *miR-124* mutants following each other in a chain-like manner when groups of males were housed together in a vial. It is known that *Drosophila* males normally pay little sexual attention to other sexually mature males. However, males with altered sexual orientation elicit a behavior called chaining, in which groups of males follow each other while attempting courtship [22, 155], which is very similar to what I have observed among groups of mature *miR-124* males. This indicates that there is abnormal courtship behavior among *miR-124* mutant males.

Male-male courtship among *Drosophila* males can result from a change in the expression of inhibitory or stimulatory cues, from an inability to recognize inhibitory courtship cues, or both. To examine the mutant behavior more closely and to distinguish between these possibilities, I quantified the courtship behavior of mutant and control males when placed with mutant or control male targets. In these assay, I used decapitated targets to ensure that target behavior did not influence the behavior of the test subject. There was no difference in the amount of time that *miR-124* mutant or CS control males devoted to courtship of CS target males, suggesting that the sexual orientation of the *miR-124* male was not altered (Figure 3.29A). By contrast, when decapitated *miR-124* mutant males were used as targets, both CS control and *miR-124* males were induced to perform significantly more courtship activity towards them (Figure 3.29A, ** $P<0.01$). This effect was suppressed when *miR-124* expression was restored in its endogenous domain (Figure 3.29B; ** $P<0.01$).

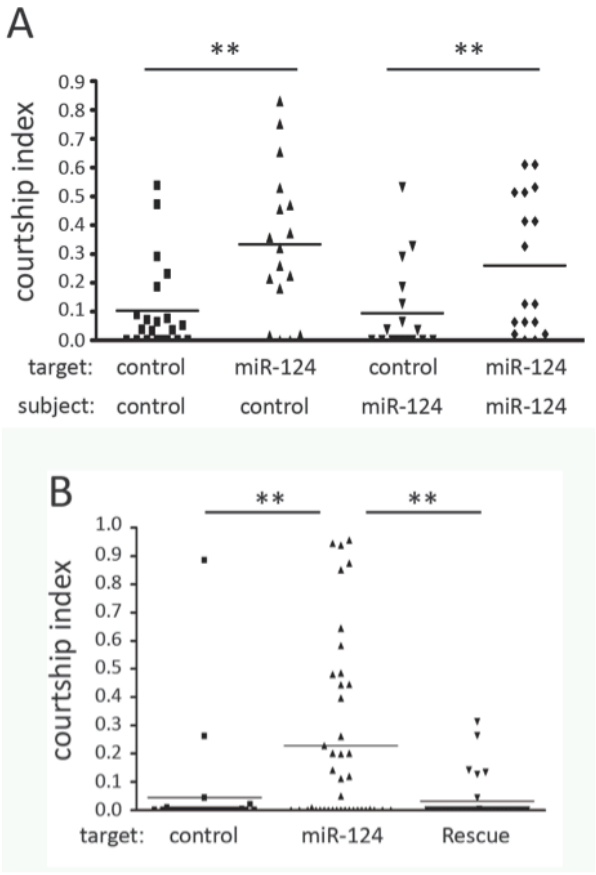

Figure 3.29 Performance of *miR-124* males in male-male courtship assay.

(A) Courtship index comparing CS control and *miR-124* mutant flies using decapitated CS or *miR-124* mutant males as targets. ** = P<0.01. (B) Courtship index for CS control males toward decapitated targets. The target genotypes used are CS control, *miR-124* mutant and rescued mutant. ** = P<0.01.

As an independent test for the higher level of male courtship elicited by *miR-124* mutant males, I performed a courtship choice assay. In this assay, I placed a wild-type CS male in a 20mm petri dish in the presence of a decapitated wild-type male on one end and a decapitated *miR-124* mutant male on the other, and recorded the amount of time the CS male spent courting either target within an observation window of 30 minutes. While wild-type CS males devoted about 10% of their time courting the wild type target, a level that is near the basal courtship elicitation by wild type males, males devoted more than twice as much time to courting the *miR-124* target (Figure 3.30; ** $P<0.01$). Thus, when presented with a choice of decapitated control or *miR-124* target males, CS males appeared to be more attracted by *miR-124* males than by CS males, and the effect did not depend on the behavior of the courtship target.

Based on these observations, I conclude that *miR-124* LOF does not affect sexual orientation of the males per se. The increased courtship induced by *miR-124* mutant males is more likely due to a change in chemical cues provided by *miR-124* males.

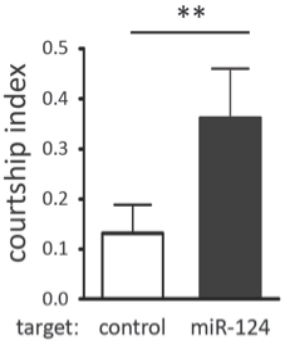

Figure 3.30 Courtship choice assay.

Courtship index (CI) using CS test males and *miR-124* mutant target males perfumed with hexane solvent alone as a control, or with hexane containing cVA. No significant difference was observed between CI of CS males towards *miR-124* target males perfumed with hexane (average CI = 0.320) or with cVA (average CI = 0.315).

3.2.5.3 Aberrant pheromone production by *miR-124* mutant males

Drosophila males produce several types of cuticular hydrocarbons that mediate chemical communication between males and females and among males [141, 148, 205, 206]. The observation that immobilized *miR-124* mutant males were sufficient to elicit an abnormal response in other males led me to postulate that the basis of the defect in the male-male courtship assay likely lay in chemical communications.

To test this hypothesis, I examined the pheromone profiles of the mutants. With the help of Dr. Joanne Yew and her student Ms. Jacquiline Chin from the Temasek LifeSciences Laboratory, I generated comprehensive cuticular hydrocarbon (CHC) profiles of sexually mature *miR-124* mutant and control male flies using gas chromatography/mass spectrometry (GC-MS). Interestingly, GC-MS analysis showed that the level of cVA was significantly reduced in *miR-124* mutant males (Figure 3.31A, ***P<0.001; Appendix 6.1), and was partially restored in rescued mutants (Figure 3.31A, ***P<0.001; Appendix 6.1). Conversely, pentacosenes were recovered at elevated levels from *miR-124* mutant males by GC-MS (Figure 3.31B, *P<0.05; Appendix 6.2) and were found at near normal levels in the rescue mutants (Figure 3.31B, **P<0.01; Appendix 6.2).

These results suggest that *miR-124* mutant males produce elevated levels of compounds that behave as male aphrodisiacs, and lower levels of compounds that have anti-aphrodisiac activity on males, leading to increased male-male courtship.

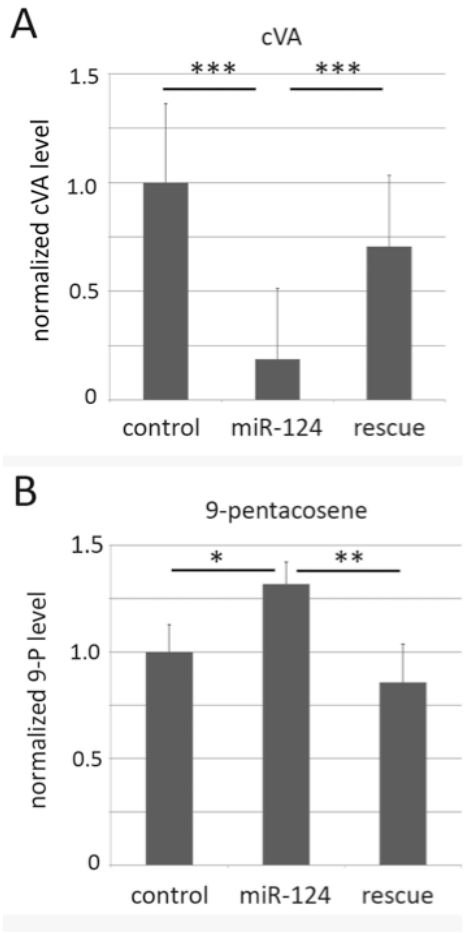

Figre 3.31 Aberrant pheromone production in *miR-124* mutant males.

(A) Normalized cVA level measured by GC-MS in extracts from control, *miR-124* mutant, and rescued mutant males. Data represent the average of 6 independent preparations ± SEM. *** = P<0.001. (B) Normalized 9-pentacosene level measured by GC-MS from from control, *miR-124* mutant, and rescued mutant males. Data represent the average of 6 independent preparations ± SEM. * = P<0.05, ** = P<0.01.

3.2.5.4 Aberrant pheromone level contributes to *miR-124* courtship phenotypes

The observation that *miR-124* mutant males show elevated levels of cuticular hydrocarbons, which behave as male aphrodisiacs, and lower levels of compounds that have male anti-aphrodisiac activity strongly support my initial hypothesis that the male-male behavioral abnormalities induced by *miR-124* mutant was due to aberrant chemical communications.

To ask whether these changes might be sufficient to account for the reduced mating success of *miR-124* mutant males, I carried out perfuming experiments. In these experiments, I perfumed control and *miR-124* mutant males either cVA or hexane as a solvent control and tested their copulation latency with mature CS female virgins in the classical male courtship assay. Strikingly, Mutant males perfumed with cVA showed a significant improvement in their ability to achieve copulation with control females (Figure 3.32A, * $P<0.05$). This indicates that the reduction in cVA level was at least partially responsible for the reduced mating success of *miR-124* mutant males

Since cVA has also been implicated as an inhibitor of male-male courtship, the reduction in cVA level in *miR-124* mutant males might contribute to the increased courtship induction by the mutant. To test this possibility, I also examined the effects of cVA perfuming on male courtship behavior. In this case, *miR-124* mutant males were similarly perfumed with cVA or hexane as a solvent control, decapitated and used as targets in the male-male courtship assay. However, I did not observe any significant difference between courtship of targets perfumed with cVA or with the hexane solvent alone (Figure 3.32B).

To measure the efficiency of the perfuming procedures, I measured the level of cVA on siblings of perfumed flies using mass spectrometry. The results indicated that the perfuming protocol restored cVA to <50% the level on control flies (Figure 3.32C). While this level of perfuming efficiency seemed to restore the mating success of *miR-124* mutant males, it failed to rescue the increased male courtship induction by the mutant males. Since the cVA-perfumed *miR-124* mutant target males also have elevated levels of one of the male aphrodisiacs, the pentacosene phenomones, the perfumed mutant males are expected to give mixed excitatory and inhibitory courtship signals. In this context, the level of cVA reached by perfuming may be insufficient to fully rescue male-male courtship, while being sufficient to restore male-female courtship. Another possibility is that cVA might be more effective at inhibiting male courtship if presented at a higher local concentration. While cVA is normally concentrated on the tip of the male ejaculatory apparatus, the perfuming experiment distributes cVA over the entire body.

Together, the perfuming experiments suggest that the changes in some of the pheromone compounds in *miR-124* mutant males contribute, at least partially, to the behavior abnormalities of the mutant.

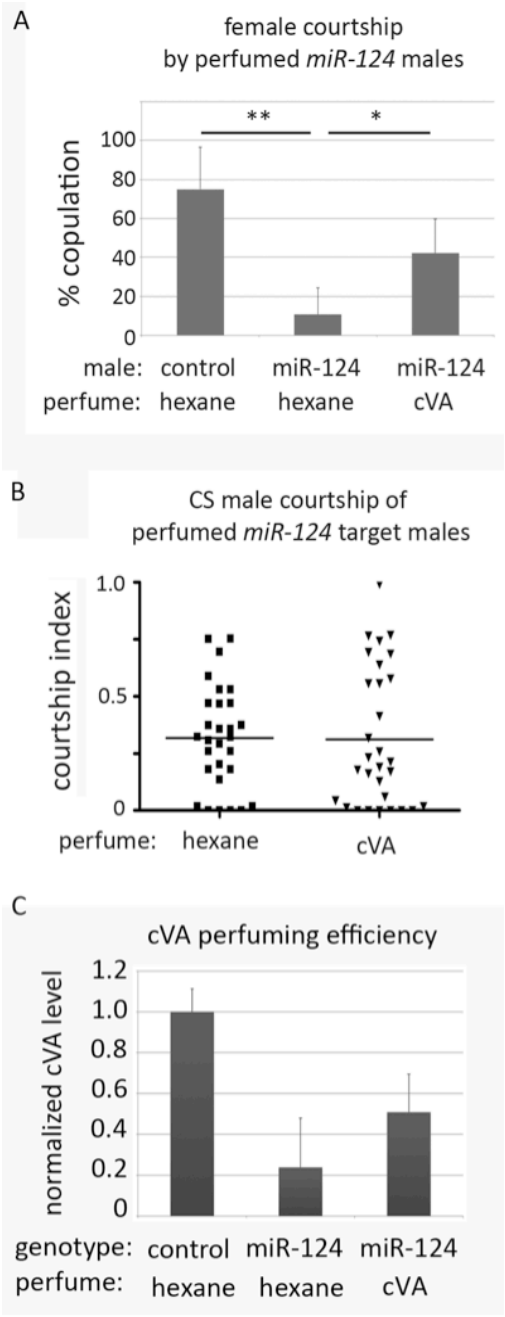

Figure 3.32: Effects of cVA perfuming on *miR-124* mutant phenotypes.

(A) Percentage of males achieving copulation in 30 min, comparing miR-124 mutant flies with or without cVA perfuming. Hexane perfuming was used as a control. Data represent the mean of more than 20 movies per genotype ± SD. * = P<0.05, ** = P<0.01 (B) Courtship index (CI) using CS test males and *miR-124* mutant target males perfumed with hexane solvent alone as a control, or with hexane containing cVA. No significant difference was observed between CI of CS males towards *miR-124* target males perfumed with hexane (average CI = 0.320) or with cVA (average CI = 0.315). (C) DART mass spectometry was used to assess the efficiency of the perfuming method. *miR-124* mutant males perfumed with cVA exhibited more cVA than solvent-perfumed *miR-124* mutant males and approximately 50% the amount of cVA found on control flies.

3.2.5.5 *miR-124* courtship phenotype is probably not due to mis-regulation of *ana*

Since mis-regulation of *ana* in *miR-124* loss-of-function during development caused a reduction in the total number of neurons, it is possible that this might have a consequence on adult behavior. To test this possibility, using the same RNAi line that has been used in the developmental study, I selectively knocked down *ana* in the cells that endogenously express *miR-124* in *miR-124* mutant background, and measured the copulation efficiency of these males. However, even though limiting the expression of *ana* this way has restored the reduction in MARCM clone size, it did not rescue the reduction in copulation efficiency of *miR-124* males (Figure 3.33). This suggests that the adult courtship defect is unlikely due to the mis-regulation of *ana* during development.

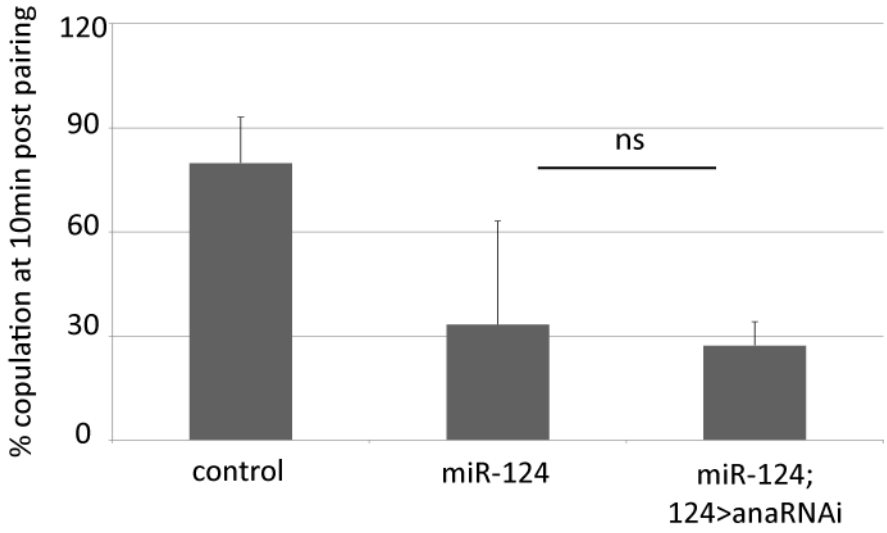

Figure 3.33 *ana* knockdown failed to rescue *miR-124* copulation defect.

Percentages of fly-pairs of the indicated genotypes in copulation at 10min post pairing. ns: not significant, comparing *miR-124* mutants and flies expressing a anaRNAi driven by *miR-124p-Gal4* in *miR-124* mutant background. Error bar srepresent SEM.

3.2.5.6 *miR-124* acts in the sex determination pathway

It is know that sexually dimorphic behavior and chemical communication are under the control of the sex determination pathway. In particular, the Dsx proteins have been shown to direct male vs female sexual differentiation, including pheromone production, as well as sexual behavior [174, 175, 206], whereas Fru^M controls male sexual behavior but not pheromone production [177, 178, 206]. Therefore, my next question was to ask whether *miR-124* might act in the sex determination pathway in its control on courtship behavior and pheromone level.

To selectively manipulate *miR-124* within the endogenous expression domain of the sex determination pathway, I made use of a miRNA sponge to deplete *miR-124* in *doublesex*-expressing cells and asked if manipulating *miR-124* level in these cells contributes to the male courtship elicitation phenotype. The *miR-124* sponge is a construct in which 10 copies of *miR-124* complementary sequences have been introduced in tandem at the 3'UTR of a UAS-dsRED reporter (Figure 3.34A). Induced expression of dsRED reporter under the effect of a Gal4 driver will lead to depletion of *miR-124* in the Gal4-expressing tissues, due to binding between the miRNA mature sequence and the miRNA sites in the 3'UTR of the reporter.

In *Drosopihla, doublesex* expression is sexually dimorphic in the brains of males and females [175, 206, 207]. In the male, Dsx^M is required for differentiation of Fru^M-expressing neurons [175, 206]. To increase efficacy, I expressed the sponge in males lacking one copy of the endogenous *miR-124* gene. Interestingly, while the *miR-124* heterozygous mutants did not elicit increased male courtship, further depletion of miR-124 in *dsx*-expressing cells elicited male courtship at a level comparable to that

elicited by homozygous *miR-124* null mutant target males (Figure 3.34B). This indicates that *miR-124* expression within the sex determination pathway could account for this phenotype.

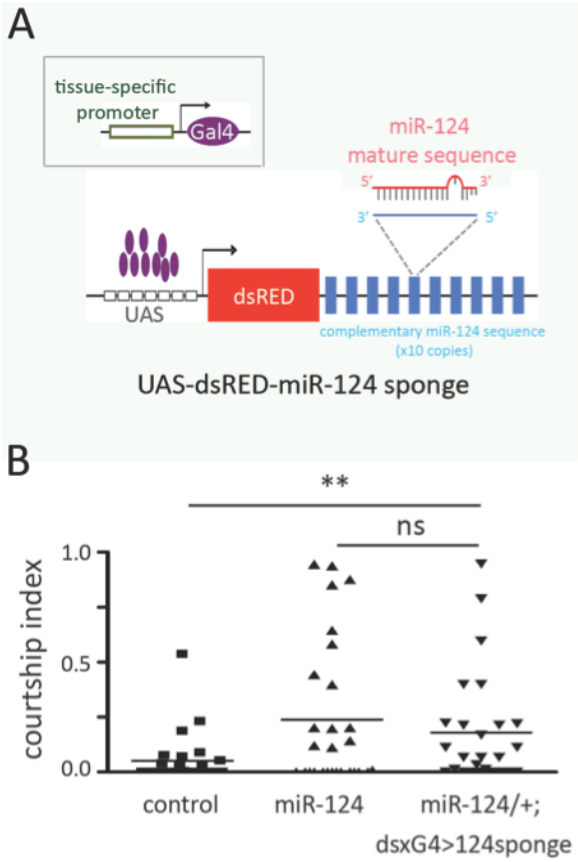

Figure 3.34 *miR-124* acts in the sex-determination pathway.

(A) Schematics showing the design of the UAS-dsRED-miR-124 sponge for tissues-specific depletion of *miR-124* in combination with the use a tissue-specific Gal4 driver (insert). (B) Courtship index comparing *miR-124* mutants and flies expressing a *miR-124* sponge under *dsx-Gal4* control with CS controls. ** = P<0.01 comparing flies expressing the *miR-124* sponge and CS control. ns: not significant, comparing *miR-124* mutants and flies expressing a *miR-124* sponge.

3.2.5.7 miR-124 acts directly on *transformer* to regulate pheromone production

I next sought to identify the target(s) of *miR-124*, which might be responsible for this phenotype. I thought that the most likely candidates in this context would be components and/or target(s) of the sex determination pathway since manipulations of this pathway have been shown to result in pheromone production errors and/or courtship behavior abnormalities.

Computational target prediction datasets do not list any of the known components of the sex determination pathway among predicted *miR-124* targets. To allow for the possibility that the prediction algorithms might miss sites with specific features, I scanned sex determination pathway transcripts using the RNAhybrid prediction tool ([22, 208]; *bibiserv.techfak.uni-bielefeld.de/rnahybrid/*) and found two potential sites for *miR-124* in the 3' UTR of *transformer* (Figure 3.35A). The *transformer* transcript is spliced in a sexually dimorphic manner, giving rise to a female-specific and a male-specific form. The first *miR-124* site is present in the 3' UTR region common to both the female-specific and non-sex-specific *tra* transcripts, while the second one is located in sequences unique to the non-sex-specific form. Pairing to residues 2-8 of the miRNA, called the seed region, is important in miRNA target identification [22, 184]. Each of the sites in *tra* would require 3 G:U base pairs with the *miR-124* seed. G:U base pairs in the seed region are compatible with miRNA function, but reduce the efficiency of target regulation [22, 184].

To ask if these *miR-124* sites on *tra* 3'UTR are functional, I carried out a luciferase reporter assay as described earlier on. Interestingly, co-expression of *miR-124* with a luciferase reporter carrying the 3'UTR sequence of the non-sex-specific *tra* transcript

showed repression of luciferase activity, showing that these sites can mediate regulation by *miR-124* (Figure 3.35B).

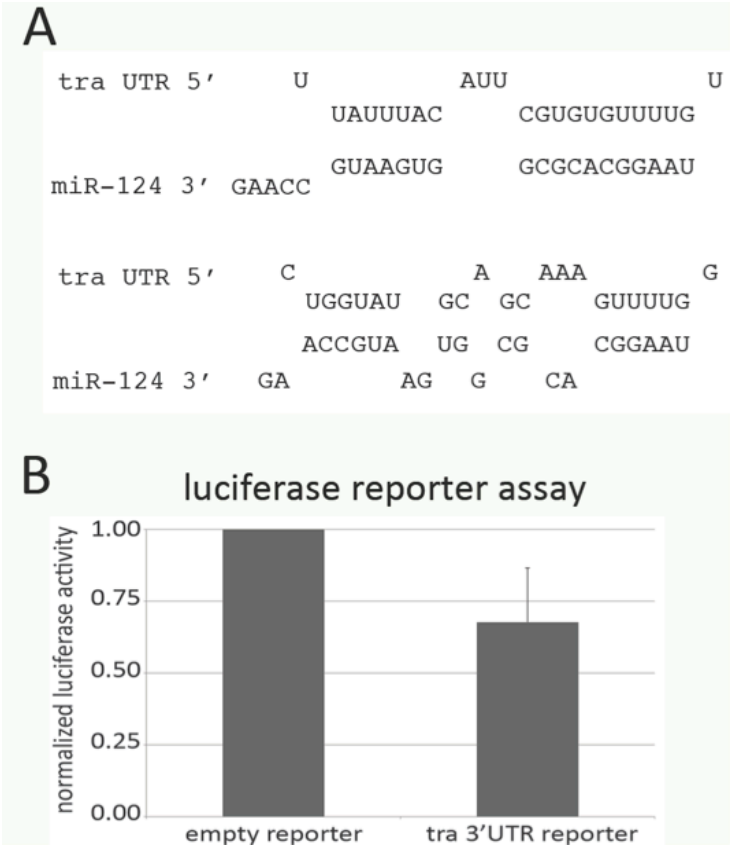

Figure 3.35 *miR-124* sites on *tra* 3'UTR are functional.

(A) Predicted pairing of *miR-124* to two sites in the tra^F transcript. (B) Luciferase reporter assay showing regulation of *miR-124* target sites on *tra* UTR by *miR-124*. Data show the mean ratio of firefly to Renilla luciferase activity based on three independent biological replicates. Error bars represent SEM. $P<0.05$ using two-tailed unpaired Student's t-test.

As a first step to determine whether *tra* might be a functionally important target of *miR-124* in vivo, I measured *tra* transcript levels by quantitative RT-PCR in RNA samples from control and *miR-124* mutant male heads. The *tra* primary transcript undergoes sex-specific splicing in females to produce tra^F, which encodes a splicing factor. In males an alternate splice form is produced, tra^M, which is thought to produce a non-functional protein (Figure 3.36A).

Using primers that recognize both splice forms, I observed that *tra* mRNA increased ~1.5 fold in the mutant and was restored to near normal levels in the rescued mutant (Figure 3.36B, * $P<0.05$).

Very interestingly, the use of a pair of primers that detects only the female-sepcific tra^F transcript showed a significant elevation of this isoform in RNA from *miR-124* mutant males (Figure 3.36C). This was intriguing since earlier studies on the sex determination pathway reported that the female-sepcific tra^F transcript is not present in males due to the absence of a functional Sxl protein expression (reviewed in [156]). Strikingly, the same primer pair detected low levels of this female-specific splice form in control males, albeit at a few percent of the level in females (Figure 3.36D). To confirm that the amplification signal obtained reflects the specificity of the primer pair from processed mRNA transcript of *tra*, rather than from contaminated genomic DNA, I performed the qRT-PCR measurement with this primer pair using nonRT RNA sample from the same experiment as the template. Under this condition, no specific qRT-PCR amplification curve was obtained (Figure 3.35E), confirming that the detection of tra^F mRNA in control males indeed reflects low level leaky tra^F expression in wild-type males.

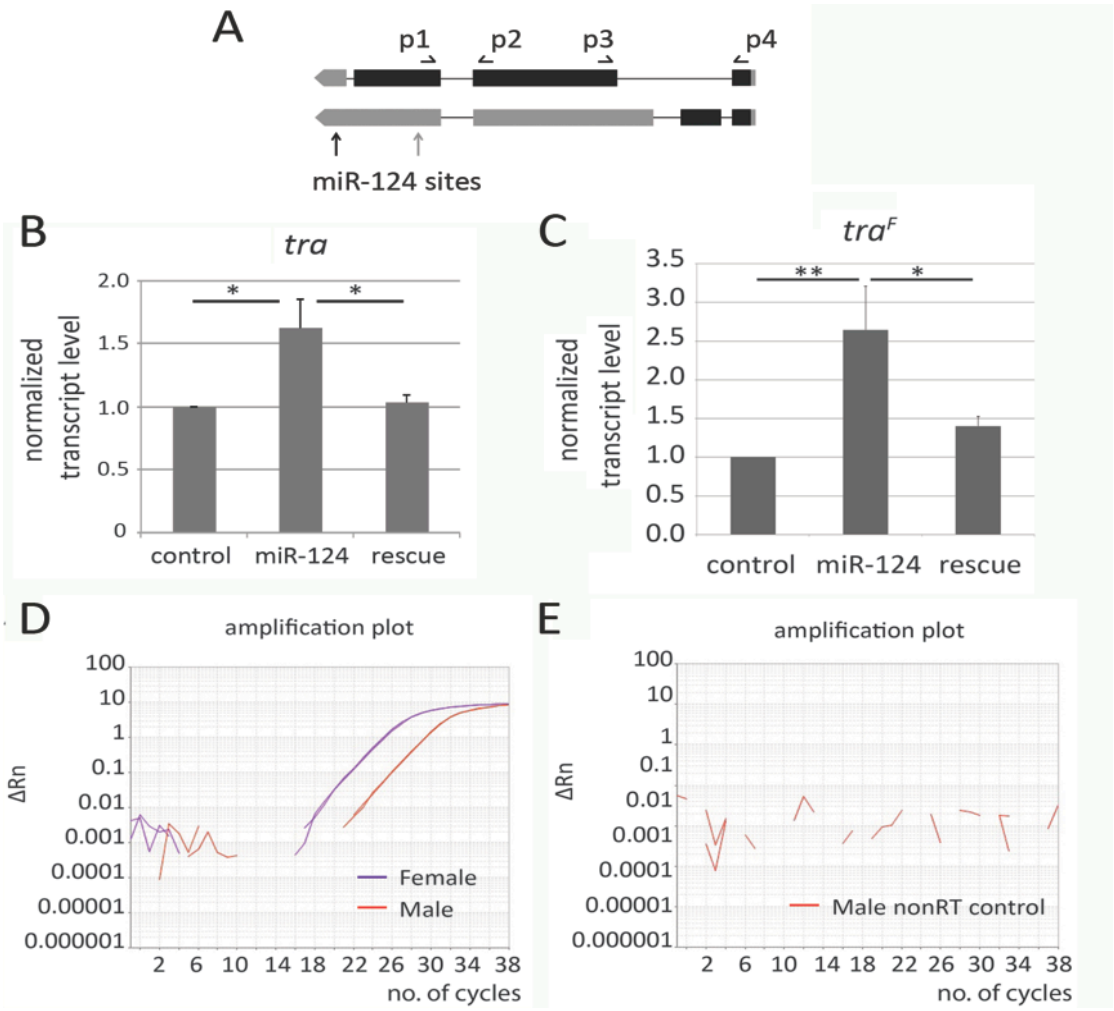

Figure 3.36 Upregulation of *tra* transcript in *miR-124* mutant males.

(A) Schematics showing female-specific tra^F isoform and non-sex-specific isoform tra^M. Exons are represented by black boxes, 5' UTR and 3' UTR by grey boxes. Sites for the primer-pairs used for detection of both isoforms (p1 and p2) and of the tra^F – specific isoform (p3 and p4) are indicated. The positions of the 2 *miR-124* target sites are indicated. (B) Elevated expression of *tra* transcript measured by quantitative real-time PCR using RNA isolated from male flies of the indicated genotypes. Data represent the average of 5 independent experiments ± SEM.* = P<0.05. (C) Normalized tra^F mRNA levels measured by quantitative RT-PCR in RNA from heads of 5-day old socially naïve males of the indicated genotypes. Actin42A was used as the internal control. Data are presented as the mean based on 6 independent biological replicates and error bars represent SD. * P<0.05, ** P<0.01 using the Wilcoxon two-sample test, comparing mutant to control or to rescue. (D) Detection of tra^F transcript in heads from 5-day old control females (purple line) and 5-day old males (orange line) was shown by the amplification curves from real-time quantitative RT-PCR experiments. The difference was ~4 cycles, or 32 fold. (E) No amplification was observed in controls not treated with reverse transcriptase (nonRT).

The observations from the measure of *tra* transcript level in *miR-124* mutant male samples indicate that *tra* is being regulated in a manner that is consistent with a regulation by *miR-124*. Therefore, the next step to take was to ask if the regulation of *tra* by *miR-124* contributes functionally to the mutant phenotypes.

To assess whether elevated *tra* expression contributes to the *miR-124* mutant phenotype, I asked if reducing *tra* levels would be sufficient to suppress the mutant phenotypes. For these experiments, I expressed a *UAS-tra*^{RNAi} transgene under *miR-124-Gal4* control in the *miR-124* mutant background. The transgene targets a region common to both female and non-sex-specific splice forms. As shown in Figure 3.36, lowering *tra* levels in the *miR-124* expressing cells was sufficient to rescue a range of *miR-124* mutant phenotypes, including restoration of normal male-female courtship behavior in *miR-124* mutant males (Figure 3.37A), suppression of the elevated male-male courtship (Figure 3.37B) and rescue of cVA production by several fold (Figure 3.37C; Appendix 2). In addition, depletion of *tra* lowered 9-pentacosene levels to within control levels, even though the change was not statistically significant. This could be due to the small sample size used for this experiment (Figure 3.37D; Appendix 2). These findings indicate that upregulation of *transformer* in the *miR-124* mutant is causally linked to both the pheromone production and behavioral abnormalities in the mutant males.

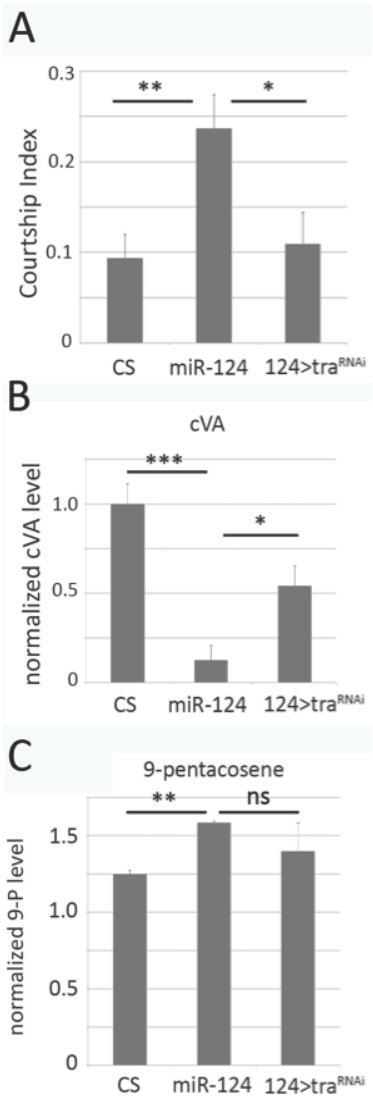

Figure 3.37 Functional rescue of *miR-124* mutant phenotypes by *tra* depletion.

(A) Percentage of males achieving copulation with CS females during the 30 min measurement period. Data represent the mean of more than 20 movies per genotype ± SD. Genotypes: CS: canton S control; *miR-124*: *miR-124* mutant; *124>tra*^{RNAi}: *miR-124*^{KO}*/miR-124*^{Gal4}*; UAS-traRNAi.* Depletion of *tra* significantly improved performance of the *miR-124* mutant males. * = P<0.05, ** = P<0.01. (B) Proportion of time CS males spent courting decapitated males of genotypes indicated in A. Data represent the mean of more than 35 movies per genotype ± SD. Depletion of *tra* significantly reduced the attractiveness of the *miR-124* mutant males to normal levels. * = P<0.05, ** = P<0.01. (C) Quantification of cVA levels in males of the indicated genotypes by GC-MS. Knocking down of *tra* in using *miR-124Gal4* driver significantly rescued the changes cVA levels in *miR-124* mutant males. Data represent the average of 2 (for *miR-124>tra*^{RNAi}) or 3 replicates (CS and *miR-124*) ± SEM * = P<0.05, *** = P<0.001. (D) Quantification of 9-pentacosene levels in males of the indicated genotypes by GC-MS. Depletion of *tra* lowered 9-pentacosene levels to within control levels. Data represent the average of 2 (for *miR-124>tra*^{RNAi}) or 3 replicates (CS and *miR-124*) ± SEM. * = P<0.05, ns: not significant.

3.2.5.8 *miR-124* is important for pre-mating reproductive fitness of the fly

Although *miR-124* mutant males showed less mating success in the courtship assay, they are fertile in laboratory conditions, as I have shown above. However, the reduced mating success might be expected to confer a disadvantage in a competitive situation, where the female has a choice of mates.

To test this, I performed a female mate-choice assay. In this assay, I placed single CS female virgins in mating chambers with one CS control male and one *miR-124* mutant or rescued mutant male and scored the choice of mate made by the female in each grouping. *miR-124* mutant males were rarely selected in the presence of a wild type male. Females did not distinguish between wild-type and rescued mutant males, with the rescued male achieving copulation at almost the equal chance as the wild-type male (Figure 3.38). This suggests that mutant males would likely be at a disadvantage in a natural competitive setting, whereby males normally have to compete with other males for successful mating with female flies.

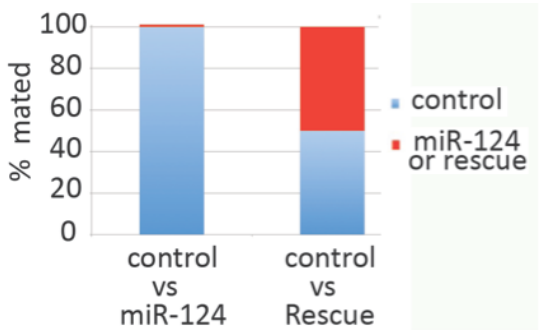

Figure 3.38 Performance of *miR-124* males in female mate choice assay.

Female mate choice was monitored by videotaping in chambers containing single females and two males of the indicated genotypes. The genotype of the male that succeeded in copulating was recorded. More than 95% of control male achieved copulation, in the presence of *miR-124* mutant males (left bar) compared with ~50% in the presence of rescued mutant males (right bar).

The result of the female choice assay described above led me to wonder if *miR-124* might be important for the reproductive fitness of male flies. In flies, mating success was found to be correlated with the aggressiveness of wild-type males in flies. More specifically, males that are less aggressive are often less successful in competing for the females [209]. Aggression is another social behavior commonly observed among *Drosophila* males, and is promoted by chemical cues such as cVA [209, 210]. The observation that *miR-124* mutant males are defective in its pheromone profile, particularly with respect to cVA, led me to ask if loss of *miR-124* influences aggressiveness of the males.

To do this, I analyzed the fighting behavior between pairs of mutant or wild-type male. In this setting, wild-type males typically fight for sole occupancy of the food patch, resulting in the establishment of a hierarchy [209, 211]. Interesting, *miR-124* mutant males exhibited overall lower levels of aggression based on several parameters. First, mutant males experienced more encounters before any fighting took place (latency, Figure 3.39A, ** $P<0.01$). In addition, mutant males exhibited lower frequency of fighting behaviors, including lunging and fencing (Figure 3.39B, ** $P<0.01$) and were often observed sharing the food patch after a few encounters.

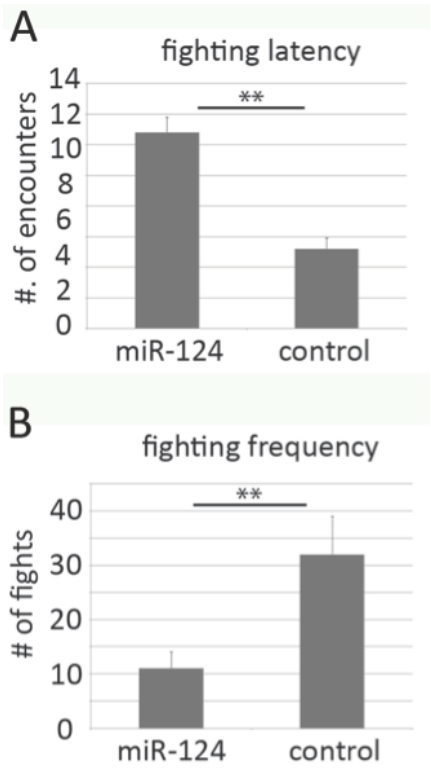

Figure 3.39 *miR-124* males are less aggressive than control males.

(A) Fighting latency was monitored by videotaping encounters between pairs of males in chambers containing a patch of food. Latency is the number of encounters that do not elicit aggressive behavior prior to the first fight. Data represent the mean of more than 16 movies per genotype ± SD. ** = P<0.01. (B) Fighting frequency was monitored by videotaping encounters between pairs of males in chambers containing a patch of food. Frequency records the number of aggressive encounters in 30 min. Data represent the mean of more than 16 movies per genotype ± SD. ** = P<0.01.

A reduction in fighting behavior overall could be due to reduced locomotion of the male. To rule out this possibility, I quantified the locomotion activity of control and *miR-124* mutant males by tracking the locomotion of single 5-day old control or mutant males placed in a 10mm courtship chamber. Quantification of the velocities of both genotypes showed no obvious difference in overall activity level between control and *miR-124* males (Figure 3.40). In addition, no obvious locomotor defects were observed during the aggression assay. These observations confirm that the reduced fighting behavior was not due to a reduction in overall mobility of *miR-124* mutant males.

Lower cVA production in the *miR-124* mutant may contribute to the lowered intensity of aggressive behaviors observed in these flies. By contrast, cVA has been reported to be the pheromone that promotes aggression in *Drosophila melanogaster* [212]. Therefore, this observation that *miR-124* mutant males are less aggressive is consistent with the observation that cVA production was significantly impaired by *miR-124* loss of function mutant males.

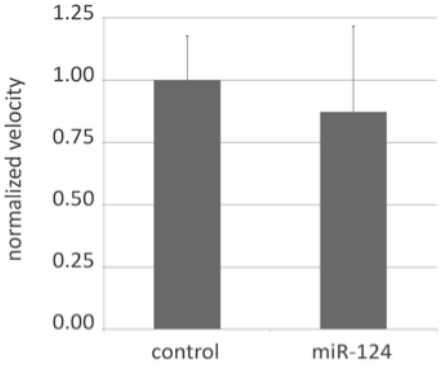

Figure 3.40 Performance of *miR-124* mutant males in locomotion assay.

The total distance travelled by single 5-day old males of the indicated genotypes in a 10mm courtship chamber was traced and measured for 10min. The velocity of each genotype was calculated and normalized to control level. 14 flies were recorded per genotype. There was no significant difference between the control and mutant flies.

4 Discussion

4.1 Advantages of modified ends-out gene targeting vectors

4.1.1 The pW25-RMCE vector

I have shown how incorporation of the recombinase-mediated cassette exchange (RMCE) strategy into the existing ends-out vector could increase the versatility of current gene targeting strategies by allowing repeated manipulations of a mutant genome after an initial targeting event.

An important genetic test for the specificity of any mutant phenotype is to ask if the phenotype is caused specifically by the loss of the targeted gene by re-introducing the gene of interest to the animal genome. However, the outcome of these experiments is, very often, dependent on the level of expression of the transgene. It is therefore difficult to interpret the results of such experiments when the genetic approach adopted either fails to achieve sufficient expression required for a particular biological process or when it results in overexpression or misexpression of the gene of interest. The advantage of using the knocked-in RMCE cassette at the targeted locus for 'genetic rescue' experiments is the wild-type sequence for the gene of interest can be re-introduced into its endogenous locus with just a few genetic crosses. Since expression of the replaced fragment will be driven under its endogenous promoter, this approach allows the 'rescue' gene to be expressed at more or less its wild-type level and perhaps more importantly, in its normal spatial and temporal expression pattern.

Similarly, combinations of protein-coding exons can be replaced using the knocked-in RMCE cassette to allow direct comparison of protein sequence variants at the

endogenous locus. This would be very useful in functional studies of protein domains and/or sequences.

During the course of this thesis work, two other independent groups have reported the use of RMCE strategies in gene targeting in flies. While Choi *et al.* [213] demonstrated use of RMCE for gene replacement at the *atonal* locus. Huang *et al.* [214] demonstrated the use of single *attP* and *loxP* sites in the generation of knockout flies that can serve as a docking site for recombinase-mediated integration for later manipulation. Compared to our system, the vectors generated by both groups have utilized shorter *attP* sequence of 54bp as compared to the 242bp sequence of the *attP* site in our vector. At the end of each gene-targeting event, the sequences between the homology arms and the *mini-white* marker are inserted at the targeted locus together with *mini-white*. This fragment, consisting of the FRT, the *loxP* and *att*P site might sometimes disrupt the endogenous locus. Therefore, the use of shorter *att*P sequence should result in even less disruptions to the flanking genomic sequence of the targeted locus. The functionality of the shorter, 54bp, *att*P site was not tested at the time when I was modifying the gene-targeting vector, thus not used in my modifications. By contrast, our RMCE system is faster and more efficient than the method described by Huang *et al.* [214].

4.1.2 The attB series of vectors

I have also shown how the use of *φC31*-mediated site-specific transformation can improve overall efficiency of the gene targeting strategy. Compared to the conventional *P*-element-mediated transformation, bacteriophage *φC31* integrase-mediated transformation can improve the efficiency of generating the transgenic stain carrying the targeting vector [216, 239]. In addition, it ensures that the donor

transgene is located on the desired chromosome, which eliminates two generations of crosses that would otherwise be needed to map donor transgenes generated by conventional *P*-element integration strategies to the desired chromosome.

The series of vectors modified in this study can provide useful flexibility to the current ends-out gene targeting strategy. The efficiency and high throughput provided by the *attB* series of vectors makes these the vectors of choice in large-scale mutagenesis studies. By contrast, the versatility provided by the pW25-RMCE vector makes it the vector of choice for in-depth genetic and functional characterization of the targeted gene/locus.

4.2 Functions and significance of *miR-124* in *Drosophila melanogaster*

The second half of this thesis aimed to elucidate the functions of a highly conserved miRNA, *miR-124*, in *Drosophila melanogaster*, focusing on its roles in the development and functions of the fly nervous system. I have presented evidence that *miR-124* is crucial in both development and in the control of adult functions.

4.2.1 Role of *miR-124* in *Drosophila* neurogenesis

In the first part of this analysis, I show that *miR-124* is required for larval neurogenesis in the central brain of the developing larvae. Two interesting and significant points from this part of the study are worth mentioning. The first point concerns the roles of this miRNA in invertebrate vs vertebrate neurogenesis. The second point is about the new insights provided by this study on the regulation and function of its functionally relevant target, *anachronism*, in the larval brain.

4.2.1.1 Roles of *miR-124* in invertebrate and vertebrate neurogenesis

In this part of the thesis work, I have provided evidence that the activity of *miR-124* in the larval neuroblast lineage is required to support proliferation, and that loss of *miR-124* activity in these cells results in under-proliferation of the neuronal progenitors and subsequently a reduction in total number of progeny, the mature neurons. This is in contrast with most results from various vertebrate systems, which were published prior to and during the course of this work. Despite some discrepancies, analysis of *miR-124* in vertebrates mainly point towards its roles as a positive regulator of neural differentiation and a negative regulator for neural progenitor proliferation.

In mammals, *miR-124* was first thought to behave like a determinant factor for neuronal cell fate by suppressing non-neuronal transcripts while promoting neuronal

transcripts expression. This was supported by evidence obtained from manipulation of *miR-124* levels in cultured cell lines using over-expression and antisense inhibition [95, 215, 216]. In one study, the authors showed that *miR-124*, in combination with another NS-specific miRNA, *miR-9*, stimulates neuronal and represses glial differentiation of cultured ES cells [215]. Consistently, expression of *miR-124* in the non-neuronal HeLa cells led to downregulation of non-neuronal mRNAs, changing its transcriptome profile significantly more similar to that of the brain [216]. Conversely, antisense inhibition of *miR-124* using 2'-OMe-RNA in primary cortical neurons led to increases in non-neuronal transcripts expression [95]. These initial analyses has led to the first notion of *miR-124* function in promoting neuronal cell fate while suppressing non-neuronal cell fate in the mammalian systems.

This notion that *miR-124* is both necessary and sufficient for mammalian neurogenesis was further supported by studies using *in vitro* neural differentiation models [55] [53]. In the first study, *miR-124* was shown to stimulate neuronal differentiation in the developing chick spinal cord and in a pluripotent embryonic carcinoma cell line, P19, through its repression on its target, SCP1. SCP1 is a small phosphatase that is specific for phosphoserines in the C-terminal domain of RNA polymerase II. It is involved in the function of the NRSF/REST complex, a global repressor of NS-specific transcription in non-neuronal cells. Similarly, overexpression of *miR-124* in two different mouse neuroblastoma cell lines induced neuronal differentiation by targeting a global repressor of alternative pre-mRNA splicing, PTBP1. PTBP1 is a repressor of alternative splicing, and suppression of PTBP1 led to the alternative splicing of another splicing regulator, PTBP2, resulting in correctly spliced and functional PTBP2. Increased level of PTBP2 in the

neuroblastoma cells caused a switch from non-neuronal to neuronal alternative splicing patterns and promotes neuronal differentiation. Together, these studies provide support to the idea that *miR-124* is acting in the neurons, where it is endogenously expressed, to repress NS-specific gene transcription globally [55].

The *in vitro* analysis mentioned above was further supported by subsequent *in vivo* experiments conducted by Chang *et al.* [54]. These authors have shown that *miR-124* depletion using antisense oligonucleotides in neuronal progenitors isolated from the subventricular zone (SVZ) of the mouse embryonic CNS has resulted in enhanced proliferation and reduced differentiation of these isolated neuronal progenitors. What is more interesting was that the authors were able to obtain similar results in *in vivo* experiments when they injected a pump to deliver antisense oligonucleotides against this miRNA to deplete endogenous *miR-124* in the SVZ of the mouse brain [54]. Therefore, it was concluded that mammalian *miR-124* functions by limiting neuronal progenitor proliferation while promoting neuronal differentiation.

However, this conclusion was at odds with another *in vivo* study performed in the chicken neural tube [99]. This study was reported contemporaneously with a study by Visvanatha *et al* [217]. Both studies were performed using similar experimental approaches. Visvanatha *et al* showed that depletion of *miR-124* by antisense injection resulted in reduced neuronal differentiation and ectopic proliferation. The study by Cao *et al.* reported that neither overexpression nor inhibition of *miR-124* by antisense injection significantly changed the acquisition of neuronal fate of chicken spinal cord neurons. Therefore, whether *miR-124* inhibits neuronal precursor proliferation and/or promotes neuronal differentiation in mammals remains ambiguous.

Overall, analysis of *miR-124* in vertebrates mainly point towards its roles as a positive regulator of neural differentiation and a negative regulator for neural progenitor differentiation through its negative regulation on several negative regulators of the neuronal differentiation pathway.

Given that *miR-124* has been 100% conserved in nucleotide sequence in all the animal models, including *Drosophila melanogaster* and all the vertebrates, I was initially surprised by the apparently contradictory roles revealed by my study in *Drosophila melanogaster* and reports in the vertebrate systems. Nevertheless, more in-depth comparisons and analysis suggest a few possibilities for this difference.

Could the phenotypic difference observed be due to methodological differences used in my study and the vertebrate studies? All of my analysis has been based on a genetic null mutant whereas the vertebrate studies have been based on either artificial over-expression or depletion of the miRNA using injected or transfected antisense oligonucleotides to reduce miRNA activity. Antisense depletion might not be efficient in reducing miRNA level to a functionally insufficient level, thus it allows only partial reduction of function. In addition, the possibility of off-target effects by antisense oligonucleotides means that antisense methods may introduce a certain degree of experimental variability. For example, conclusions based on miRNA depletion by antisense injection in *Drosophila* embryos [218] have been inconsistent with studies based on phenotypic analysis of genetic null mutants [219]. The availability of mouse knockouts of *miR-124* would allow one to ask if the analysis of

genetic null mutant animal support the findings reported using antisense methods, and thus would provide the means to address this possibility.

Perhaps a more biological basis for the discrepancy in function could be due to the subtle differences in the expression pattern of *miR-124* in the various systems. While *miR-124* expression has been thought to be broadly specific in the CNS of the various animal models, I have observed some level of differences in the characterizations of *miR-124* expression in *Drosophila melanogaster*. The observation of *miR-124* being expressed in both neural progenitors and mature neurons in my hand is consistent with only one report in the vertebrate system, which showed detection of *miR-124* activity in mouse neural progenitor cells using an *in vivo* GFP sensor for miRNA activity [220]. By contrast, most other vertebrate studies have reported the expression of *miR-124* in differentiating neurons but not in the neural progenitors. These conclusions were made based on results of *in situ* hybridization experiments using RNA probes directed against the mature and/or primary transcript of *miR-124* [53, 54, 99, 217, 221]. Therefore, there remains a possibility that there might be a corresponding function of *miR-124* in the neural progenitors of the vertebrate CNS, which might have been overlooked due to low-level expression of the mature miRNA.

Last but not least, yet another interesting possibility is that the different effects of *miR-124* of neuronal progenitor proliferation might reflect evolutionary divergence of *miR-124* function. This would be addressed in an independent session at the end of this chapter.

4.2.1.2 Expression of *anachronism* and its function

I present evidence that *miR-124* positively controls neural progenitor proliferation in the larval central brain by acting directly on its target *anachronism*. Sequence analysis suggests that *ana* encodes a secreted glycoprotein and a previous study has provided evidence that Ana protein acts as a negative regulator of neuroblast proliferation by acting on quiescent larval NB to prevent their premature entry into the proliferative phase [200]. The authors have shown that loss of *ana* function resulted in premature onset of NB proliferation. However, the authors have suggested that *ana* expression was specific to a subset of glial cells and proposed that Ana protein acts non-autonomously from glia to regulate NB proliferation. Unexpectedly, results of my analysis show that *miR-124* reduces *ana* to functionally inconsequential levels in the central brain NB lineage, and that failure to do so results in elevated *ana* level in these cells, leading to impaired NB proliferation. Contrary to the earlier report that *ana* expression was glia-specific, I have provided direct molecular evidence of presence of *ana* transcript in central brain NBs. In addition, I have presented evidence of function of elevated Ana in these cells.

Again, the lack of detection for the low level of *ana* in the NB lineages in the original study could be due to technical difficulties in the detection of a low abundance transcript using *in situ* hybridization, the main method used by these authors in the characterization of *ana* expression. I have used a more quantitative biochemical approach whereby the detection of the transcript was performed directly on an enriched pool of neuronal lineage cells, which was technically more sensitive in the identification of low abundance transcript.

Based on observations from this work, I hypothesize that the absence of *miR-124* in the glia cells in the larval brain allows a detectable level of *ana* expression in the cortex glia, as was proposed by the original study on *ana*. Expression of *ana* in the glia cells may serve as the functional source of Ana protein in early larval brains to control of the timing of onset of NB proliferation. By contrast, expression of *ana* in the NB lineage is limited by the presence of *miR-124* and failure to do so, as in the case where miR-124 has been genetically deleted from these cells, results in impairment of NB proliferation.

Another point of note is that the *UAS-ana RNAi* MARCM clonal analysis affect *ana* levels in the NB, in the GMC cells as well as in their post-mitotic progeny since the driver used in this experiment, the Elav-Gal4 driver, is expressed in all the cells in the NB lineages. Therefore, it is possible that Ana protein produced by any or all of the cells in the NB clonal lineage could act on the NB and GMC to affect their proliferation. As a result, it remains to be explored whether the effect of Ana protein within the NB lineages is a result of a non-autonomous activity of this secreted protein or a more local cellular interaction.

4.2.2 Role of *miR-124* in the adult

In the second part, I show that *miR-124* contributes to the regulation of adult fly social behaviors, such as courtship and aggression, by controlling the level of important fly pheromones.

4.2.2.1 Reinforcement of male sexual identity by suppressing leaky expression in the sex determination pathway

In this study, I have presented evidence that *miR-124* may be required for the reinforcement of male sexual identity by suppressing the consequences of leaky splicing in the sex determination pathway. I have also identified the sex-specific splicing factor *transformer* as the functionally significant target of miR-124 in this process. I suggest a role for *miR-124* in the control of male sexual differentiation and behavior, by limiting inappropriate expression of the female form of *transformer*.

It is generally thought that the sex determination pathway acts in a binary fashion, with particular spliced forms of the pathway being turned on or off, depending on the genetic sex of the cells [222, 223]. However, I was able to detect low-levels of the female-specific transcripts, tra^F and dsx^F in adult males. This has also been supported by observations made in another study in the literature [223, 224]. In the case of tra^F, this presumably reflects low-level leaky expression of Sxl in males. Inappropriate splicing to produce tra^F transcript in males would then lead to inappropriate splicing to produce dsx^F. Under normal conditions, the levels of these transcripts found in males are probably far below their respective functional threashold, although the kinetics of these molecules have yet to be studied. Indeed, quantification made in this study suggests that the level of tra^F in females are almost 30-fold higher than that amount detectable in males, suggesting that the leaky expression of tra^F is probably

far below its functional threshold. However, such leaky expression should be limited as higher levels of tra^F or dsx^F have been shown to compromise male sexual differentiation and behavior [181, 223, 225].

Findings from this work provide evidence that a modest elevation in the expression of tra^F in *miR-124* expressing cells interferes with male pheromone production. In this scenario, *miR-124*-mediated regulation ensures that leakiness in the production of tra^F is kept at levels that are functionally insignificant in the male. A modest increase in tra^F is not expected to have much effect in females, where the endogenous level is higher, which explains the lack of female phenotypes in this aspect. In this case, *miR-124* provides a secondary means of controlling the cascade of sex-specific splicing events that controls sexual differentiation in *Drosophila*. In this way, *miR-124* ensures the establishments of sexual identities, particularly male identities, which are crucial for the reproductive fitness of its species.

4.2.2.2 *miR-124* is required for proper male-specific pheromone production

I have presented evidence that *miR-124* is required to ensure fidelity of gender-appropriate pheromone production in males, which is an important element of male sexual identity.

Drosophila pheromones are sexually dimorphic in expression. The sex-specific biosynthesis of pheromone is controlled by the sex determination pathway. Genetic experiments have demonstrated the role of the Dsx protein in the regulation of male and female specific pheromone profiles. Genetic ablation of *dsx* locus in chromosomal females led to the loss of female-specific pheromones. Instead, they

produced pheromones that are normally made by the males. This suggests that expression of Dsx^F in females ensures the production of female-specific hydrocarbons while suppressing the production of male-specific hydrocarbons and other male-specific pheromones such as cVA. By contrast, such genetic ablation of the *dsx* locus in chromosomal males did not affect production of male-specific hydrocarbons. However, these 'males' expressed traces of female-specific hydrocarbons such as the *cis*-*cis*, 7-11-hetocosadiene, and a reduced amount of the males-specific lipid cVA. These observations have led to a few interesting conclusions. Firstly, it indicates the *dsx* locus is not required for production of male hydrocarbons, suggesting that male compounds represents the 'default state' of hydrocarbon production in *Drosophila melanogaster*. However, the presence of Dsx^M protein in males is probably required for biosynthesis of cVA, hinting at a possible differential genetic regulation for cVA and the hydrocarbons. Additionally, this observation shows that Dsx^M protein is required in males to ensure that synthesis of female-specific hydrocarbons is suppressed [174, 176, 223].

In this study, I have observed elevated level of *tra* transcripts in animals lacking *miR-124*. Although constitutive over-expression of Tra^F has been shown to masculinize the pheromone profile of chromosomal female *Drosophila* [176], a modest increase of Tra^F has not resulted in obvious phenotypes. By contrast, the presence of Tra^F is expected to affect sexual differentiation in males. For example, it has been shown that ectopic expression of Tra^F in males led to overall feminization of gender-specific traits in *Drosophila.* Similarly, tissue-specific expression of Tra^F in the oenocytes of chromosomally male flies caused the ectopic over-production of female-specific pheromones in these males. The molecular effect of Tra^F over-expression was

mediated through its regulation on gender-specific splicing of the downstream components of the sex-determination pathway. Likewise, Gal4-directed expression of Dsx^F in an otherwise wild-type male (also expressing Dsx^M) has been reported to reduce cVA levels, whereas Dsx^F expression in *dsx* mutant males abolished cVA production completely [174, 223]. This is consistent with the observation of low cVA production in *miR-124* mutant males, where an increase in expression of the tra^F isoform is expected to affect the downstream splicing of *dsx*.

Ectopic expression of Dsx^F in XY males has also been shown to cause production in female-specific diene-hydrocarbons such as 7,11-heptacosadiene and 7,11-nonacosadiene [174, 176]. If the effect of *miR-124*-mediated regulation on tra^F is consistent, we would then expect to observe these compounds in cuticular extracts from *miR-124* mutant males. However, this was not the case. None of the female-specific pheromones were detected in samples obtained from *miR-124* males. This is likely due to the absence of *miR-124* expression in the oenocytes where the Tra^F - Dsx^F cascade is thought to exert its effect on female hydrocarbon production.

By contrast, regulation of male-specific hydrocarbons is probably more complex. The male-specific hydrocarbons are also synthesized by the abdominal epidermal oenocytes, since genetic ablation of these cells abolished all male hydrocarbon production, but does not affect levels of cVA, which is made in the male ejaculatory bulb instead [147, 176]. Interestingly, while the site of hydrocarbons synthesis is generally thought to be oenocytes, manipulation of the sex determination cascade in the nervous system has affected production of subset of pheromones. For example, feminization of the nervous system in XY males by directing ectopic tra^F expression

using the pan-neuronal *elav-gal4* driver has led to significant elevations of the male hydrocarbons such as *cis*-7-tricosene and *cis*-9-pentacosene, although no gain of female hydrocarbons was observed [150, 176]. Additionally, brain specific RNAi-mediated depletion of a desaturase enzyme involved in pheromone biosynthesis was shown to alter pheromone production [176, 226], suggesting that the genetic sex of the central nervous system might indirectly modulate pheromone production in peripheral tissues. While *miR-124* is highly enriched in the *Drosophila* nervous system, particularly in the brain, I have also observed expression of this miRNA in the male reproductive organs, including the ejaculatory bulb. Therefore, it is likely that the regulation of pheromone production by *miR-124* could be mediated through its local expression in the ejaculatory bulb as well as its expression from the adult nervous system. However, exactly how the brain or its peripheral branches might affect pheromone production remains to be studied. In moth, the neuropeptide PBAN has been linked to control pheromone production, hinting that *miR-124* regulation of *transformer* could potentially act in the context of neuroendocrine control of male pheromone production. Further analysis would be required to address such possibilities.

4.2.2.3 Combinatorial code of action of pheromones on fly courtship behavior

While most studies on the roles of pheromones on social behaviors such as courtship and aggression have focused on the effect of a given class of compounds in isolation, observations made in this work leads to the hypothesis that a cocktail of several pheromonal compounds, each at its appropriate level, is used to control aspects of courtship behavior.

First of all, this hypothesis can be supported by the studies on the effects of cVA on mating behaviors in *Drosophila melanogaster*. The literature on cVA may appear rather controversial on a first glance. Some studies show that cVA mediates the classical male-female courtship behavior by promoting mating behavior in females, while inhibiting male-male courtship behavior [154]. Other studies report the lack of such observations [174, 234]. The differences probably could have arisen from the varied experimental context used in the different studies.

The study by Kurtovic *et al.* shows that female mutants of *Or67d* which encodes for one of the cVA receptors, are far less receptive than wild-type females. Mutant males of *Or67d* engage in vigorous male-male courtship. These observations suggest that activation of the cVA response pathway is necessary for both the induction of female receptivity and the inhibition of male-male courtship behavior.

By contrast, Billeter *et al.* shows that, despite the presence of wild-type level of cVA, male flies with their oenocytes genetically ablated and therefore do not express any hydrocarbons take much longer to copulate with wild-type females. These males also induce vigorous male-male courtship from sibling or wild-type males, suggesting that in the absence of the other courtship-mediating pheromones, cVA alone is not sufficient to induce female receptivity or to prevent male-male courtship.

The presence of multiple pheromones, with the corresponding response pathways, probably provide contextual information about the specific situation facing the fly, allowing it to make a particular behavior decision based on the combinatorial output of pathway activation. For example, when cVA is detected in the absence of nearby

flies, a scenario similar to the presence of oenocyteless males, a male fly might respond by moving toward this odor source. By contrast, if cVA is detected in combination with a close encounter with male cuticular hydrocarbons, the male fly might curb courtship behavior.

Evidence from this thesis work provides further support to this hypothesis. The observation that addition of cVA, while restoring mating success of *miR-124* mutant males with females in the classical mating assay, failed to suppress the high level of male courtship induced by mutant males could probably due to the elevated level of a male aphrodisiac, the cis-9-pentacosene, present on *miR-124* males. While further genetic tests and pheromone manipulation experiments are required to address this, I think that this study provides an interesting case to demonstrate the importance of understanding the combinatory output of several pheromones on animal behaviors.

4.3 Context-depending roles of miRNAs

I have presented evidence on how *miR-124* regulates 1) *Drosophila* neurogenesis by controlling neural progenitor proliferation; and 2) *Drosophila* adult functions by regulating male pheromone production. Results of these characterizations provide an example on the context-depending roles of animal miRNAs. In this case, depending on the developmental and biological contexts, *miR-124* may regulate vastly different targets.

Even though most vertebrate studies on *miR-124* have converged on its roles in limiting neuronal proliferation while promoting neural differentiation, there has been little overlap in the relevant targets identified in each report. In mouse studies alone, *miR-124* has been shown to regulate multiple targets, such as the high mobility group box transcription factor Sox9 in the subventricular zone of the adult mouse cortex, ephrin-B1 in the developing mouse cortex and the polypyridine tract-binding protein 1 (PTBP1) in non-neuronal cells [73, 74, 128, 248]. Evidently, *miR-124* regulates different targets during neuronal differentiation in a cellular context-dependent manner.

In addition, studies on the role of *miR-124* in the development of *Xenopus* eyes have presented evidences for a developmental stage-dependent role of *miR-124*. The authors first showed that overexpression of *miR-124* repressed cell proliferation and induced neurogenesis in the *Xenopus* optic cup. Using similar approaches, the same authors showed evidence for an opposite, anti-neural role for *miR-124* at the earlier optic vesicle stage [227, 228].

4.4 Evolution of miRNAs and their targets

It has been suggested that at least a third of miRNA families are highly conserved across species [229], and that more than 60% of miRNA loci are conserved from mouse to human [97]. In addition, among the highly conserved animal miRNAs, many have been broadly conserved in expression pattern. However, very few functional conserved miRNA:target relationships have been reported so far. Global analysis of miRNAs and their respective targets based on computational prediction suggested that conservation of predicted miRNA targets among nematodes, flies and vertebrates is close to what would be expected from chance [230]. One proposed underlying mechanism for this is that the miRNA regulatory networks have been substantially modulated during the course of animal evolution. One well-studied example is the highly conserve miRNA *let-7*. While *let-7* functions in the regulation of developmental timing in both worms and flies, the functional targets mediating such regulation by the miRNA differ in the two organisms [231-233]. Similar observations have been made in studies of another highly conserved miRNA in the nervous system, the miRNA *miR-9*. *miR-9* appears to be critical in early neural development in both mouse and zebrafish models, by controlling the expression of completely different subsets of targets [79, 234]. Furthermore, while *miR-9* appears to be grossly nervous system-specific in its expression, differs subtly in the specific region of expression in the nervous system of different organisms. As a result, the role of *miR-9* in *Drosophila* development is entirely unrelated to its known roles in the vertebrates [49, 78].

In the case of *miR-124*, the conclusion resulting from this work that *miR-124* activity is required in the neuroblast lineage to support proliferation seems to contradict with

findings from vertebrate systems, which have, mainly, suggested a role for *miR-124* in limiting neuronal progenitor proliferation and in promoting neuronal differentiation. The different effects of *miR-124* of neuronal progenitor proliferation in the different animal models could reflect evolutionary divergence of *miR-124* function. *miR-124* is predicted to target hundreds of genes according to computational prediction, expression profilings of miRNA overexpression and/or depletion, and biochemical experiments involving immunopurification of miRNA containing RNPs [124, 125, 128, 255-257]. However, there is little evidence of conservation of the identified or predicted targets between insects, nematodes and vertebrates. In this study, I have identified the *anachronism* gene as a functionally relevant target of *Drosophila miR-124 in vivo*, and provided direct genetic evidence that downregulation of *ana* expression in neuronal progenitors is required to support a normal level of proliferation within the larval central brain. The observation that the *ana* gene is not conserved beyond the *Drosophila* family suggests that the *miR-124* regulatory network could have been substantially altered during animal evolution. It is likely that the acquisition of this novel target in *Drosophila* that results from the parallel evolution of *miR-124* and its targets across animal kingdoms has led to an entirely distinct function in control of CNS proliferation in *Drosophila*.

Nevertheless, this leaves us with the puzzle of why *miR-124* is so strongly conserved. Perhaps some yet uncharacterized ancient functions of its role in neuronal development and/or functions await discovering, despite considerable diversification in gene regulatory networks. Similar observations have been made in highly conserved protein-coding genes, such as the bHLH-O family of protein, Hey (eg. [186]).

5 Bibliography

1. Allen, J.W. and C.W. Gwaltney, *Sister chromatid exchanges in mammalian meiotic chromosomes.* Basic life sciences, 1984. 29 Pt B: p. 629-45.
2. Spradling, A.C., et al., *The Berkeley Drosophila Genome Project gene disruption project: Single P-element insertions mutating 25% of vital Drosophila genes.* Genetics, 1999. 153(1): p. 135-77.
3. Salz, H.K., T.W. Cline, and P. Schedl, *Functional changes associated with structural alterations induced by mobilization of a P element inserted in the Sex-lethal gene of Drosophila.* Genetics, 1987. 117(2): p. 221-31.
4. Tower, J., et al., *Preferential transposition of Drosophila P elements to nearby chromosomal sites.* Genetics, 1993. 133(2): p. 347-59.
5. Zhang, P. and A.C. Spradling, *Efficient and dispersed local P element transposition from Drosophila females.* Genetics, 1993. 133(2): p. 361-73.
6. Preston, C.R. and W.R. Engels, *P-element-induced male recombination and gene conversion in Drosophila.* Genetics, 1996. 144(4): p. 1611-22.
7. Preston, C.R., J.A. Sved, and W.R. Engels, *Flanking duplications and deletions associated with P-induced male recombination in Drosophila.* Genetics, 1996. 144(4): p. 1623-38.
8. Golic, M.M., et al., *FLP-mediated DNA mobilization to specific target sites in Drosophila chromosomes.* Nucleic Acids Res, 1997. 25(18): p. 3665-71.
9. Gong, M. and Y.S. Rong, *Targeting multi-cellular organisms.* Curr Opin Genet Dev, 2003. 13(2): p. 215-20.
10. Gong, W.J. and K.G. Golic, *Ends-out, or replacement, gene targeting in Drosophila.* Proc Natl Acad Sci U S A, 2003. 100(5): p. 2556-61.
11. Rong, Y.S., *Gene targeting by homologous recombination: a powerful addition to the genetic arsenal for Drosophila geneticists.* Biochem Biophys Res Commun, 2002. 297(1): p. 1-5.
12. Rong, Y.S. and K.G. Golic, *Gene targeting by homologous recombination in Drosophila.* Science, 2000. 288(5473): p. 2013-8.
13. Rong, Y.S. and K.G. Golic, *A targeted gene knockout in Drosophila.* Genetics, 2001. 157(3): p. 1307-12.
14. Bateman, J.R. and C.T. Wu, *A simple polymerase chain reaction-based method for the construction of recombinase-mediated cassette exchange donor vectors.* Genetics, 2008. 180(3): p. 1763-6.
15. Bateman, J.R., A.M. Lee, and C.T. Wu, *Site-specific transformation of Drosophila via phiC31 integrase-mediated cassette exchange.* Genetics, 2006. 173(2): p. 769-77.
16. Bushati, N. and S.M. Cohen, *microRNA functions.* Annual review of cell and developmental biology, 2007. 23: p. 175-205.
17. Lee, Y., et al., *MicroRNA genes are transcribed by RNA polymerase II.* The EMBO journal, 2004. 23(20): p. 4051-60.
18. Cai, X., C.H. Hagedorn, and B.R. Cullen, *Human microRNAs are processed from capped, polyadenylated transcripts that can also function as mRNAs.* RNA, 2004. 10(12): p. 1957-66.
19. Rodriguez, A., et al., *Identification of mammalian microRNA host genes and transcription units.* Genome research, 2004. 14(10A): p. 1902-10.
20. Morlando, M., et al., *Primary microRNA transcripts are processed co-transcriptionally.* Nature structural & molecular biology, 2008. 15(9): p. 902-9.

21. Okamura, K., et al., *The mirtron pathway generates microRNA-class regulatory RNAs in Drosophila.* Cell, 2007. 130(1): p. 89-100.
22. Ruby, J.G., et al., *Evolution, biogenesis, expression, and target predictions of a substantially expanded set of Drosophila microRNAs.* Genome research, 2007. 17(12): p. 1850-64.
23. Yi, R., et al., *Exportin-5 mediates the nuclear export of pre-microRNAs and short hairpin RNAs.* Genes & development, 2003. 17(24): p. 3011-6.
24. Jiang, F., et al., *Dicer-1 and R3D1-L catalyze microRNA maturation in Drosophila.* Genes & development, 2005. 19(14): p. 1674-9.
25. Forstemann, K., et al., *Normal microRNA maturation and germ-line stem cell maintenance requires Loquacious, a double-stranded RNA-binding domain protein.* PLoS biology, 2005. 3(7): p. e236.
26. Schwarz, D.S., et al., *Asymmetry in the assembly of the RNAi enzyme complex.* Cell, 2003. 115(2): p. 199-208.
27. Khvorova, A., A. Reynolds, and S.D. Jayasena, *Functional siRNAs and miRNAs exhibit strand bias.* Cell, 2003. 115(2): p. 209-16.
28. Matranga, C., et al., *Passenger-strand cleavage facilitates assembly of siRNA into Ago2-containing RNAi enzyme complexes.* Cell, 2005. 123(4): p. 607-20.
29. O'Donnell, K.A., et al., *c-Myc-regulated microRNAs modulate E2F1 expression.* Nature, 2005. 435(7043): p. 839-43.
30. Viswanathan, S.R., G.Q. Daley, and R.I. Gregory, *Selective blockade of microRNA processing by Lin28.* Science, 2008. 320(5872): p. 97-100.
31. Piskounova, E., et al., *Determinants of microRNA processing inhibition by the developmentally regulated RNA-binding protein Lin28.* The Journal of biological chemistry, 2008. 283(31): p. 21310-4.
32. Rybak, A., et al., *A feedback loop comprising lin-28 and let-7 controls pre-let-7 maturation during neural stem-cell commitment.* Nature cell biology, 2008. 10(8): p. 987-93.
33. Heo, I., et al., *Lin28 mediates the terminal uridylation of let-7 precursor MicroRNA.* Molecular cell, 2008. 32(2): p. 276-84.
34. Heo, I., et al., *TUT4 in concert with Lin28 suppresses microRNA biogenesis through pre-microRNA uridylation.* Cell, 2009. 138(4): p. 696-708.
35. Heo, I., et al., *Mono-uridylation of pre-microRNA as a key step in the biogenesis of group II let-7 microRNAs.* Cell, 2012. 151(3): p. 521-32.
36. Bartel, D.P., *MicroRNAs: target recognition and regulatory functions.* Cell, 2009. 136(2): p. 215-33.
37. Stark, A., et al., *Animal MicroRNAs confer robustness to gene expression and have a significant impact on 3'UTR evolution.* Cell, 2005. 123(6): p. 1133-46.
38. Lim, L.P., et al., *Vertebrate microRNA genes.* Science, 2003. 299(5612): p. 1540.
39. Doench, J.G. and P.A. Sharp, *Specificity of microRNA target selection in translational repression.* Genes & development, 2004. 18(5): p. 504-11.
40. Bushati, N. and S.M. Cohen, *microRNA functions.* Annu Rev Cell Dev Biol, 2007. 23: p. 175-205.
41. Filipowicz, W., S.N. Bhattacharyya, and N. Sonenberg, *Mechanisms of post-transcriptional regulation by microRNAs: are the answers in sight?* Nat Rev Genet, 2008. 9(2): p. 102-14.
42. Hatfield, S.D., et al., *Stem cell division is regulated by the microRNA pathway.* Nature, 2005. 435(7044): p. 974-8.

43. Grishok, A., et al., *Genes and mechanisms related to RNA interference regulate expression of the small temporal RNAs that control C. elegans developmental timing.* Cell, 2001. 106(1): p. 23-34.
44. Jin, Z. and T. Xie, *Dcr-1 maintains Drosophila ovarian stem cells.* Current biology : CB, 2007. 17(6): p. 539-44.
45. Wienholds, E., et al., *The microRNA-producing enzyme Dicer1 is essential for zebrafish development.* Nature genetics, 2003. 35(3): p. 217-8.
46. Murchison, E.P., et al., *Characterization of Dicer-deficient murine embryonic stem cells.* Proceedings of the National Academy of Sciences of the United States of America, 2005. 102(34): p. 12135-40.
47. Li, X. and R.W. Carthew, *A microRNA mediates EGF receptor signaling and promotes photoreceptor differentiation in the Drosophila eye.* Cell, 2005. 123(7): p. 1267-77.
48. Karres, J.S., et al., *The conserved microRNA miR-8 tunes atrophin levels to prevent neurodegeneration in Drosophila.* Cell, 2007. 131(1): p. 136-45.
49. Bejarano, F., P. Smibert, and E.C. Lai, *miR-9a prevents apoptosis during wing development by repressing Drosophila LIM-only.* Developmental biology, 2010. 338(1): p. 63-73.
50. Shibata, M., et al., *MicroRNA-9 regulates neurogenesis in mouse telencephalon by targeting multiple transcription factors.* The Journal of neuroscience : the official journal of the Society for Neuroscience, 2011. 31(9): p. 3407-22.
51. Pietrzykowski, A.Z., et al., *Posttranscriptional regulation of BK channel splice variant stability by miR-9 underlies neuroadaptation to alcohol.* Neuron, 2008. 59(2): p. 274-87.
52. Coolen, M., et al., *miR-9 controls the timing of neurogenesis through the direct inhibition of antagonistic factors.* Developmental cell, 2012. 22(5): p. 1052-64.
53. Makeyev, E.V., et al., *The MicroRNA miR-124 promotes neuronal differentiation by triggering brain-specific alternative pre-mRNA splicing.* Molecular cell, 2007. 27(3): p. 435-48.
54. Cheng, L.C., et al., *miR-124 regulates adult neurogenesis in the subventricular zone stem cell niche.* Nat Neurosci, 2009. 12(4): p. 399-408.
55. Visvanathan, J., et al., *The microRNA miR-124 antagonizes the anti-neural REST/SCP1 pathway during embryonic CNS development.* Genes & development, 2007. 21(7): p. 744-9.
56. Yu, J.Y., et al., *MicroRNA miR-124 regulates neurite outgrowth during neuronal differentiation.* Experimental cell research, 2008. 314(14): p. 2618-33.
57. Sun, K., et al., *Neurophysiological defects and neuronal gene deregulation in Drosophila mir-124 mutants.* PLoS genetics, 2012. 8(2): p. e1002515.
58. Xu, X.L., et al., *The steady-state level of the nervous-system-specific microRNA-124a is regulated by dFMR1 in Drosophila.* The Journal of neuroscience : the official journal of the Society for Neuroscience, 2008. 28(46): p. 11883-9.
59. Rajasethupathy, P., et al., *Characterization of small RNAs in Aplysia reveals a role for miR-124 in constraining synaptic plasticity through CREB.* Neuron, 2009. 63(6): p. 803-17.
60. Hollander, J.A., et al., *Striatal microRNA controls cocaine intake through CREB signalling.* Nature, 2010. 466(7303): p. 197-202.
61. Magill, S.T., et al., *microRNA-132 regulates dendritic growth and arborization of newborn neurons in the adult hippocampus.* Proceedings of the

National Academy of Sciences of the United States of America, 2010. 107(47): p. 20382-7.
62. Lusardi, T.A., et al., *Ischemic preconditioning regulates expression of microRNAs and a predicted target, MeCP2, in mouse cortex.* Journal of cerebral blood flow and metabolism : official journal of the International Society of Cerebral Blood Flow and Metabolism, 2010. 30(4): p. 744-56.
63. Alvarez-Saavedra, M., et al., *miRNA-132 orchestrates chromatin remodeling and translational control of the circadian clock.* Human molecular genetics, 2011. 20(4): p. 731-51.
64. Schratt, G.M., et al., *A brain-specific microRNA regulates dendritic spine development.* Nature, 2006. 439(7074): p. 283-9.
65. Khudayberdiev, S., R. Fiore, and G. Schratt, *MicroRNA as modulators of neuronal responses.* Communicative & integrative biology, 2009. 2(5): p. 411-3.
66. Choi, P.S., et al., *Members of the miRNA-200 family regulate olfactory neurogenesis.* Neuron, 2008. 57(1): p. 41-55.
67. Cheng, H.Y. and K. Obrietan, *Revealing a role of microRNAs in the regulation of the biological clock.* Cell Cycle, 2007. 6(24): p. 3034-5.
68. Chang, S., et al., *MicroRNAs act sequentially and asymmetrically to control chemosensory laterality in the nematode.* Nature, 2004. 430(7001): p. 785-9.
69. Cayirlioglu, P., et al., *Hybrid neurons in a microRNA mutant are putative evolutionary intermediates in insect CO2 sensory systems.* Science, 2008. 319(5867): p. 1256-60.
70. Luo, W. and A. Sehgal, *Regulation of circadian behavioral output via a MicroRNA-JAK/STAT circuit.* Cell, 2012. 148(4): p. 765-79.
71. Giraldez, A.J., et al., *Zebrafish MiR-430 promotes deadenylation and clearance of maternal mRNAs.* Science, 2006. 312(5770): p. 75-9.
72. Giraldez, A.J., et al., *MicroRNAs regulate brain morphogenesis in zebrafish.* Science, 2005. 308(5723): p. 833-8.
73. De Pietri Tonelli, D., et al., *miRNAs are essential for survival and differentiation of newborn neurons but not for expansion of neural progenitors during early neurogenesis in the mouse embryonic neocortex.* Development, 2008. 135(23): p. 3911-21.
74. Davis, T.H., et al., *Conditional loss of Dicer disrupts cellular and tissue morphogenesis in the cortex and hippocampus.* The Journal of neuroscience : the official journal of the Society for Neuroscience, 2008. 28(17): p. 4322-30.
75. Schaefer, A., et al., *Cerebellar neurodegeneration in the absence of microRNAs.* The Journal of experimental medicine, 2007. 204(7): p. 1553-8.
76. Wang, Y., et al., *DGCR8 is essential for microRNA biogenesis and silencing of embryonic stem cell self-renewal.* Nature genetics, 2007. 39(3): p. 380-5.
77. Johnston, R.J. and O. Hobert, *A microRNA controlling left/right neuronal asymmetry in Caenorhabditis elegans.* Nature, 2003. 426(6968): p. 845-9.
78. Li, Y., et al., *MicroRNA-9a ensures the precise specification of sensory organ precursors in Drosophila.* Genes & development, 2006. 20(20): p. 2793-805.
79. Shibata, M., et al., *MicroRNA-9 modulates Cajal-Retzius cell differentiation by suppressing Foxg1 expression in mouse medial pallium.* The Journal of neuroscience : the official journal of the Society for Neuroscience, 2008. 28(41): p. 10415-21.
80. Sutton, M.A. and E.M. Schuman, *Dendritic protein synthesis, synaptic plasticity, and memory.* Cell, 2006. 127(1): p. 49-58.

81. Sutton, M.A., et al., *Miniature neurotransmission stabilizes synaptic function via tonic suppression of local dendritic protein synthesis.* Cell, 2006. 125(4): p. 785-99.
82. Lugli, G., et al., *Expression of microRNAs and their precursors in synaptic fractions of adult mouse forebrain.* Journal of neurochemistry, 2008. 106(2): p. 650-61.
83. Siegel, G., et al., *A functional screen implicates microRNA-138-dependent regulation of the depalmitoylation enzyme APT1 in dendritic spine morphogenesis.* Nature cell biology, 2009. 11(6): p. 705-16.
84. Fiore, R., et al., *Mef2-mediated transcription of the miR379-410 cluster regulates activity-dependent dendritogenesis by fine-tuning Pumilio2 protein levels.* The EMBO journal, 2009. 28(6): p. 697-710.
85. Impey, S., et al., *Defining the CREB regulon: a genome-wide analysis of transcription factor regulatory regions.* Cell, 2004. 119(7): p. 1041-54.
86. Berdnik, D., et al., *MicroRNA processing pathway regulates olfactory neuron morphogenesis.* Current biology : CB, 2008. 18(22): p. 1754-9.
87. Caudy, A.A., et al., *Fragile X-related protein and VIG associate with the RNA interference machinery.* Genes & development, 2002. 16(19): p. 2491-6.
88. Jin, P., R.S. Alisch, and S.T. Warren, *RNA and microRNAs in fragile X mental retardation.* Nature cell biology, 2004. 6(11): p. 1048-53.
89. Li, Z., et al., *The fragile X mental retardation protein inhibits translation via interacting with mRNA.* Nucleic acids research, 2001. 29(11): p. 2276-83.
90. Parsons, M.J., et al., *Using hippocampal microRNA expression differences between mouse inbred strains to characterise miRNA function.* Mammalian genome : official journal of the International Mammalian Genome Society, 2008. 19(7-8): p. 552-60.
91. Cheng, H.Y., et al., *microRNA modulation of circadian-clock period and entrainment.* Neuron, 2007. 54(5): p. 813-29.
92. Kadener, S., et al., *A role for microRNAs in the Drosophila circadian clock.* Genes & development, 2009. 23(18): p. 2179-91.
93. Yang, M., et al., *Circadian regulation of a limited set of conserved microRNAs in Drosophila.* BMC genomics, 2008. 9: p. 83.
94. Chen, P.Y., et al., *The developmental miRNA profiles of zebrafish as determined by small RNA cloning.* Genes & development, 2005. 19(11): p. 1288-93.
95. Conaco, C., et al., *Reciprocal actions of REST and a microRNA promote neuronal identity.* Proceedings of the National Academy of Sciences of the United States of America, 2006. 103(7): p. 2422-7.
96. Gao, F.B., *Context-dependent functions of specific microRNAs in neuronal development.* Neural development, 2010. 5: p. 25.
97. Griffiths-Jones, S., et al., *miRBase: tools for microRNA genomics.* Nucleic acids research, 2008. 36(Database issue): p. D154-8.
98. Kapsimali, M., et al., *MicroRNAs show a wide diversity of expression profiles in the developing and mature central nervous system.* Genome biology, 2007. 8(8): p. R173.
99. Cao, X., S.L. Pfaff, and F.H. Gage, *A functional study of miR-124 in the developing neural tube.* Genes & development, 2007. 21(5): p. 531-6.
100. Shkumatava, A., et al., *Coherent but overlapping expression of microRNAs and their targets during vertebrate development.* Genes & development, 2009. 23(4): p. 466-81.

101. Fischbach, S.J. and T.J. Carew, *MicroRNAs in memory processing.* Neuron, 2009. 63(6): p. 714-6.
102. Deo, M., et al., *Detection of mammalian microRNA expression by in situ hybridization with RNA oligonucleotides.* Developmental dynamics : an official publication of the American Association of Anatomists, 2006. 235(9): p. 2538-48.
103. Lagos-Quintana, M., et al., *Identification of tissue-specific microRNAs from mouse.* Current biology : CB, 2002. 12(9): p. 735-9.
104. Krichevsky, A.M., et al., *A microRNA array reveals extensive regulation of microRNAs during brain development.* RNA, 2003. 9(10): p. 1274-81.
105. Miska, E.A., et al., *Microarray analysis of microRNA expression in the developing mammalian brain.* Genome biology, 2004. 5(9): p. R68.
106. Smirnova, L., et al., *Regulation of miRNA expression during neural cell specification.* The European journal of neuroscience, 2005. 21(6): p. 1469-77.
107. Clark, A.M., et al., *The microRNA miR-124 controls gene expression in the sensory nervous system of Caenorhabditis elegans.* Nucleic acids research, 2010. 38(11): p. 3780-93.
108. Miska, E.A., et al., *Most Caenorhabditis elegans microRNAs are individually not essential for development or viability.* PLoS genetics, 2007. 3(12): p. e215.
109. Yang, Y., et al., *EPAC null mutation impairs learning and social interactions via aberrant regulation of miR-124 and Zif268 translation.* Neuron, 2012. 73(4): p. 774-88.
110. Younossi-Hartenstein, A., et al., *Early neurogenesis of the Drosophila brain.* The Journal of comparative neurology, 1996. 370(3): p. 313-29.
111. Campos-Ortega, J.A., *Genetic mechanisms of early neurogenesis in Drosophila melanogaster.* Journal of physiology, Paris, 1994. 88(2): p. 111-22.
112. Ito, K. and Y. Hotta, *Proliferation pattern of postembryonic neuroblasts in the brain of Drosophila melanogaster.* Developmental biology, 1992. 149(1): p. 134-48.
113. Ashraf, S.I. and Y.T. Ip, *The Snail protein family regulates neuroblast expression of inscuteable and string, genes involved in asymmetry and cell division in Drosophila.* Development, 2001. 128(23): p. 4757-67.
114. Egger, B., et al., *Regulation of spindle orientation and neural stem cell fate in the Drosophila optic lobe.* Neural development, 2007. 2: p. 1.
115. Kraut, R. and J.A. Campos-Ortega, *inscuteable, a neural precursor gene of Drosophila, encodes a candidate for a cytoskeleton adaptor protein.* Developmental biology, 1996. 174(1): p. 65-81.
116. Kraut, R., et al., *Role of inscuteable in orienting asymmetric cell divisions in Drosophila.* Nature, 1996. 383(6595): p. 50-5.
117. Yu, F., et al., *Analysis of partner of inscuteable, a novel player of Drosophila asymmetric divisions, reveals two distinct steps in inscuteable apical localization.* Cell, 2000. 100(4): p. 399-409.
118. Cai, Y., et al., *Apical complex genes control mitotic spindle geometry and relative size of daughter cells in Drosophila neuroblast and pI asymmetric divisions.* Cell, 2003. 112(1): p. 51-62.
119. Giansanti, M.G., M. Gatti, and S. Bonaccorsi, *The role of centrosomes and astral microtubules during asymmetric division of Drosophila neuroblasts.* Development, 2001. 128(7): p. 1137-45.
120. Kaltschmidt, J.A., et al., *Rotation and asymmetry of the mitotic spindle direct asymmetric cell division in the developing central nervous system.* Nature cell biology, 2000. 2(1): p. 7-12.

121. Hirata, J., et al., *Asymmetric segregation of the homeodomain protein Prospero during Drosophila development.* Nature, 1995. 377(6550): p. 627-30.
122. Knoblich, J.A., L.Y. Jan, and Y.N. Jan, *Asymmetric segregation of Numb and Prospero during cell division.* Nature, 1995. 377(6550): p. 624-7.
123. Shen, C.P., L.Y. Jan, and Y.N. Jan, *Miranda is required for the asymmetric localization of Prospero during mitosis in Drosophila.* Cell, 1997. 90(3): p. 449-58.
124. Spana, E.P. and C.Q. Doe, *The prospero transcription factor is asymmetrically localized to the cell cortex during neuroblast mitosis in Drosophila.* Development, 1995. 121(10): p. 3187-95.
125. Doe, C.Q. and E.P. Spana, *A collection of cortical crescents: asymmetric protein localization in CNS precursor cells.* Neuron, 1995. 15(5): p. 991-5.
126. Betschinger, J., K. Mechtler, and J.A. Knoblich, *Asymmetric segregation of the tumor suppressor brat regulates self-renewal in Drosophila neural stem cells.* Cell, 2006. 124(6): p. 1241-53.
127. Spana, E.P., et al., *Asymmetric localization of numb autonomously determines sibling neuron identity in the Drosophila CNS.* Development, 1995. 121(11): p. 3489-94.
128. Ghysen, A. and C. O'Kane, *Neural enhancer-like elements as specific cell markers in Drosophila.* Development, 1989. 105(1): p. 35-52.
129. White, K., *Defective neural development in Drosophila melanogaster embryos deficient for the tip of the X chromosome.* Developmental biology, 1980. 80(2): p. 332-44.
130. Cubas, P., et al., *Proneural clusters of achaete-scute expression and the generation of sensory organs in the Drosophila imaginal wing disc.* Genes & development, 1991. 5(6): p. 996-1008.
131. Skeath, J.B. and S. Thor, *Genetic control of Drosophila nerve cord development.* Current Opinion in Neurobiology, 2003. 13(1): p. 8-15.
132. Hartenstein, V., et al., *The development of the Drosophila larval brain.* Advances in experimental medicine and biology, 2008. 628: p. 1-31.
133. Boone, J.Q. and C.Q. Doe, *Identification of Drosophila type II neuroblast lineages containing transit amplifying ganglion mother cells.* Developmental neurobiology, 2008. 68(9): p. 1185-95.
134. Bello, B.C., et al., *Amplification of neural stem cell proliferation by intermediate progenitor cells in Drosophila brain development.* Neural development, 2008. 3: p. 5.
135. Bowman, S.K., et al., *The tumor suppressors Brat and Numb regulate transit-amplifying neuroblast lineages in Drosophila.* Developmental cell, 2008. 14(4): p. 535-46.
136. Carney, T.D., et al., *Functional genomics identifies neural stem cell sub-type expression profiles and genes regulating neuroblast homeostasis.* Developmental biology, 2012. 361(1): p. 137-46.
137. San-Juan, B.P. and A. Baonza, *The bHLH factor deadpan is a direct target of Notch signaling and regulates neuroblast self-renewal in Drosophila.* Developmental biology, 2011. 352(1): p. 70-82.
138. Bayraktar, O.A., et al., *Drosophila type II neuroblast lineages keep Prospero levels low to generate large clones that contribute to the adult brain central complex.* Neural development, 2010. 5: p. 26.
139. Jallon, J.M. and Y. Hotta, *Genetic and behavioral studies of female sex appeal in Drosophila.* Behavior genetics, 1979. 9(4): p. 257-75.

140. Tompkins, L., et al., *Conditioned courtship in Drosophila and its mediation by association of chemical cues.* Behavior genetics, 1983. 13(6): p. 565-78.
141. Jallon, J.M., *A few chemical words exchanged by Drosophila during courtship and mating.* Behavior genetics, 1984. 14(5): p. 441-78.
142. Scott, D. and R.C. Richmond, *A genetic analysis of male-predominant pheromones in Drosophila melanogaster.* Genetics, 1988. 119(3): p. 639-46.
143. Cobb, M., *Genotypic and phenotypic characterization of the Drosophila melanogaster olfactory mutation Indifferent.* Genetics, 1996. 144(4): p. 1577-87.
144. Amrein, H., *Pheromone perception and behavior in Drosophila.* Current Opinion in Neurobiology, 2004. 14(4): p. 435-42.
145. Boll, W. and M. Noll, *The Drosophila Pox neuro gene: control of male courtship behavior and fertility as revealed by a complete dissection of all enhancers.* Development, 2002. 129(24): p. 5667-81.
146. Ferveur, J.F. and J.M. Jallon, *Genetic control of male cuticular hydrocarbons in Drosophila melanogaster.* Genetical research, 1996. 67(3): p. 211-8.
147. Billeter, J.C., et al., *Specialized cells tag sexual and species identity in Drosophila melanogaster.* Nature, 2009. 461(7266): p. 987-91.
148. Pechine, J.M., et al., *A further characterization of Drosophila cuticular monoenes using a mass spectrometry method to localize double bonds in complex mixtures.* Analytical biochemistry, 1985. 145(1): p. 177-82.
149. Arienti, M., et al., *Ontogeny of Drosophila melanogaster female sex-appeal and cuticular hydrocarbons.* Integrative zoology, 2010. 5(3): p. 272-82.
150. Fernandez, M.P., et al., *Pheromonal and behavioral cues trigger male-to-female aggression in Drosophila.* PLoS biology, 2010. 8(11): p. e1000541.
151. Siwicki, K.K., et al., *The role of cuticular pheromones in courtship conditioning of Drosophila males.* Learning & memory, 2005. 12(6): p. 636-45.
152. Guiraudie-Capraz, G., D.B. Pho, and J.M. Jallon, *Role of the ejaculatory bulb in biosynthesis of the male pheromone cis-vaccenyl acetate in Drosophila melanogaster.* Integrative zoology, 2007. 2(2): p. 89-99.
153. Yew, J.Y., et al., *A new male sex pheromone and novel cuticular cues for chemical communication in Drosophila.* Current biology : CB, 2009. 19(15): p. 1245-54.
154. Kurtovic, A., A. Widmer, and B.J. Dickson, *A single class of olfactory neurons mediates behavioural responses to a Drosophila sex pheromone.* Nature, 2007. 446(7135): p. 542-6.
155. Hall, J.C., *Courtship among males due to a male-sterile mutation in Drosophila melanogaster.* Behavior genetics, 1978. 8(2): p. 125-41.
156. Salz, H.K. and J.W. Erickson, *Sex determination in Drosophila: The view from the top.* Fly, 2010. 4(1): p. 60-70.
157. Erickson, J.W. and J.J. Quintero, *Indirect effects of ploidy suggest X chromosome dose, not the X:A ratio, signals sex in Drosophila.* PLoS biology, 2007. 5(12): p. e332.
158. Zhu, C., J. Urano, and L.R. Bell, *The Sex-lethal early splicing pattern uses a default mechanism dependent on the alternative 5′ splice sites.* Molecular and cellular biology, 1997. 17(3): p. 1674-81.
159. Boggs, R.T., et al., *Regulation of sexual differentiation in D. melanogaster via alternative splicing of RNA from the transformer gene.* Cell, 1987. 50(5): p. 739-47.
160. Inoue, K., et al., *Binding of the Drosophila sex-lethal gene product to the alternative splice site of transformer primary transcript.* Nature, 1990. 344(6265): p. 461-3.

161. Valcarcel, J., et al., *The protein Sex-lethal antagonizes the splicing factor U2AF to regulate alternative splicing of transformer pre-mRNA.* Nature, 1993. 362(6416): p. 171-5.
162. Amrein, H., M. Gorman, and R. Nothiger, *The sex-determining gene tra-2 of Drosophila encodes a putative RNA binding protein.* Cell, 1988. 55(6): p. 1025-35.
163. Hoshijima, K., et al., *Control of doublesex alternative splicing by transformer and transformer-2 in Drosophila.* Science, 1991. 252(5007): p. 833-6.
164. Hedley, M.L. and T. Maniatis, *Sex-specific splicing and polyadenylation of dsx pre-mRNA requires a sequence that binds specifically to tra-2 protein in vitro.* Cell, 1991. 65(4): p. 579-86.
165. Ryner, L.C. and B.S. Baker, *Regulation of doublesex pre-mRNA processing occurs by 3'-splice site activation.* Genes & development, 1991. 5(11): p. 2071-85.
166. Burtis, K.C. and B.S. Baker, *Drosophila doublesex gene controls somatic sexual differentiation by producing alternatively spliced mRNAs encoding related sex-specific polypeptides.* Cell, 1989. 56(6): p. 997-1010.
167. Ryner, L.C., et al., *Control of male sexual behavior and sexual orientation in Drosophila by the fruitless gene.* Cell, 1996. 87(6): p. 1079-89.
168. Villella, A., et al., *Functional analysis of fruitless gene expression by transgenic manipulations of Drosophila courtship.* Proceedings of the National Academy of Sciences of the United States of America, 2005. 102(46): p. 16550-7.
169. Kimura, K., et al., *Fruitless specifies sexually dimorphic neural circuitry in the Drosophila brain.* Nature, 2005. 438(7065): p. 229-33.
170. Vrontou, E., et al., *fruitless regulates aggression and dominance in Drosophila.* Nat Neurosci, 2006. 9(12): p. 1469-71.
171. Kimura, K., et al., *Fruitless and doublesex coordinate to generate male-specific neurons that can initiate courtship.* Neuron, 2008. 59(5): p. 759-69.
172. Siwicki, K.K. and E.A. Kravitz, *Fruitless, doublesex and the genetics of social behavior in Drosophila melanogaster.* Current Opinion in Neurobiology, 2009. 19(2): p. 200-6.
173. Ejima, A., et al., *Generalization of courtship learning in Drosophila is mediated by cis-vaccenyl acetate.* Current biology : CB, 2007. 17(7): p. 599-605.
174. Waterbury, J.A., L.L. Jackson, and P. Schedl, *Analysis of the doublesex female protein in Drosophila melanogaster: role on sexual differentiation and behavior and dependence on intersex.* Genetics, 1999. 152(4): p. 1653-67.
175. Rideout, E.J., et al., *Control of sexual differentiation and behavior by the doublesex gene in Drosophila melanogaster.* Nat Neurosci, 2010. 13(4): p. 458-66.
176. Baker, B.S. and J.M. Belote, *Sex determination and dosage compensation in Drosophila melanogaster.* Annual review of genetics, 1983. 17: p. 345-93.
177. Manoli, D.S., et al., *Male-specific fruitless specifies the neural substrates of Drosophila courtship behaviour.* Nature, 2005. 436(7049): p. 395-400.
178. Demir, E. and B.J. Dickson, *fruitless splicing specifies male courtship behavior in Drosophila.* Cell, 2005. 121(5): p. 785-94.
179. Lee, W.J., et al., *Inhibition of mitogen-activated protein kinase by a Drosophila dual-specific phosphatase.* The Biochemical journal, 2000. 349 Pt 3: p. 821-8.
180. Villella, A. and J.C. Hall, *Neurogenetics of courtship and mating in Drosophila.* Advances in genetics, 2008. 62: p. 67-184.
181. Villella, A. and J.C. Hall, *Courtship anomalies caused by doublesex mutations in Drosophila melanogaster.* Genetics, 1996. 143(1): p. 331-44.

182. Ferveur, J.F., *The pheromonal role of cuticular hydrocarbons in Drosophila melanogaster.* BioEssays : news and reviews in molecular, cellular and developmental biology, 1997. 19(4): p. 353-8.
183. Tompkins, L. and S.P. McRobert, *Behavioral and pheromonal phenotypes associated with expression of loss-of-function mutations in the sex-lethal gene of Drosophila melanogaster.* Journal of neurogenetics, 1995. 9(4): p. 219-26.
184. Brennecke, J., et al., *Principles of microRNA-target recognition.* PLoS Biol, 2005. 3(3): p. e85.
185. Brennecke, J., et al., *bantam encodes a developmentally regulated microRNA that controls cell proliferation and regulates the pro-apoptotic gene hid in Drosophila.* Cell, 2003. 113: p. 25-36.
186. Ledent, V. and M. Vervoort, *The basic helix-loop-helix protein family: comparative genomics and phylogenetic analysis.* Genome research, 2001. 11(5): p. 754-70.
187. Miller, M.R., et al., *TU-tagging: cell type-specific RNA isolation from intact complex tissues.* Nature methods, 2009. 6(6): p. 439-41.
188. Wu, J.S. and L. Luo, *A protocol for mosaic analysis with a repressible cell marker (MARCM) in Drosophila.* Nature protocols, 2006. 1(6): p. 2583-9.
189. Kozomara, A. and S. Griffiths-Jones, *miRBase: integrating microRNA annotation and deep-sequencing data.* Nucleic acids research, 2011. 39(Database issue): p. D152-7.
190. Jones, W.D., et al., *Two chemosensory receptors together mediate carbon dioxide detection in Drosophila.* Nature, 2007. 445(7123): p. 86-90.
191. Bischof, J., et al., *An optimized transgenesis system for Drosophila using germ-line-specific phiC31 integrases.* Proc Natl Acad Sci U S A, 2007. 104(9): p. 3312-7.
192. Klemenz, R., U. Weber, and W.J. Gehring, *The white gene as a marker in a new P-element vector for gene transfer in Drosophila.* Nucleic Acids Res, 1987. 15(10): p. 3947-59.
193. Ruby, J.G., et al., *Large-scale sequencing reveals 21U-RNAs and additional microRNAs and endogenous siRNAs in C. elegans.* Cell, 2006. 127(6): p. 1193-207.
194. Brand, A. and N. Perrimon, *Targeted gene expression as a means of altering cell fates and generating dominant phenotypes.* Development, 1993. 118: p. 401-415.
195. Lee, T. and L. Luo, *Mosaic analysis with a repressible cell marker for studies of gene function in neuronal morphogenesis.* Neuron, 1999. 22(3): p. 451-61.
196. Maiorano, N.A. and A. Mallamaci, *Promotion of embryonic cortico-cerebral neuronogenesis by miR-124.* Neural development, 2009. 4: p. 40.
197. Weng, R., et al., *Recombinase-mediated cassette exchange provides a versatile platform for gene targeting: knockout of miR-31b.* Genetics, 2009. 183(1): p. 399-402.
198. Chen, Y.W., R. Weng, and S.M. Cohen, *Protocols for use of homologous recombination gene targeting to produce microRNA mutants in Drosophila.* Methods in molecular biology, 2011. 732: p. 99-120.
199. Goto, H., et al., *Identification of a novel phosphorylation site on histone H3 coupled with mitotic chromosome condensation.* The Journal of biological chemistry, 1999. 274(36): p. 25543-9.
200. Ebens, A.J., et al., *The Drosophila anachronism locus: a glycoprotein secreted by glia inhibits neuroblast proliferation.* Cell, 1993. 74(1): p. 15-27.

201. Park, Y., M.C. Caldwell, and S. Datta, *Mutation of the central nervous system neuroblast proliferation repressor ana leads to defects in larval olfactory behavior.* Journal of neurobiology, 1997. 33(2): p. 199-211.
202. Choi, W.Y., A.J. Giraldez, and A.F. Schier, *Target protectors reveal dampening and balancing of Nodal agonist and antagonist by miR-430.* Science, 2007. 318(5848): p. 271-4.
203. Varghese, J., S.F. Lim, and S.M. Cohen, *Drosophila miR-14 regulates insulin production and metabolism through its target, sugarbabe.* Genes & development, 2010. 24(24): p. 2748-53.
204. Rezaval, C., et al., *Neural circuitry underlying Drosophila female postmating behavioral responses.* Current biology : CB, 2012. 22(13): p. 1155-65.
205. Stowers, L. and D.W. Logan, *Sexual dimorphism in olfactory signaling.* Current Opinion in Neurobiology, 2010. 20(6): p. 770-5.
206. Vosshall, L.B., *Scent of a fly.* Neuron, 2008. 59(5): p. 685-9.
207. Robinett, C.C., et al., *Sex and the single cell. II. There is a time and place for sex.* PLoS biology, 2010. 8(5): p. e1000365.
208. Rehmsmeier, M., et al., *Fast and effective prediction of microRNA/target duplexes.* RNA, 2004. 10(10): p. 1507-17.
209. Dow, M.A. and F. von Schilcher, *Aggression and mating success in Drosophila melanogaster.* Nature, 1975. 254(5500): p. 511-2.
210. Wang, L. and D.J. Anderson, *Identification of an aggression-promoting pheromone and its receptor neurons in Drosophila.* Nature, 2010. 463(7278): p. 227-31.
211. Chen, S., et al., *Fighting fruit flies: a model system for the study of aggression.* Proceedings of the National Academy of Sciences of the United States of America, 2002. 99(8): p. 5664-8.
212. Wang, L., et al., *Hierarchical chemosensory regulation of male-male social interactions in Drosophila.* Nature neuroscience, 2011. 14(6): p. 757-62.
213. Choi, C.M., et al., *Conditional mutagenesis in Drosophila.* Science, 2009. 324(5923): p. 54.
214. Huang, J., et al., *Directed, efficient, and versatile modifications of the Drosophila genome by genomic engineering.* Proceedings of the National Academy of Sciences of the United States of America, 2009.
215. Krichevsky, A.M., et al., *Specific microRNAs modulate embryonic stem cell-derived neurogenesis.* Stem cells, 2006. 24(4): p. 857-64.
216. Lim, L.P., et al., *Microarray analysis shows that some microRNAs downregulate large numbers of target mRNAs.* Nature, 2005. 433(7027): p. 769-73.
217. Visvanathan, J., et al., *The microRNA miR-124 antagonizes the anti-neural REST/SCP1 pathway during embryonic CNS development.* Genes Dev, 2007. 21(7): p. 744-9.
218. Leaman, D., et al., *Antisense-mediated depletion reveals essential and specific functions of microRNAs in Drosophila development.* Cell, 2005. 121(7): p. 1097-108.
219. Bushati, N. and S.M. Cohen, *microRNA functions.* Annu Rev Cell Dev Biol, 2007. 23: p. 175–205.
220. De Pietri Tonelli, D., et al., *Single-cell detection of microRNAs in developing vertebrate embryos after acute administration of a dual-fluorescence reporter/sensor plasmid.* BioTechniques, 2006. 41(6): p. 727-32.
221. Wienholds, E., et al., *MicroRNA Expression in Zebrafish Embryonic Development.* Science, 2005. 309: p. 310-1.

222. Cline, T.W. and B.J. Meyer, *Vive la difference: males vs females in flies vs worms.* Annual review of genetics, 1996. 30: p. 637-702.
223. Groth, A.C., et al., *Construction of transgenic Drosophila by using the site-specific integrase from phage phiC31.* Genetics, 2004. 166(4): p. 1775-82.
224. Tarone, A.M., Y.M. Nasser, and S.V. Nuzhdin, *Genetic variation for expression of the sex determination pathway genes in Drosophila melanogaster.* Genetical research, 2005. 86(1): p. 31-40.
225. McKeown, M., J.M. Belote, and R.T. Boggs, *Ectopic expression of the female transformer gene product leads to female differentiation of chromosomally male Drosophila.* Cell, 1988. 53(6): p. 887-95.
226. Bousquet, F., et al., *Expression of a desaturase gene, desat1, in neural and nonneural tissues separately affects perception and emission of sex pheromones in Drosophila.* Proceedings of the National Academy of Sciences of the United States of America, 2012. 109(1): p. 249-54.
227. Liu, K., et al., *MiR-124 regulates early neurogenesis in the optic vesicle and forebrain, targeting NeuroD1.* Nucleic acids research, 2011. 39(7): p. 2869-2879.
228. Qiu, R., et al., *The role of miR-124a in early development of the Xenopus eye.* Mechanisms of development, 2009. 126(10): p. 804-16.
229. Lim, L.P., et al., *The microRNAs of Caenorhabditis elegans.* Genes & development, 2003. 17(8): p. 991-1008.
230. Chen, K. and N. Rajewsky, *The evolution of gene regulation by transcription factors and microRNAs.* Nature reviews. Genetics, 2007. 8(2): p. 93-103.
231. Reinhart, B.J., et al., *The 21-nucleotide let-7 RNA regulates developmental timing in Caenorhabditis elegans.* Nature, 2000. 403(6772): p. 901-6.
232. Caygill, E.E. and L.A. Johnston, *Temporal regulation of metamorphic processes in Drosophila by the let-7 and miR-125 heterochronic microRNAs.* Current biology : CB, 2008. 18(13): p. 943-50.
233. Sokol, N.S., et al., *Drosophila let-7 microRNA is required for remodeling of the neuromusculature during metamorphosis.* Genes & development, 2008. 22(12): p. 1591-6.
234. Leucht, C., et al., *MicroRNA-9 directs late organizer activity of the midbrain-hindbrain boundary.* Nature neuroscience, 2008. 11(6): p. 641-8.

6 Appendices

Appendix 1. GC-MS analysis of cuticular hydrocarbon extracts from control, mir-124 mutant, and rescued mutant males.

Compound and elemental composition[1]	Control[2] (n=6)	mir-124 mutant[2] (n=6)	Rescued mutant[2] (n=6)
C21:0 (nC21)	0.46±0.08	0.32±0.05	0.76±0.11
C22:1	0.24±0.01	0.27±0.02	0.35±0.02
cVA (cis-vaccenyl acetate)	9.36±3.40	1.75±0.57***	6.60±2.17***
C22:0	0.74±0.06	0.62±0.02	0.95±0.05
7,11-C23:2	0.13±0.01	0.07±0.001	0.12±0.02
9-C23:1 (9-tricosene)	1.39±0.13	1.76±0.25	1.84±0.14
7-C23:1 (7-tricosene)	23.52±1.17	24.92±1.74	32.80±2.03***
5-C23:1 (5-tricosene)	2.71±0.11	3.06±0.20	3.01±0.18
C23:0 (nC23)	10.57±0.40	11.21±0.25	12.66±0.63**
C24:1	0.32±0.11	0.37±0.09	0.30±0.07
C24:0	0.36±0.02	0.43±0.04	0.35±0.03
2-MeC24	1.44±0.08	1.58±0.15	2.03±0.12
C25:2	0.52±0.06	0.71±0.07	0.70±0.04
9-C25:1 (9-pentacosene)	4.80±0.61	6.33±0.65*	4.11±0.74
7-C25:1 (7-pentacosene)	22.99±1.55	25.62±0.63***	11.61±1.16***
5-C25:1 (5-pentacosene)	1.10±0.33	0.79±0.02	2.38±0.01
C25:0 (nc25)	2.34±0.15	3.13±0.03	2.52±0.15
2-MeC26	6.75±0.49	5.37±0.08	6.55±0.13
9-C27:1	0.16±0.02	0.19±0.03	0.12±0.04
7-C27:1	0.97±0.10	0.77±0.07	0.29±0.06**
C27:0 (nC27)	1.66±0.33	2.42±0.60	1.86±0.39
2-MeC28	5.90±0.81	5.95±0.71	6.18±0.77
C29:0	0.37±0.11	0.78±0.26	0.54±0.17
2-MeC30	0.64±0.16	0.99±0.27	0.87±0.25

[1]The elemental composition is listed as the carbon chain length followed by the number of double bonds; 2-Me indicates the position of methyl branched compounds.

[2]The normalized signal intensity for each compound and SEM is indicated; * P<0.05, **P<0.01, ***P<0.001 when compared to control (ANOVA followed by post-hoc Tukey HSD test).

Appendix 2. GC-MS analysis of cuticular hydrocarbon extracts from control, *mir-124* mutant, rescued mutants, and *mir-124>tra-RNAi* males.

Compound and elemental composition[1]	Control[2] (n=3)	mir-124 mutant[2] (n=3)	Rescued mutant[2] (n=3)	mir-124> tra-RNAi[2] (n=2)
C21:0 (nC21)	0.28±0.1	0.21±0.01	0.51±0.03	0.35±0.04
C22:1	0.22±0.02	0.24±0.01	0.31±0.02	0.34±0.03
cVA (cis-vaccenyl acetate)	3.86±0.43	0.48±0.04***	2.57±0.47*	2.09±0.23*
C22:0	0.61±0.03	0.60±0.01	0.87±0.05	0.70±0.05
7,11-C23:2	0.14±0.01	0.07±0.001	0.17±0.02	0.11±0.02
9-C23:1 (9-tricosene)	1.10±0.05	1.20±0.02	1.57±0.12	1.94±0.07
7-C23:1 (7-tricosene)	21.68±1.14	21.04±0.29	29.07±2.12***	28.95±2.20***
5-C23:1 (5-tricosene)	2.56±0.05	2.62±0.05	2.71±0.25	3.11±0.40
C23:0 (nC23)	9.84±0.15	10.66±0.06	11.33±0.2*	10.35±0.33
C24:1	0.09±0.05	0.19±0.01	0.16±0.02	0.22±0.01
C24:0	0.41±0.01	0.52±0.01	0.40±0.03	0.44±0.01
2-MeC24	1.52±0.13	1.24±0.02	1.81±0.15	1.78±0.09
C25:2	0.41±0.02	0.54±0.02	0.74±0.01	0.76±0.06
9-C25:1 (9-pentacosene)	6.13±0.12	7.78±0.05**	5.74±0.21	6.86±1.02
7-C25:1 (7-pentacosene)	26.01±0.69	26.97±0.25	14.09±0.46***	23.23±1.15***
5-C25:1 (5-pentacosene)	1.41±0.68	0.75±0.01	023±0.02	0.59±0.03
C25:0 (nc25)	2.65±0.06	3.79±0.05	2.85±0.07	2.68±0.26
2-MeC26	7.72±0.28	5.22±0.01***	6.64±0.27	5.23±0.21***
9-C27:1	0.20±0.01	0.25±0.01	0.20±0.02	0.18±0.05
7-C27:1	1.15±0.09	0.92±0.02	0.41±0.01	0.60±0.08
C27:0 (nC27)	2.38±0.12	3.77±0.08*	2.72±0.16	1.92±0.21
2-MeC28	7.66±0.13	7.53±0.05	7.85±0.37	5.76±0.33**
C29:0	0.62±0.06	1.37±0.01	0.92±0.1	0.52±0.05
2-MeC30	0.98±0.06	1.59±0.03	1.41±0.13	0.66±0.02

[1]The elemental composition is listed as the carbon chain length followed by the number of double bonds; 2-Me indicates the position of methyl branched compounds.

[2]The normalized signal intensity for each compound and SEM is indicated; * $P<0.05$, **$P<0.01$, ***$P<0.001$ when compared to control (ANOVA followed by post-hoc Tukey HSD test).